



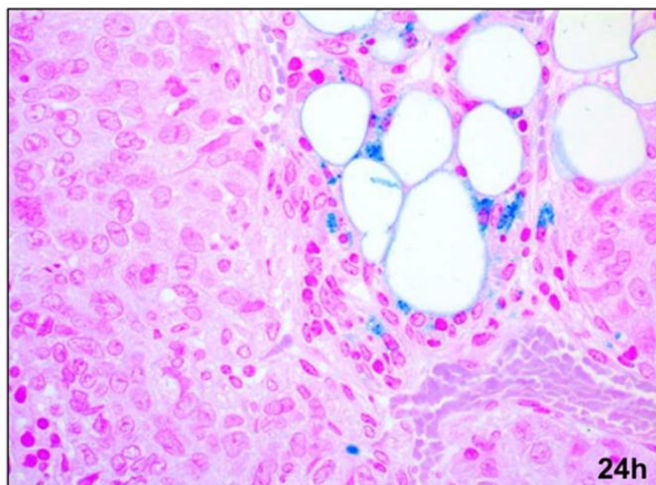
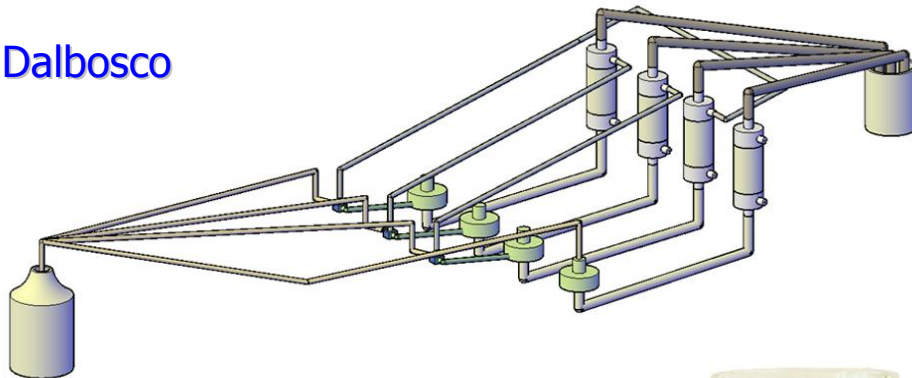
UNIVERSITY  
OF TRENTO - Italy

Department of Materials Engineering  
and Industrial Technologies

Doctoral School in Materials Science and Engineering – XXIV cycle

# Synthesis, Characterization and Functionalization of Iron Oxide Magnetic Nanoparticles for diagnostics and therapy of tumors

Luca Dalbosco



April 2012



# Contents

<b>Introduction</b>	<b>5</b>
<b>I Preliminaries</b>	<b>7</b>
<b>1 On Nanoparticles and their Application</b>	<b>9</b>
1.1 Nanoscience and Nanotechnology . . . . .	10
1.1.1 General introduction on nanomaterials . . . . .	14
1.2 Nanoparticles . . . . .	18
1.2.1 Properties, Characteristics and Applications . . . . .	22
1.2.2 Biomedical application . . . . .	24
1.3 Iron oxide Nanoparticles . . . . .	39
1.3.1 Introduction . . . . .	39
1.3.2 Properties and Characteristics . . . . .	41
1.3.3 Specific properties for biomedical applications . . . . .	49
<b>2 The Nanosmart Project</b>	<b>57</b>
2.1 State-of-art of commercial nanoparticles . . . . .	58
2.1.1 Interaction lived tissue and application . . . . .	61
2.1.2 Pharmacokinetics . . . . .	63
2.2 Nanosmart Project . . . . .	65
<b>II Experimental Part: Production</b>	<b>67</b>
<b>3 Introduction</b>	<b>71</b>
<b>4 UNITN MNPs</b>	<b>73</b>
4.1 MNP Synthesis and chemical-physical characteristics . . . . .	73
4.1.1 Nanoparticle size measurement using DLS and TEM . . . . .	74
4.1.2 X-ray photoelectron spectroscopy XPS . . . . .	76

<b>5</b>	<b>GATECH MNPs</b>	<b>79</b>
5.1	Synthesis and coating . . . . .	79
5.1.1	Nanoparticle size measurement using DLS . . . . .	84
5.1.2	Nanoparticle size measurement using TEM . . . . .	85
5.1.3	Nanoparticle size measurement using AFM . . . . .	86
5.1.4	Change of coating recipe . . . . .	87
5.1.5	Change of coating protocol . . . . .	89
5.1.6	Protocol for the determination of Fe concentration . . . . .	91
5.1.7	Stability of MNPs . . . . .	91
5.1.8	Chemical surface analysis of MNPs using $\zeta$ -potential . . . . .	95
5.1.9	Magnetic $T_2$ relaxivity of PEG-MNPs . . . . .	97
5.1.10	X-ray photoelectron spectroscopy . . . . .	99
5.2	Functionalization . . . . .	105
5.2.1	Labeling with fluorescent dye . . . . .	105
5.2.2	Antibody conjugation to MNP . . . . .	107
5.3	Drug loading . . . . .	112
5.4	Material, Reagent and Instruments . . . . .	117
5.4.1	Experiment materials of chapter 4 . . . . .	117
5.4.2	Experiment materials of chapter 5 . . . . .	118
<b>III</b>	<b>Experimental Part: Biological Tests</b>	<b>123</b>
<b>6</b>	<b><i>In vitro</i> tests</b>	<b>125</b>
6.1	Introduction . . . . .	125
6.2	Cell characterization . . . . .	126
6.3	Production of EGFr antibodies . . . . .	127
6.3.1	Hybridoma Adaptation to Medium without Horse Serum . . . . .	129
6.3.2	IgG production . . . . .	129
6.3.3	IgG purification . . . . .	130
6.3.4	EGFr IgG quality testing . . . . .	131
6.4	GATECH MNPs . . . . .	133
6.4.1	Interaction NP-cell . . . . .	133
6.4.2	Toxicity of MNPs . . . . .	134
6.4.3	Measurement of uptake of AB-MNP by cells . . . . .	134
6.4.4	Effectiveness of DOX entrapped in MNPs . . . . .	137
6.4.5	Bioreactor experiment: Introduction part . . . . .	142
6.4.6	Bioreactor experiment: Results and Comments . . . . .	148
<b>7</b>	<b><i>In vivo</i> tests</b>	<b>157</b>
7.0.7	Results . . . . .	157
	<b>Conclusions</b>	<b>165</b>

<i>CONTENTS</i>	3
<b>Acknowledgment</b>	<b>169</b>
<b>References</b>	<b>171</b>



# Introduction

In the last decade nanotechnologies have greatly developed in many research fields such as engineering, electronic, biological and many others. They can offer several possibilities to design tools, to create new techniques or improve the already existing ones, to discover innovative applications. And nanotechnology research is just at the beginning.

One of the most interesting thing of this topic is the size of nanostructures. These materials are thousand times smaller than a cell and have a compatible size with proteins, enzymes and a lot of biological molecules.

For this reason many research groups specialized in biotechnology started to invest people and resources in this new scientific possibility. Following this very promising trend, BIOtech, a research group for biotechnology at the University of Trento, has proposed the Nanosmart project.

Developed together with many prestigious institutes all over the world, this project aims to exploit the nanotechnology possibilities in biological research.

The purpose of this challenge is the design, development and production of magnetic nanoparticles to use them in diagnostics and therapy of cancer disease.

Magnetic nanoparticles (MNP) are spherical agglomerates of iron oxide, few tens of nanometers, which can be exploited in many ways. Being magnetic they can

be used as contrast agents in magnetic resonance imaging MRI. Together having a high absorbing coefficient in the radio frequency band, they can locally increase the temperature of the tissues hosts and this being used for hyperthermia treatments.

Entrapping some drugs in one of their multilayers, MNP can be used as inert carriers for drug delivery: due to their small size they can enter biological tissues, cross the plasma membrane of cells and release the drug only on predetermined targets.

My Ph.D. started together with the project; so I had the possibility to follow this research from the beginning. In this years many problems have been handled, many errors have been made, many brilliant ideas have been shelved but also new abilities have been acquired, important collaborations were born and alternative structures have been thought and, fortunately, realized.

Trying to eliminate unnecessary things and focusing on main purpose of this work, in this thesis I want to illustrate just the long "*fil rouge*" that connects the idea of producing a nanoparticle that can cure tumor to the point of verify its effectiveness.

## Part I

# Preliminaries



## Chapter 1

# On Nanoparticles and their Application

Starting a new project is always a new challenge also for a laboratory with great experience. Challenge that becomes more charming when the topic of the project is almost totally new. One of the first difficulty is to acquire knowledge of the *state of art* of the topic and to use literature to get *know how* to handle research with the best possible performance; this permit to save time and money, to avoid useless experiments and, hence, to focus on changes and evolutions of tests already carried out and well documented in the scientific literature.

To better understand what are the properties characterizing magnetic iron oxide nanoparticles (MNPs), we need to deepen their purpose and usage. For this reason it is important to learn the possibilities offered by field of nanotechnology and its applications in diagnosis and therapy for medicine, in particular those offered by nanoparticles. Most of the attention will be on magnetic iron oxide nanoparticles

(simply called MNP) in particular on their composition, structure, characterization, functionalization and analysis.

Taking into account these properties and characteristics of MNP, University of Trento, in collaboration with other six research centers from different countries, carried on the “NANOSMART” project, which at the use of nanoparticles in diagnosis and therapy of tumors.

## 1.1 Nanoscience and Nanotechnology

In the first studies and in earlier publications, the terms “nanoscience” and “nanotechnology” had quite similar meaning. As years goes by the two terms have taken slightly different meanings. Nanoscience is the study of phenomena and manipulation of materials at atomic, molecular and macromolecular scales, where properties differ significantly between these scales and major scales. Conversely, nanotechnology refers to the design, characterization, production and the application of structures, devices and systems for the control of the form and size of nanoscale components.

The prefix *nano* comes from the Greek word  $\nu\alpha\nu\phi\varsigma$ . A nanometer (nm) is equal to one billionth of a meter,  $10^{-9}m$ . A human hair is approximately 80 thousand nm wide, while a red blood cell approximately 7 thousand nanometers (Figure 1.1). Atoms are smaller than a nanometer, while some molecules, such as proteins or antibodies, are compatible with this size.

The main effects that characterize the properties of nanoparticles compared to the same material at the macroscopic scale are two: size-dependent and quantum effects. Nanosciences study how they affect the properties of materials, while nanotechnologies aim to exploit this peculiarity to create structures and systems with new properties and functions by modulating these effects as desired.

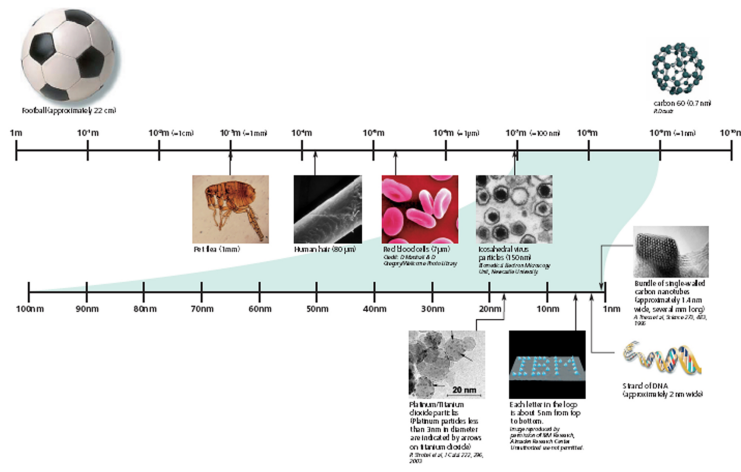


Figure 1.1: Size scale, for each dimension is represented a characteristic structure [1]

The use of nanocomposites is very ancient; for instance, already in the tenth century, nanoscale pigments were used to color glass and ceramics. But it is just in recent years that the necessity to investigate and manipulate nanoscale materials has led an improving and evolution in consideration and in design of instruments that can exploit these possibilities.

The highest leap forward in this research field was designed and developed in the 80's with the design of two instruments: the scanning tunneling microscope (STM) in 1982 and the atomic force microscope (AFM) in 1986. These apparatus use nanometric approach to produce atomic resolution images. They also have the ability to move atoms or molecules on surfaces, building rudimentary nanostructures; one of the most famous example is the word IBM made by Eigler and Schweizer in 1990 (Figure 1.1).

Nanomaterials can be constructed with *top down* or *bottom up* approaches. With *top down* very small structures are produced starting with a large part of material through processes of mass removal. On the contrary, with *bottom up* technique

nanoscale materials is produced building up atom by atom, molecule by molecule. The evolution of this technique is self-assembling, in which the atoms or molecule are able to create structures according to their natural properties. Another aspect of the *bottom up* technique is the use of tools that can move individual atoms or molecules.

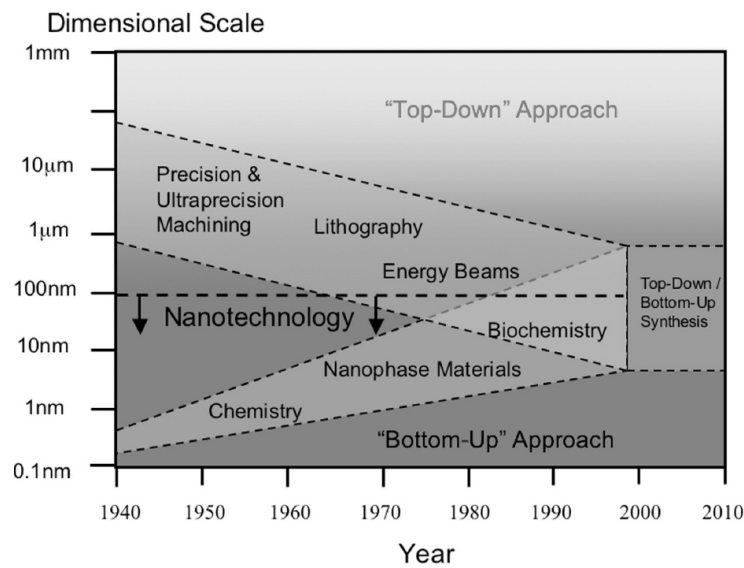


Figure 1.2: The convergence of technique production “top-down” and “bottom-up” [1]

The main challenge of *top-down* method is the creation of small structures with sufficient precision, while for *bottom-up* is the creation of large structures with a good quality and resistance that can be used as a material. These two methods have evolved separately but the objective was always the same: the production of nanoscale structures.

In recent years the scientific community is trying to develop a hybrid technique able to take the positive aspects of both methods. Nanosciences and nanotechnologies encompass a large number of fields: chemical, physical, biological, medical, engineer-

ing and electronics. The four main subdivisions of nanosciences are: nanomaterials, nanometrology, bionanotechnology and optoelectronics for information and communication.

The current applications of nanomaterials include the use of these materials as thin films of coverage, for example, in electronics and as active surfaces such as windows self-cleaning. In most cases nanoscale materials are bound or placed on some supports, but some types of nanoparticles are used free, as in commercial sunscreen. The particles of these creams have a composition able to absorb the ultraviolet rays UV of the sun, to protect the skin from diseases carried by a typical long exposure to sunlight. The skill and the precision of the production of nanomaterials, with size less than 100 nm, are so high to bring benefits in the production of components in various fields such as information technology and automobile and aerospace industry. In the coming years nanomaterials will increase performance in a variety of products such as silicon electronics, displays, paints, catalysts and microsensors.

Are also very promising carbon nanotubes, hollow tubes products with carbon molecules which have a great resistance, a good flexibility and great electrical conductivity; probably they will revolutionize the field of electronics and communications. In the future lubricants based on inorganic nanospheres will be used; they are magnetic materials that take advantage of nanocrystalline grains, medical nanoceramics that have more durability and better prosthetics applications and nanomembranes for a better water purification. Nanometrology, which is the science of measurement, can be used by nanotechnology because it allows the morphology and electric characterization of a lot of materials.

Regarding the optoelectronic information and communication, nanotechnology is making great strides. An example is the evolution of the size of a transistor from 90 nm in 2004 to future 22 nm in 2016. Other applications are the use of magnetic

materials for the storage of data. In information technology field nanoscience were not limited only to the electronics of silicon, for example the use of plastic electronics to produce flexible displays. Quantum dots are semiconductor nanoparticles developed in recent years; they can be adjusted to emit or absorb light of a particular color for use in solar cells or in the fluorescence labeling for biological experiments.

Applications of nanotechnology in medicine are especially promising, with several areas of study as the diagnosis of diseases, the drug delivery in specific areas of the body and molecular imaging. In medical field, research seeks to produce materials and tools as a scaffold for cell and tissue engineering and sensors that can be used for monitoring of human parameters. In the coming years nanotechnology can help to produce complex structures as the retina and cochlea and using biotechnology it will be easier to understand how complex biological structures are composed. [2]

### 1.1.1 General introduction on nanomaterials

Nanomaterials are defined as those structures that do not even have all dimensions in the nanoscale. For example, there are some materials, such as films or coating surfaces of computer chips, which are nanoscale only in one dimension and the other two are macroscopic. Nanotubes or nanowires are examples of 2-dimensional nanostructures with nanometer scale. With regard to compounds that have all three nanosized, there are colloids, precipitates and quantum dots. In this definition it is possible to find also materials with macroscopic scale; they are nanocrystalline materials made of nanometer-sized grains.

Materials that have well defined physical properties, at the nanometer scale, can express quite different properties; an example is the copper, that is malleable and ductile, which, if produced in spheres or tubes of size below 50 nm, completely loses

its malleability and ductility becoming a very hard material.

As already mentioned, the two main factors that give different properties of nanoscale materials are the increase of the ratio between surface and volume and quantum effects.

Fundamental properties for a material, as surface reactivity, resistance and electrical characteristics are size-dependent and that depends on the number of atoms on the surface respect to total amount of atoms while for a microstructure this ratio between surface atoms and total atoms tends to zero. For instance a particle with size of 30 nm has 5% of atoms on its surface, while at 10 nm are 20% and for nanoparticles with size of 3 nm on the surface atoms are the half of the total.

So a material will be very more reactive in its nanometric form compared to the coarse one.

Quantum effects modify optical, electrical and magnetic properties; the effect is more significant decreasing the size of the object. In some cases a very small size can also modify the mechanical properties; this happens in metals made of small crystalline grains. The neighboring regions of these grains slow or completely stop the propagation of defects when the material is stressed. If the grain are nanometric, the number of interaction between them becomes huge increasing the effectiveness of the material under stress. For example, in experimental tests the nanocrystals of nickel resulted to be much more resistant than the steel, the harder one.

### **One nanometric dimension**

Materials with one nanometric dimension, such as films and active surfaces, have been developed and used for decades in electronics, chemistry and engineering; probably greatest development occurred in the industry of silicon integrated circuits. The

monolayer thickness of an atom or molecule, are frequently used in chemistry. The formation and properties of these layers can reasonably be understood from an atomic point of view, even in the case of complex layers, such as lubricants. Progress has been made in controlling the composition of the surface polishing and the film growth.

The engineering of surfaces, such as the choice of the size or modulation of reactivity, finds many applications as cells with fuel or catalysts. The large surface area, full of nanoparticles, can be used in many applications, especially in the chemical and energy sector where the great reactivity and selectivity is exploited to save money reducing the main resources for the production of energy.

### **Two nanometric dimension**

Research and investigation of nanostructures with two nanoscale dimensions is quite recent, about the last 15 years. The interest increased when the first results emphasized the great Electrical and mechanical properties of these structures. Carbon nanotubes (CNTs) are graphene sheets and are of 2 types: single wall, a single tube or multi-wall, a series of concentric tubes, as shown in Figure 1.3. In both cases, the diameter is a few nanometer and the length ranges from several micrometers to few centimeters. Nanotubes are mechanically very strong: indeed, the value of the Young's modulus is greater than 1 terapascal, very similar to diamond. In addition to the mechanical strength, they are very flexible and are good electrical conductors; actually they behave like semiconductors or metals.

Applications of carbon nanotubes are several: the reinforcement of composite materials, nanoelectronics, sensors and displays. In addition to the carbon nanotubes there are nanotubes of inorganic compounds of molybdenum disulfide; they have excellent properties as lubricants, high impact resistance and high reactivity in catalytic capability to store oxygen and lithium. Nanotubes based on oxides, such as titanium

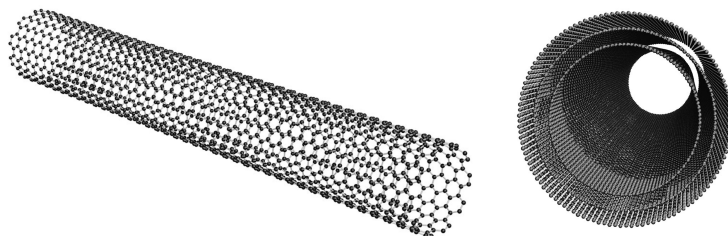


Figure 1.3: Single-wall or multi-walled carbon nanotubes [1]

dioxide, may instead find good applications in the field of catalysis, photocatalysis and energy storage.

Another example of materials with two nanometric dimensions are nanowires. These structures are composed of incredibly thin cables, or even by a linear series of points, self-assembled. Nanowires can be produced by a wide range of materials, such as silicon, gallium nitrate, and the indium phosphide. These structures have been shown to have magnetic, electronic and optical properties; for example silicon nanowires can bend the light also around a narrow angle. For these reasons, the applications of the nanowires are different as the storage of data at high density for magnetic heads for writing on electronic media, for electronic devices and optoelectronic and metal interconnections between quantum devices and nanodevices.

### **Three nanometric dimension**

All three dimensions of this kind of material are nanometric and as a consequence the volume of these structures is contained in a sphere-form structure with a size less than 100 nm. The main structures of this type are fullerenes, dendrimers, quantum dots and nanoparticles especially.

This is only a short introduction on nanoparticles. Next section provides a deep description of them.

## 1.2 Nanoparticles

Nanoparticles are aggregates of molecules with a size less than 100 nm. The term nanoparticle is extended to include sub-categories such as nanopowders, nanoclusters and nanocrystals. Nanocrystals are compounds with a crystalline form and a size less than 100 nm. Nanopowders and nanoclusters are compounds that do not have a crystalline form and which have, respectively, size less than 100 nm and between 2 and 10 nm with a very narrow size distribution.

There are many type of structures, the most important are four.

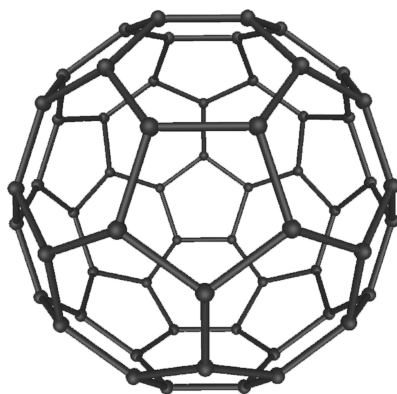
### **Nanoparticles**

These compounds exhibit new and interesting properties that depend on the size, which is less than 100 nm. Nanoparticles are widely present in the natural world as photochemical reactions, as result of volcanic activity or produced by plants or algae. They have also been created, unintentionally, by humans in the form of products of combustion residues and cooked food or, more recently, as the remains of the exhausted fuel of vehicles. In comparison to the quantity of nanoparticles produced naturally or accidentally, nanoparticles synthesized for research or industrial purposes are a small minority. This minority increased in recent years and will grow even more in the next, thanks to developments that these special size-dependent properties carried out in the various fields in which they are exploited. For example, titanium dioxide or zinc oxide become transparent if they form nanometer-sized structures and absorb and reflect UV rays.

Nanoparticles have a large range of applications: in a short time in the cosmetics industry, textile and paint industries; in long times such as contrast agents for diagnostic imaging or carriers for drug delivery and hyperthermia. Nanoparticles can be arranged in layers placed on top of other structures, increasing the surface and improving the reactivity, finding many applications in the field of catalysts. Currently, nanoparticles are not produced for direct use, but they are exploited as additives or ingredients in already existing products, in order to improve some properties. The diffusion of nanoparticles is very low compared to other nanoscale materials, because there is not yet in-depth information of their toxicity. Toxicity, that can be decreased attaching them on the surface or binding with other composites. In fact, if nanoparticles are free or attached, you can have different impacts on health and safety man or nature if the nanoparticles are free or bound to other molecules or structures. [19]

### Fullerene

In the mid-80's was discovered a new class of materials based on carbon called fullerenes: "carbon 60" ( $C_{60}$ ) is the most famous (following figure).



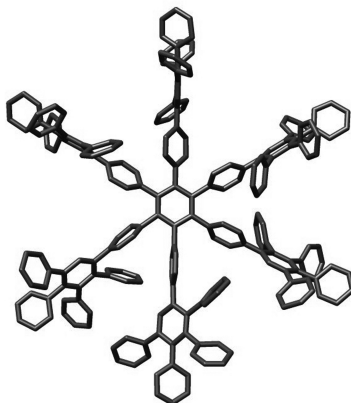
This is a spherical molecule of 1 nm in diameter with 60 carbon atoms distributed in 20 hexagons and 12 pentagons; this is the same configuration of a classic soccer ball. The term derives from the name of the architect Buckminster Fuller became famous for the construction of geodesic domes.

A technique to produce large quantities of fullerene consists in heating small rods of graphite in environment helium. There are many applications of fullerenes: as lubricant for surfaces, carrier for drug delivery and electronic circuits.

### Dendrimers

Another structure with all nanoscale dimensions is the dendrimer.

Dendrimers are highly branched molecules, which are characterized by their structural perfection; in fact the name comes from the greek term *dendron*, which means *tree* (following figure).



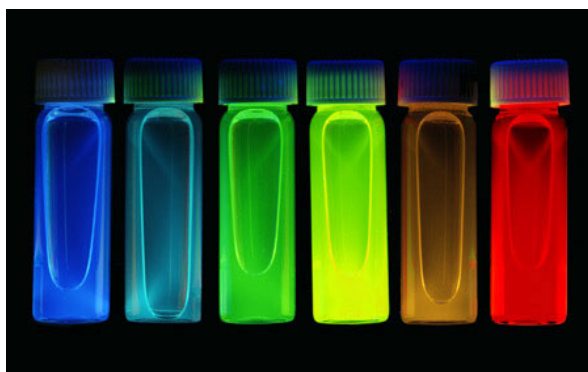
The structural perfection is based on evaluation of the symmetry and polydispersity. The dendritic molecules can be divided into low and high molecular weight species. The dendrimers are formed through a process of hierarchical self-assembly at the nanoscale. There are various types of these molecules: the smaller have size of

several nanometers, and are used in conventional applications such as coatings and inks, but can be exploited as molecular carriers for drug delivery or as a filter to trap metal ions for purify water, for example. [4]

### Quantum dots

Quantum dots are semiconductor nanoparticles; they have been theorized in the 70's, but were created only in the 80's.

If the particles of semiconductors are small, quantum effects come into play, because the surface is not more homogeneous but shows electrons or area of absence of charge. The energy of these particles depends on the wavelength of the quantum state that characterizes the surface and the color yields information on their size. Moreover, the quantum dots can be produced in order to absorb and emit the required wavelength, just modifying the size. In the following figure the different absorptions of quantum dots.



Recently, semiconductor particles have found applications in the field of composites, solar cells and as a tool for biological fluorescence analysis to trace the behavior and localization of biological molecules. In all these fields the quantum dots can be prepared to emit at certain energy levels. The latest developments have resulted in

the production of high quality particles, coated, monodisperse and crystalline that can reach dimensions smaller than 2 nm in diameter, which can be exploited as marker in the treatments of chemical reagents or processes. [4]

### 1.2.1 Properties, Characteristics and Applications

Nanoparticles have great scientific interest because they have behaviors that are halfway between those in macroscopic and the atomic or molecular scale. The mechanics regulating the interaction of nanoparticles with themselves are complicated. For instance, a suspension of nanoparticles is possible because the interaction of their surface with the solvent is strong enough to prevail on the density difference, which would push the nanoparticles to precipitate or float in the solvent.

The interaction between surface and solvent also depends on their polar or non-polar nature.

There are two meaningful examples; the first concerns nanoparticles coated with hydrophobic molecules. It is very easy to suspend this NP in a non-polar solvent as toluene, consequently it is impossible to resuspend them in polar solvent as water (figure 1.4). The second is about nanoparticles that have specific surface charge. They can be suspended only in solvent with compatible amounts of ions, in the reverse case the NP agglomerate and precipitate.

Nanoparticles also have properties in the visible because they are small enough to confine their electrons, that produce quantum effects.

Those are the main properties of nanoparticles; there are many other properties but they depend on the material and production process of NP.

Although it is impossible to determine what are the advantages and disadvan-

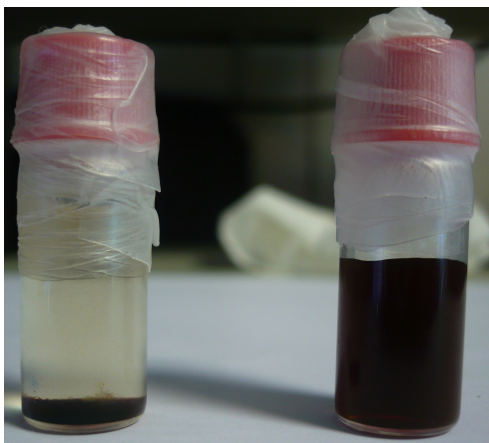


Figure 1.4: Iron oxide core of nanoparticles in water (left) and in toluene (right)

tages for each type of nanoparticle, it is interesting to analyze which are the common positive and negative characteristics. Among the positive properties there are tensile strength, hardness, stability in the size, conductivity and thermal expansion, chemical resistance and the ablation and the ability to strengthen. With regard to the negative aspects have to be reported the increase of suspension viscosity, the emission in the visible light, the great opacity and sedimentation.

The fields of study and research and applications of nanoparticles are several ranging from engineering to quantum physics of materials, from biology to computer science, from specific purpose in particular experiments to commercial use for everyday objects.

In-depth illustration of main research and industrial fields where NP are used would take a entire book probably, so that is just a table list of most recent applications: sunscreen and cosmetic, composites, buildings clay, optoelectronic, industrial glass coating and protection, painting, fuel cell, display, ceramics, sensing. [4]

### 1.2.2 Biomedical application

Probably the most interesting area for nanoparticles application and the field where their use and their research is more developed, especially in the last 10 years, is the field of biology and medicine.

At the base of living organisms are the cells, which have a characteristic dimension of about  $10\ \mu m$ . The structures that constitute cells are reaching a sub-micrometer size. The smallest structures are proteins which have size of about 5 nm, which is compatible with the size of a nanoparticle synthesized in the laboratory.

This simple dimensional comparison suggests to use nanoparticles as probes to analyze and mimic the mechanisms and interactions that occur within the cell without causing too much interference. Better understand how biological processes occur at the nanometer level is one of the primary goals of bio-nanotechnology. The properties of nanoparticles are several but those that have interest in biomedical practice are those that depend on the size, such as optical and magnetic effects.

More studied biomedical application and with the best results for future are:

- Fluorescence bio-marker [5][6]
- Controlled drug release and gene therapy [7][8]
- Photogenic bio-sensors [9][10]
- Genetic structure probe [11]
- Tissue engineering [12][2]
- Hyperthermia [13][19]
- Separation and purification of bio-molecules or cells [14]

- MRI contrast agents [15][16][17]
- Phagokinetic tracks [18]

As previously mentioned, nanoparticles and proteins have comparable size, this means that nanomaterials may be adapted for mark or label biomolecules.

Labeling different molecules or cells, you can exploit the different sizes of nanoparticles or bind NP on the structure surface that interact with them. These interactions modify the structure of the ligands that can be viewed with ultraviolet or fluorescence probes.

Ligands can be contained in the NP external layer (polymers, proteins, small molecules); this is a further properties for the external shell beyond make NP biocompatible. To exploit optical properties of nanoparticles, fluorescent molecules can be bind in the outer layer to change optical characteristics.

The approach used for the design and definition of a nano-biomaterial is represented in Figure 1.5.

Basically, in most cases the structure of nanoparticles is obtained with one or more layer. The NP core (or inner layer) gives to NP the main characteristics or properties (for iron oxide NP is super paramagnetic behavior). The outer layer can be exploited to form bonds with other molecules, inorganic or polymer for example. These structures can be represented as nanovesicle or layer surrounding the nanoparticle. The general forms are spherical and cylindrical, but many other shapes are possible.

The size and the size distribution especially are very important in some cases when the nanoparticles are designed to penetrate through the cell membrane, for example; an incompatible size of NP can cause a complete lack of penetration inside the cell. These two parameters are essential when size dependent quantum effects are used to

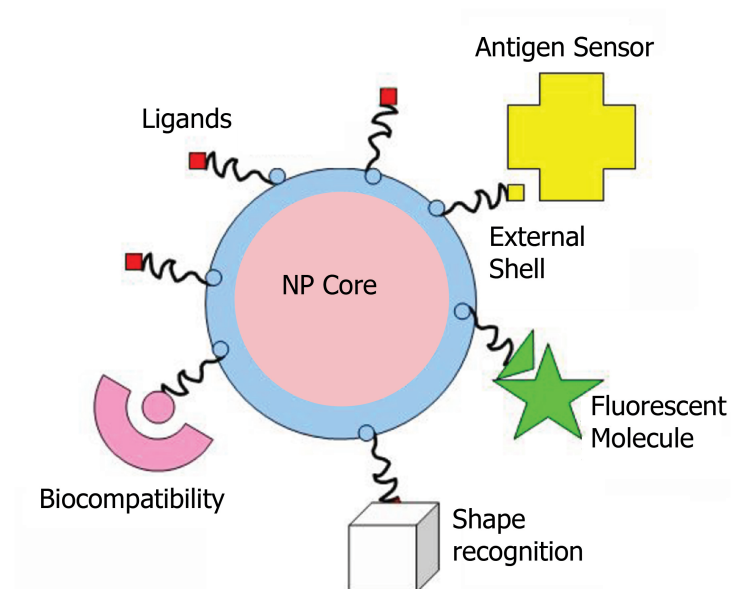


Figure 1.5: Configuration scheme used applied to medical or biological problems in biomaterials approach [20].

control some properties of the materials. An average size very precise and a narrow distribution are required to have very efficient fluorescence probe.

The outer layers may be multifunctional; combining magnetic and luminescent properties it is possible to detect and manipulate various types of particles. The core of these biostructures is often protected by several monolayers of inert materials, such as silicon. For this reason organic molecules are absorbed or chemio-absorbed on the surface of the nanoparticles, and the same layer can act as a biocompatible material. However, very often an extra layer of ligands is necessary to proceed with further functionalization.

The ligand is a molecule that has reactive groups on both ends. A group is specialized for binding with the nanoparticles, the other for binding to biocompatible molecules, such as dextran or poly-ethyleneglycol (PEG), antibodies, fluorophores

and other molecules which depend on the function required by the application. [20]

### **Diagnosis using nanoparticles**

One of main biomedical applications for nanoparticles is diagnosis to understand and analyze the symptoms of diseases. These tools are used for several activities such as to determine tissue type prior to organ transplantation, to determine blood type for patients requiring blood transfusions, and to monitor the progression of disease and the effects of therapy. It would be ideal the diagnosis of diseases before appearance of symptoms. Catching a disease early would allow the patient to take appropriate precautions to slow, halt or possibly reverse the progression of the ailment. It will be possible to use diagnostic tests and genetic screening at the same time to have the possibility of personalized therapy.

A general list of diagnosis application can be filled with:

- Screening for blood transfusions
- Monitor therapy activity
- Check disease progression
- Personalized medicine
- Genetic screening
- Diagnose disease susceptibility, risk assessment
- Infectious disease assessment
- Tissue typing for organ transplants

One of last ideas is to perform a combination of techniques or tests with the same nanotechnology tools or probe to perform accurate diagnosis. Current diagnostic techniques include immunoassay, genetic-based tests, cell-based assays, tissue or histological tests and medical imaging.

Until now the research fields with best results about use and application of nanotechnology and in particular nanoparticles are tissue engineering, drug discovery, drug delivery and diagnostics . Nanotechnology is enabling a variety of diagnostic methods, including optical, electrical, magnetic, electrochemical and mechanical Functionalized nanoparticles can enable multiplexed bioassays for simultaneous diagnostic screening of multiple diseases High-capacity screening and combined molecular and immunological diagnostics will play a role in establishing a broader range of testing capabilities. Finally, smart nanostructures such as nanotubes, dendrimers and nanoparticles are designed and fabricated with capability for diagnosis and therapy [3][21][22][23][24][21][25][26]

For each diagnosis technique a lot of nanotechnology structures can be used; main methods are described in following bullet point:

- *Optical*: enhanced fluorescence, quantum dots, surface plasmon resonance (SPR), **nanoparticles**, nanoshells and fiber optics;
- *Raman spectroscopy*: surface enhanced Raman spectroscopy (SERS), tip enhanced Raman spectroscopy (TERS) and **gold nanoparticles**;
- *Electrical*: potentiometric, amperometric, conductimetric, enzymatic and **nanoparticles for hyperthermia**;
- *Mechanical*: nanocantilevers, surface acoustic waves (SAWs) and quartz crystal balance;

- *Mass spectrometry*: **nanoparticles pre-concentrator**
- *Magnetic*: immunoassay, magnetofection and magnetoresistive
- *Imaging*: **contrast agents nanoparticles** and multifunctional agents
- *Genetics*: nanopore sequencing and **nanoparticles carriers**
- *Immunoassays*: **luminescent nanoparticles**

A lot of structure in biological system have nanoscale size. Viruses, proteins, small molecule drugs and fluorescent dyes are all less than 100 nm, as shown in fig. 1.1 Through the manipulation of organic and inorganic materials at the atomic level, novel materials, structures and devices can be realized enhancing thermal, optical, electrical and mechanical properties of materials. Properties of materials at the nanoscale can be quite different than bulk material properties. For example it is possible to modify surface properties of materials, such as adhesion. As explained, the great surface area per unit volume of nanomaterials exhibits higher chemical reactivity, increased mechanical strength, and faster electrical and magnetic responses.

Medical applications show particular promise, including building blocks of nucleic acids as structural components as binding agents similar to antibodies rather than typical genetic maps, nanostructured biosensors for implantable patient monitoring and nanoparticles as imaging contrast agents.

The three big categories of diagnostic are: assays, bio-sensors and imaging. The first purpose for nanotechnology is to improve the already existing test and, in the future, to create novel diagnostic methods. [27]

In vitro assays are used extensively for diagnostics. Assays are used for: enzyme-linked immunosorbent assays (ELISAs), polymerase chain reaction (PCR)-based genetic assays and staining assays such as Giemsa and Gram for viral and bacterial

diagnostics.

With a disease that needs diagnostic assay, patients sample would be shipped to laboratory and analyzed; nanotechnology aims to reduce this procedure in order to increase test sensitivity and to catch a disease earlier.

Research on biosensor aims to exploit the acknowledgment of assays and transfer it to design implantable devices for better and faster diagnosis. Nanostructures can be used to enhance these transduction mechanisms. For example, quantum dots can be used in optical biosensors. They are more photostable respect to traditional organic fluorophores, they ave greater quantum efficiency and have much narrower emission. The main advantages could be in use such as high sensitive optical biosensors and multiplexed assays. Functionalized magnetic nanoparticles can be targeted to desired analytes and detected with miniature magnetic sensors, creating portable diagnostics.

Medical imaging for diagnostics include X-ray imaging, computed tomography (CT) scans, magnetic resonance imaging (MRI), positron emission tomography (PET) scans, ultrasound and more recent optical techniques such as optical coherence tomography (OCT).

The advantage of imaging over assays and biosensors for diagnostics is the elimination of the need for a patient sample, such as blood or tissue. So, they are not invasive totally. However, most medical imaging equipment is expensive and requires trained personnel to operate and interpret results. Another disadvantage is the low resolution of most of these techniques that limits sensitivity. Nanoparticles as contrast agents can be used to increase sensitivity which may allow earlier diagnosis of diseases or keeping the same sensitivity it is possible to reduce size and cost of diagnostic instruments, tools and apparatus. [28]

### Nanotechnology properties to improve diagnosis

As described, there are a lot of possibilities, methods and characteristics of nanotechnological material to improve quality and effectiveness of diagnosis. In this part of this work the focus will be only on these properties showed by iron oxide nanoparticles that have been developed for this Ph.D reasearch.

All properties of three nanometric dimension structures are numerated in the following list. Typical nanoparticle properties are pointed out and deepened for their general applications.

- **Fluorescent**
- Quantum dots
- Surface Plasmon Resonance (SPR)
- Electrical
- **Magnetic**
- Mechanical

**Fluorescent:** tags with this characteristic, such as fluorescein isothiocyanate (FITC) and rhodamine, have been used extensively as optical markers for a variety of biological assays. Traditional fluorophores have a broad user base and are available in many forms such as voltage-sensitivity dyes, membrane-specific chemistries and pH-sensitive structures. However, traditional fluorophores have some typical disadvantages: broad emission spectra, short emission lifetimes and photobleaching. Nanotechnology can improve use of traditional fluorophores and develop novel markers to transform optical detection methods with greater sensitivity, multiplexed assays, single-molecule detection and in vivo diagnostics. Fluorescent tags can be improved

by conjugation with receptor molecules, with coatings for improved photostability, and by combining with metals for greater emission. For example, nanoparticle platforms consisting of surface-functionalized, silica-coated nanophosphors can be used for bioimaging applications. Silica coating enhances aqueous dispersion of nanoparticles, and allows surface functionalization of peptides and nucleic acids for specificity. Fluorescence emission can be tuned by controlling the size of the nanoparticle. A range of nanoparticle sizes can be used simultaneously for multiplexed assays due to each size of nanoparticle emitting a different color. [20][29][30]

Fluorescent is a great nanomaterials property, but not all materials have that property even if they are in nanometric form. As already said, nanoparticles have a great superficial reactivity so it is very easy to bind different molecules on their surface. One of this molecule could be a fluorescent dye; a non-fluorescent nanoparticle functionalized with a dye becomes a fluorescent probe to all intents and purposes. This is the case of iron oxide nanoparticles used in this work. Iron oxide core does not emit fluorescent signal and to obtain a fluorescent nanoparticles probe it has been used a specific dye: DiI (fig. 1.6). The protocol, application and result of this procedure will be described in following parts of this work.

**Magnetic:** several structures exploit their magnetic properties for specific purpose. One of the most studied is magnetic separation: functionalizing NP with ligands that can bind specific molecules, it is possible to use a magnet to separate these molecules from other molecules in solution. It is possible to use ferrite nanoparticles coated with gold or silica. Antibody-conjugated magnetic nanoparticles can be used to tag proteins for magnetic immunoassays. Another application is binding RNA or DNA for sensing: molecular beacons can be bound to magnetic nanoparticles to enable capture of single-base mismatched DNA and target mRNAs for intracellular gene expression analysis (Fig. 1.7)

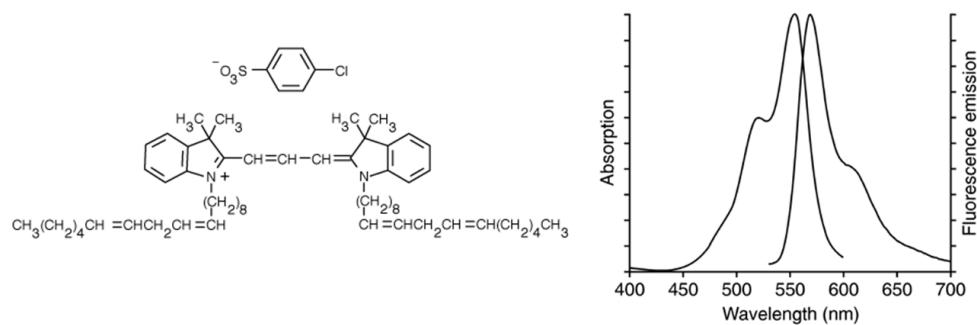


Figure 1.6: Structure (left) and absorption-emission spectra (right) of DiI fluorescent dye

Combining molecular beacons with magnetic nanoparticles, single-base mismatched DNA can be magnetically separated (Fig. 1.26)

Another application is exploiting of magnetic skill of nanoparticle to move them inside the cell; in addition to this, functionalized magnetic nanoparticles may also be internalized through magnetofection: the application of external magnetic to attract magnetic nanoparticles into the cell. [32][33][34]

Also sensing can use magnetic nanoparticles could also be used for benchtop and handheld diagnostics similar to chip-based electrical methods for biological analysis, in particular for tests regarding DNA. This instrument works in a similar way of atomic force microscope (AFM), but instead of electric interaction, this tool can map the magnetic signal of nanoparticles.

Medical imaging diagnostic techniques represent one of the most interesting research field about nanoparticles; they include MRI, PET, CT, OCT, optoacoustic or photoacoustic tomography (OAT or PAT) and NIR imaging. Nanoparticles containing hundreds of contrast agents can greatly enhance the sensitivity of these imaging methods. Examples of MRI contrast agents include gadolinium-diethylene-triamine-pentacetic acid (Gd-DTPA) and superparamagnetic iron oxide particles (SPIOs).

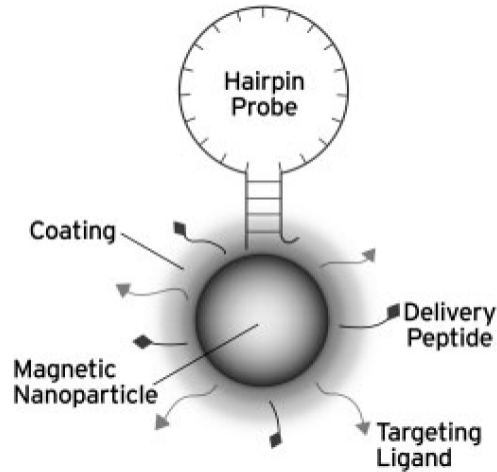


Figure 1.7: Magnetic nanoparticle tagged with molecular beacon oligonucleotide structure [1][31]

[36][37]

Ultrasound contrast agents are designed to affect the propagation of sound waves in the surrounding sample area by altering the acoustic properties. Liquid perfluorocarbon nanoparticles and liposomes are examples of ultrasound contrast agents.

The first advantage to use nanoparticles in the nanometric size, is that they can prolong the time before elimination by the body because big structures activate the inflammatory response earlier respect to nanostructure.

Noninvasive detection at the single-cell level may be possible with nanocarriers loaded with contrast agent and functionalized with biological receptors specific to the desired cell. Nanocarriers could include liposomes, dendrimers or porous polymeric nanoparticles. For example, magnetic nanoparticles acting as MRI contrast agents can be modified to target a specific cell type and can be simultaneously monitored optically due to addition of optical tags. One indirect advantage is instrument cost reduction because if more sensitive structures are used, it is possible to design appa-

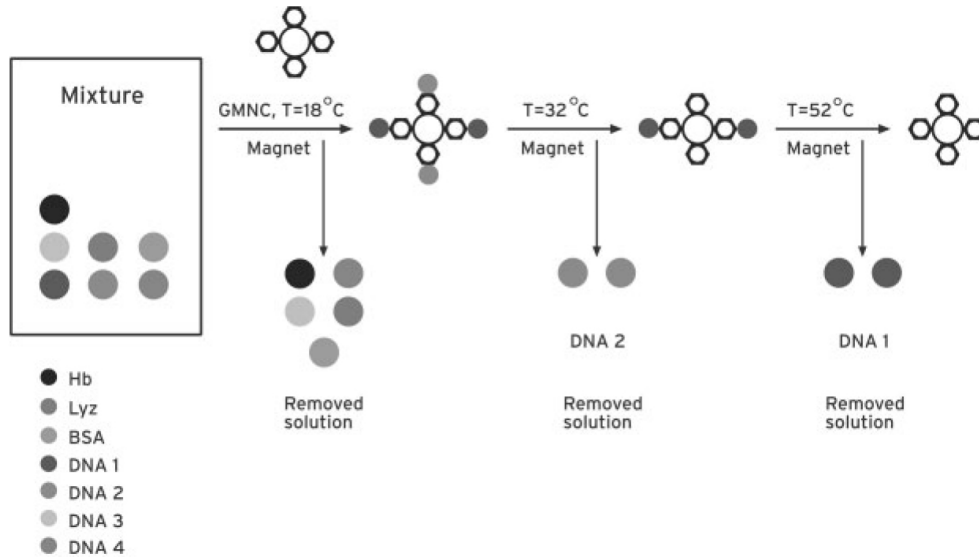


Figure 1.8: Genomagnetic capture separation [1][35]

ratus with detector and electronic not so advanced. Lasers and optical (for OCT and NIR) or acoustic (for OAT/PAT) detectors are relatively inexpensive in comparison to large magnets and X-ray machines.

Another advantage of using optics for imaging is the ability to guide the optical path with fiber optics, as in endoscopy, enabling internal imaging of vasculature, deep tissue and possibly the brain. Thermal vibrations produce acoustic waves which propagate from the underlying tissue to the skin surface. Acoustic detectors on the surface of the skin pick up the resulting acoustic waves.

One of the most promising nanoparticles type are those made by gold: they can be used as contrast agents for optoacoustic imaging. By controlling shape and structure, they can be designed to optimally absorb at a desired wavelength. AuNO can

produce luminescence from lower excitation intensities than typical bioimaging fluorophores; that is used with NIR. Gold nanoparticles are also higher photostable respect to organic fluorophores. Respect to quantum dots, they do not produce significant blinking, are easier to fabricate and can be readily modified for biological specificity and exhibit very low toxicity . All of these characteristics show promise for gold nanoparticles as an enabling technology to achieve single-molecule in vivo imaging for early diagnostics [38][39]

### **Future perspective**

As the present, the future of nanoparticles will be focused on the use of pharmaceuticals and drug delivery, although new applications appear on the horizon.

In biosciences, nanoparticles will replace increasingly most part of organic dyes which require better photostability and a high capability to multiplexing (combination of more signals into one). There are also concerns developments for direct and remote control of nanoprobe devices; for example the possibility to move the magnetic nanoparticles to the tumor and to make sure that they reach the goal: the release of the drug or locally heating to destroy diseased tissue (hyperthermia). The more interesting expectation is the development of multifunctional nanomaterials that are controlled by different types of signals: artificial and external or environmental and local. [3] [19] [20]

There are two particular fields to take into account for the distant future.

**Multifunctional Platforms** An area of future impact of nanotechnology for patient care is the development of in vivo modular, multifunctional platforms to target, detect and react Dendrimers, due to their highly branched structure, are potential multifunctional nanostructured platforms. Crosslinking to two or more different types of nanoparticles could also create a multifunctional platform.

Therapeutics could be harbored within the dendrimer core or coated onto the nontargeting nanoparticle enabling targeted drug delivery in conjunction with imaging for combination diagnosis and therapy.

**Real-time Monitoring** With this technique it is possible to remotely monitor patient in real-time. In vivo nanoscale sensors may also provide feedback, based on physiological status, as part of replacement biological systems, such as an artificial kidney or pancreas. Due to the ultraminiature form factor, identical sensors may be implanted for redundancy as a safeguard against sensor failure. If an array of these sensors is used for different targets, it is possible to monitor several parameters of patient condition simultaneously. [40][41]

#### **Effect on the health of nanostructures**

In the previous section, many advantages of nanostructures and in particular of nanoparticles have been described but these structures could represent negative effects on human and environmental health because they could be toxic for both.

Few years ago, a search of the negative impacts of plastic in the short and long term have been approved; in the same way in this year a similar research was started about compatibility nanostructure with people and environment.

The main fact that contributed to start this research is the size of the nanostructures, which is the same order of magnitude of cells and large proteins; thinking about the possibility that NPs are facilitated to evade natural defenses of the human or other species and damaging the cell, resulting cytotoxic.

These studies have to take into account that all living animals have to deal with nanoscale particles such as those resulting by chemical reactions of the atmosphere, by pollen, by forest fires or the millions of pollutant nanoparticles that can be felt during the use of a fire simply.

Then, there is a division of health impact of nanostructures in industrial and in biotechnology research. While in industry and in large distribution is taken into account in particular the impact of these materials on workers during the processing phase, in biotechnological research it is analyzed the cytotoxicity of each type of structure and concentration that can lead to effects negative test object.

The general approach of estimation and control of risk comes from identification of the hazard, which represents the potential of a substance to cause damage. Is also important the probability of exposure to this hazard and the associated consequences. The risk is usually controlled by decreasing the probability of exposure and limiting the release of the material in the air or water.

Rearging the manufacture of nanoparticles and nanotubes, the main determinants of their toxicity are: their total surface interacts with the organs, the great reactivity of the surface and the ability to liberate free radicals, their nanometric size that allows them to penetrate within the organs or cells and the ability to participate or initiate toxic reactions.

Two main ways in which the nanostructures come into contact with the organs and with the cells are inhalation and contact with the skin. The small size of the nanoparticles allows a large part to be able, by inhalation, to be deposited deep in the lungs. The size of the NP also affects their penetration into cells. In the lungs, there are localized specialized phagocytes, such as tissue macrophages or leukocytes, which are able to eliminate large particles. This mechanism has developed mainly in large animals and humans, to remove potential bacteria or unicellular organisms. But nanoparticles are able to penetrate directly to the cell membrane with the ability to interfere with important cellular functions, such as motility and the ability to remove bacteria. The size of nanoparticles is not the only reason of the possible toxicity, have great importance also the inhaled quantity and total of surface are. But while the

toxicity of nanoparticles depends strongly on the amount, the mutagenicity is not so directly. Stochastically even just a single nanoparticle can create a genetic mutation that can start tumor formation.

Regarding the inhalation of small amounts of nanoparticles, risks for health are minimal; instead when the amount becomes high, it is possible to note respiratory problems, which always depend on the type, size and reactivity of the nanoparticles. Only people at work risk to inhale so large amounts of nanomaterials, but they can protect themselves by knowing the type of nanoparticle, using appropriate, storing the NP in liquid suspension rather than powdered, monitoring with sensors the concentration of NP in air and using other attentions. [4][20]

## 1.3 Iron oxide Nanoparticles

### 1.3.1 Introduction

Superparamagnetic nanoparticles of iron oxides have become a major tool for medical imaging with a lot of applications. This is possible using one or more of properties that characterized them. There are a lot of kinds of iron oxide nanoparticles: from just discovered until something already undergoing clinical trials for cancer imaging applications.

They are also used as diagnostic tool for a vast number of diseases (from atheromatous plaques to degenerative diseases such as multiple sclerosis), hence it appeared of clinical interest to numerous researchers to investigate the relevance of nanoparticles in such indications.

It is possible to find applications also in the stem cell field which has attracted a lot of attention in both neurological and cardiologic research over recent years.

One of the most interesting research field is the production of contrast agents for magnetic resonance imaging (MRI). These are iron oxides magnetite ( $Fe_3O_4$ ), maghemite ( $\gamma Fe_2O_3$ ) or other ferrites that are insoluble in water. Unlike ferromagnetic substances and because of their size, superparamagnetic agents have no magnetic properties outside an external magnetic field [42][43]

Superparamagnetic agents are highly effective in MRI as they are strong enhancers of proton relaxation.

Superparamagnetic nanoparticles are small coated crystals of iron oxides (figure 1.9), characterized by a large magnetic moment in the presence of a static external magnetic field. This large magnetic moment is caused by a crystal ordering which induces a cooperativity between the individual paramagnetic ions constituting the crystal. Consequently, the magnetic moment of superparamagnetic particle is greater than the sum of each paramagnetic ions constituting the crystal.

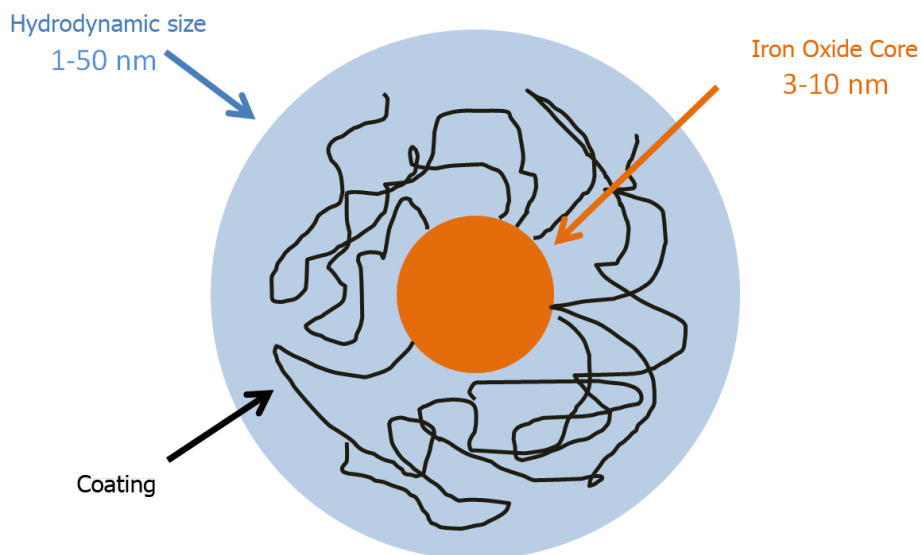


Figure 1.9: General structure of iron oxide nanoparticles.

These small superparamagnetic crystals are smaller than a magnetic domain (approximately 30 nm) and, consequently, they do not show any magnetic remanence unlike ferromagnetic materials. The interaction between surrounding protons of water molecules and the magnetic moment of superparamagnetic particles results in a decrease of relaxation time ( $t_1$  and  $t_2$ ).

The multiple components regulating the efficacy of these agents require them to be characterized as accurately as possible by information such as the size of the iron oxide crystals, the charge, the nature of the coating, the hydrodynamic size of the coated particle, etc. These physicochemical characteristics not only affect the efficacy of the superparamagnetic particles in MRI, but also their stability, biodistribution, opsonization and metabolism as well as their clearance from the vascular system. [44][43]

### 1.3.2 Properties and Characteristics

Magnetic nanoparticles have different types and different compositions: in most cases it is an oxide bonded to a metal. Some examples are:

$Al_2O_3$ ,  $Al(OH)_3$ ,  $B_2O_3$ ,  $Bi_2O_3$ ,  $CeO_2$ ,  $CoO$ ,  $Co_3O_4$ ,  $CrO_3$ ,  $Cr_2O_3$ ,  $CuO$ ,  $Dy_2O_3$ ,  $Er_2O_3$ ,  $Eu_2O_3$ ,  $FeO$ ,  $Fe_2O_3$ ,  $Fe_3O_4$ ,  $Gd_2O_3$ ,  $HfO_2$ ,  $In_2O_3$ ,  $La_2O_3$ ,  $MgO$ ,  $Mg(OH)_2$ ,  $Mn_2O_3$ ,  $Mn_3O_4$ ,  $MoO_3$ ,  $NiO$ ,  $Ni_2O_3$ ,  $PbO$ ,  $SiO_2$ ,  $SnO_2$ ,  $Ta_2O_5$ ,  $TiO_2$ ,  $ZnO$  e  $ZrO_2$

Some TEM images are showed in Figure 1.10.

The main applications of these magnetic nanoparticles are: biomaterials, catalysts, fluids for heat transfer, nanocomposites, the transparent conductive coatings and optical devices capacitors, semiconductor transistor, materials for optical fibers and lasers, additives for different types of material, dyes to glass and ceramics for the

sintering additives and many more. [45]

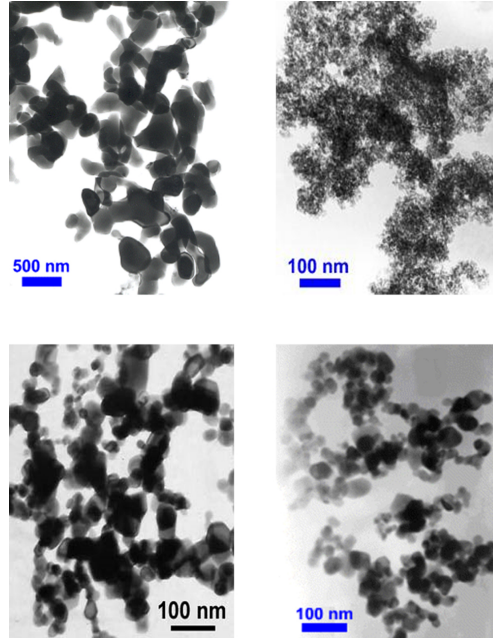


Figure 1.10: TEM images of different nanoparticles Top left:  $Al_2O_3$ ; top right:  $SiO_2$ ; bottom left:  $SnO_2$ ; bottom right:  $ZrO_2$ . [45]

### Iron Oxide

Particular significant are magnetic nanoparticles formed by iron oxide. Iron oxides are three: wustite  $FeO$ , hematite  $Fe_2O_3$  and magnetite  $Fe_3O_4$ , but only the last two are used for magnetic nanoparticles production.

The maghemite is an oxide of iron  $Fe^{3+}$ , its molecular weight is 159.69 and it is possible to find it in nature formed by weathering or oxidation at low temperature starting from magnetite; precisely its name derives from MAGnetite and HEMatite that shares the composition and the strong magnetism mineral, which is the physical properties that better characterizes it. The appearance and molecular structure are

shown in figure 1.11.

Instead, the magnetite is the most high iron content material (about 72.5%) and for this reason it is widely used in industries dealing with metals. With a large percentage of iron, it is one of minerals with the more intense magnetic properties existing in nature. It is a mixture of both oxidation of iron:  $Fe^{2+}$  and  $Fe^{3+}$ , its molecular weight is 231.54 and in nature it can be found in igneous and metamorphic rocks. Magnetite can be produced biologically by a wide variety of organisms. Appearance and molecular structure are shown in Figure 1.11.

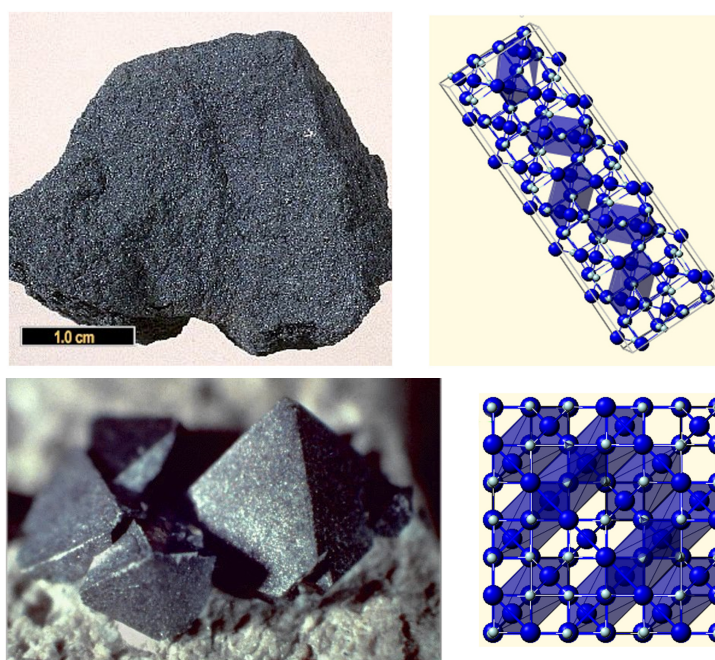


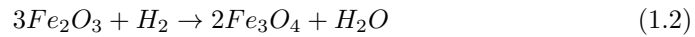
Figure 1.11: Geology and molecular structure of maghemite (top) and magnetite (bottom) [46][47]

The synthesis of iron oxide  $Fe_3O_4$ , also called synthetic magnetite, can be prepared using various processes. One of these is an oxidation of nitrobenzene with an ion of

iron derived from iron chloride  $FeCl_2$ :



Other two processes are the reduction of maghemite by hydrogen and carbon monoxide, respectively:



Although quite simple, the described processes show just the chemical principle used for synthesize IONP but until know there is not control for size and size distribution of desired nanoparticles. This is only the starting point of their production.

Iron oxides find application in several fields: in the production of ceramics and glass, also as colorants, in the preparation of cosmetic, to color and increase the strength of steel and many others. The maghemite nanoparticles are used in the following fields: anti-corrosion agents, catalysts, gas sensors, nonlinear optics, pigments, semiconductors, and biomedicine. Instead, the applications of the nanoparticles di magnetite are found in: color imaging, detoxification of biological fluids, absorption of electromagnetic waves, ferrofluids, magnetic separation of cells, magnetic coatings, magnetic detectors, coolers, magnetic contrast agents in MRI, magneto-optical devices, semiconductors, toner for printers and biomedicine [46][47][48][49].

### **Ferrofluid**

A particular application of iron oxide nanoparticles is as ferrofluid. A ferrofluid is a liquid which becomes strongly magnetized in presence of a magnetic field.

Ferrofluids are colloidal liquids made of nanoscale ferromagnetic, or ferrimagnetic, particles suspended in a carrier fluid (usually an organic solvent or water). Each tiny particle is thoroughly coated with a surfactant to inhibit clumping. Large ferromagnetic particles can be ripped out of the homogeneous colloidal mixture, forming a separate clump of magnetic dust when exposed to strong magnetic fields. The magnetic attraction of nanoparticles is weak enough so that the surfactant's Van der Waals force is sufficient to prevent magnetic clumping or agglomeration. Ferrofluids usually do not retain magnetization in the absence of an externally applied field and thus are often classified as "superparamagnets" rather than ferromagnets.

The main application of ferrofluids is the reduction of friction. If applied to the surface of a very powerful magnet, it can glide on smooth surfaces with minimal resistance [50]

### **Production and synthesis**

One of the main problems of synthesis of superparamagnetic nanoparticles is the colloidal nature of magnetic nanoparticles. Consequently, a full set of analytical methods should be used in order to characterize the efficacy (in terms of magnetization and relaxivity) and purity of nanoparticles and the reproducibility of the synthesis process. Moreover, the physicochemical and biological behavior of the particles, can be affected by the size, the geometry, the composition of the crystals, the charge of the particles and the nature of the coating. An accurate description of the physicochemical properties of these nanoparticles is crucial. The size of the crystals varies from agent to agent, but also depends on the measurement technique. The core size is generally between 4 and 10 nm. The size of the crystals can be appreciated by transmission electronic microscopy (TEM). Moreover, the sample preparation can induce aggregation of the colloids and the TEM measurements may consequently not reflect

the crystal size in solution. [43][51][52]

The hydrodynamic size of nanoparticles includes the global size of the particle: several magnetic crystal surrounded by the coating molecules and the coordinated water molecules on the surface of coating. It is measured by photon correlation spectroscopy (PCS) and dynamic light scattering (DLS). In both techniques the intensity of the diffused light is modulated by the Brownian motion of the particles in solution. The correlation between time and scattering intensity gives information on particle size in solution. Different mathematical models and weighting parameters are used, unimodal or multimodal distribution, distribution in number, volume or intensity, display result giving right size distribution of nanoparticles. The result takes into account the hydrodynamic radius of structure that greatly depends on the type of coatings; so it is very difficult to compare different types of MNPs. [53][54][55]

There are two main categories of superparamagnetic agents

- superparamagnetic iron oxides (SPIOs), larger than 50 nm in size;
- ultrasmall superparamagnetic iron oxides (USPIOs), smaller than 50 nm in size.

This difference has significant effects in the ratio of relaxivity constants  $r_1$  and  $r_2$  but also in plasma half-life and biodistribution.

Other fundamental characteristics of these agents are the nature and charge of the particle coating. The charge on the surface of the nanoparticles is usually appreciated by the  $\zeta$ -potential measurement deduced from the measurement of electrophoretic mobility. Unfortunately, the value of  $\zeta$ -potential of superparamagnetic nanoparticles is rarely described in literature.

So it is possible to affirm that the relationship between the structure, the composition and the charge of nanoparticles and their potential in terms of efficacy, biodistribution and safety, is not yet well understood and greatly depends on the types of

metal core and coating used to produce nanoparticles.

So, the synthesis is one of the most important parameters to produce nanoparticles with precise properties to exploit for applications. For this reason methods for the synthesis of nanoparticles are manifold, some simpler and some more complex. Each method will get different results regarding morphology, size, and magnetization. For all of them it is possible to define these advantages and disadvantages. [3][43]

1. **Pyrolysis/aerosols:** this technique allows to produce spherical nanoparticles with a size range between 5 and 60 nm with a very wide distribution, a magnetization value between 10 and 50 *emu/g* with good magnetic properties. The advantage of this method is the great production of nanoparticles that can be summarized in a single experiment; in the negative the produced nanoparticles make aggregate too easily. The physical principle of this technique is laser pyrolysis. Using a laser, specific material is heated and the nanoparticles are produced from it.
2. **Gas deposition:** this technique allows to produce spherical nanoparticles with a range of size between 5 and 50 nm with a narrow distribution; a magnetization value greater than 20 *emu/g*. It is a very beneficial method for the deposition of protective coating or for the production of thin films. The main disadvantage is that it requires high temperatures for the gas production. The method is based on an instrument consisting of several chambers; inside these chambers a gas containing the constituents of the nanoparticles is made to deposit on specific structures for the production of nanoparticles.
3. **Bulk solution:** this technique allows to produce spherical nanoparticles aggregates, ranging in size between 10 and 50 nm with a very wide distribution, a magnetization value between 20 and 50 *emu/g*, expressing a superparamagnetic

behavior. It represents a very advantageous method because for each synthesis a large amount of nanoparticles is produced. One disadvantage is the uncontrolled oxidation that may happen to nanoparticles and the appearance of a diamagnetic contribution of the same. The bulk solution refers just to that part of the solution where the molecules contained are influenced by other similar molecules and not from other solid or gaseous molecules. It is a sort of self assembly.

4. **Sol-gel:** this technique allows to produce spherical nanoparticles, with high porosity, ranging in size between 20 and 200 nm with a very wide distribution, a magnetization value between 10 and 40 *emu/g*, expressing behaviors paramagnetic. There are two advantages: the easy selection of the size and the ability to mix different components for the production of a type of nanoparticles. The disadvantage is that production of sol-gel matrix can remain bound to the surface of the nanoparticles. The production of nanoparticles is derived indirectly by the sol-gel method. What has been described as sol-gel is a colloidal suspension able to solidify forming a gel. Nanoparticles that are synthesized inside the obtained porous product.
5. **Microemulsion:** this technique allows to produce nanoparticles cubic or spherical, with the absence of aggregates, with a range of size between 4 and 20 nm with a very narrow distribution; a magnetization value greater than 30 *emu/g*, expressing superparamagnetic behavior. There are two advantages: the great uniformity of the properties between the produced nanoparticles and easy modulation of the size of the same. But there are also two disadvantages: surfactants are difficult to remove and only a small amount of nanoparticles can be produced at the same time.

[56][57][58][59][60][61][62]

### 1.3.3 Specific properties for biomedical applications

Biomedical applications have attracted the most interest in the nanoparticles: contrast agents for MRI, drug delivery and hyperthermia. Minor application, you can consider half way between the drug delivery and magnetic properties, it is handling by external magnetic field.

#### **MRI contrast agents**

The iron oxide and  $Fe_3O_4$ , containing 3 ions of iron, is one of the natural molecules more paramagnetic. This kind of molecule is able to decrease the relaxation times of the magnetization vector of the tissues containing them, so as to be mapped on the image of the diagnostic resonance. So, if nanoparticles can bind with tumor cells, the tumor region will be more visible than other anatomical zones helping the characterization and facilitating therapeutic practice such as export surgical or radiation therapy.

#### **Drug delivery**

The drug delivery is a process of administration of pharmaceutical components that has the purpose of producing therapeutic effects in humans or in animals. In these specific cases, the administered drugs are conveyed together with other molecules which have multiple purposes. The main tasks of these molecules are: location of the tissue or areas that require a cure and to facilitate the absorption of the drug by these areas.

The role of nanoparticles in drug delivery is secondary. Nanoparticles do not have

a direct healing power of cancer or any other disease, but there are advantages deriving from two important properties: the large surface reactivity and the nanometric size.

The large **surface reactivity** of nanoparticles yields the possibility to form bonds with different types of molecules, as shown in Figure 1.5. The main molecules are: specialized drug for the treatment of that type of cancer, various biocompatible coatings, different types of ligand, antibodies and other structures.[43]

Various biocompatible coatings play several roles, from simple to more complicated. For example, it is necessary to coat the nanoparticle of iron oxide with a polymer layer, which may be dextran or poly-ethyleneglycol (PEG), for the simple reason that the nanoparticle, already coated with oleic acid, is not soluble in pure water, but only in non-polar solvents (for example toluene).

Nanoparticles coated with polymer (PEG, for example) are soluble in water and then the suspension coated nanoparticles is more biocompatible than uncoated. There are more complicated roles for coating molecules: they have to contribute to a total compatibility and to a specific activation, for example they have to be pH,  $pCO_2$  or  $pO_2$  sensitive. They also are resistant to chemical reactions that take place at the contact with the specific tissues for which they were produced. Then for each type of application exist a lot of combination between core materials, coatings, activators and drugs.

Even the ligands, which are bound to external coat, have clear tasks. The main purpose is communication between the drug delivery carrier and tissue cells. Proper communication between these two structures can lead to three benefits that are of great importance to the basic theory of drug delivery mediated by nanoparticles. [20]

1. The regulation of immune response: communicating with the immune cells, ligands must make sure that this is not completely suppressed. This could

bring local benefits to developing tumor invalidating the work of the drug, a drug that has been developed taking into account a normal immune response to the region affected tissue. The other possibility is that the enhanced immune response is going to attack the nanoparticles, limiting the strength and action range.

2. Direct communication with the cell membrane: this type of communication can modify membrane permeability. This can happen for blood vessel endothelial so nanoparticles are able to leave the bloodstream and penetrate into tissues and in the case of the cell membrane of cancer too. So drug, just released from the MNPs, can enter easier cells into the cytoplasm.
3. Tumore targeting: making oncology analysis on the tumor it is possible to determine which proteins exposes the tumor cell on its surface. So once produced a type of nanoparticle that has this specific ligand entrapped in the polymer coatings, it will accumulate only close to tumor, limiting the dose to healthy cells and reducing the quantity of a drug required for tumor therapy.

Independently for which tumor tissue the particle is designed, the nanoparticle solution will be injected intravenously to the patient; then the first interaction of the nanoparticles and their coatings will be with the blood, in second place with the immune system. Thanks to the polymer coatings, it is possible to increase the stability of the structure, the half-lives of nanocarriers within the bloodstream and the duration of entrapment of the drug.

As the reactivity to surface, but also the **size** of the nanoparticles have a considerable importance with regard to drug delivery and in the same way also for the magnetic resonance imaging and hyperthermia, because the effectiveness of these two practices, a diagnostic and a therapeutic, depend heavily on the amount of magnetic

material content, hence on the size. [20]

Opsonization, which is the mechanism of coating of the external structure by the body, and the size determine the fate of the NP after the intravenous injection. This depends on the two organs filter our body: the venous sinuses of the spleen tend to eliminate particles larger than 200 nm and the liver removes large particles from the bloodstream. Therefore, since the half-life of life of MNPs decreases with increasing their size, the choice of the size of the NP depends on several parameters. In a healthy tissue the size of the pores of the endothelial tissue is about 10 nm, while in tumor tissue ranging from 200 nm to 1200 nm, depending on the type of tumor. Also in healthy tissue: particles much larger than 10 nm are eliminated by phagocytosis, particles slightly larger than 10 nm are eliminated by pinocytosis, a process similar to phagocytosis.

A structuring increasingly complex of the coatings can lead to a problem: the longevity and the ability of the mimetic MNPs compared to the immune system are in contrast with the presence on the surface of functionalities that allows targeted action. This can be translated as increasing number of coating layers it is possible to decrease the specificity of the nanoparticles, such as their ability to perform tasks.

The first of the two possible solutions is based on the EPR effect (Enhanced Permeation and Retention effect): this effect is caused by cancer cells that alter the porosity of the close capillaries, destroying their filtering mechanisms. Therefore, taking account of this, we can limit the number of selected ligands to facilitate nanoparticles to leave blood stream and penetrate tumor tissues. [3]

The second solution is based on the use of viruses: genetically modified virus are exploited to avoid the immune response. Although this implies the risk of unexpected behavior of the viruses that could not avoid the immune response, but make it even stronger.

A further possible solution consists in the synthesis of biological membranes that contain nanoparticles that may be free or bound to these structures. Some examples of these cages are biological: the liposomes, the lipid-based nanocapsules, the cages protein, the polymeric micelles and the cages of hydrogel.

Taking into account that liposomes are drug delivery carrier more used in clinical practice in last years, is interesting to compare them with polymer coatings. It easy to note three advantages of coatings polymer:

1. better control of the properties of the coating determine the longevity in vivo and thickness, then the volume necessary to trap the drug;
2. a selection of the polymer formulations compatible with the chemistry of drug molecules to facilitate the entrapment;
3. the design with specific properties sensitive to the pH or temperature, for the localized release of drugs.

However, they also have negative aspects: they induce easily the inflammatory response and accumulation of proteins on their surface.

Then, as happens in many similar cases, there is not a compartmentation of always suitable nanoparticles, but it depends on specific cases.

### **Hyperthermia**

Hyperthermia is a kind of therapy performed by heat. The care of patients with hyperthermia is based on two facts: the first goes back nearly 50 years ago when some studies have shown that tumor cells grown in the laboratory survive less than normal cells, when the temperature increases. Switching from regular 37C to 42-43C, there is a significant die-off of cancer cells. The second is that drugs and radiation, which are

the bases of chemotherapy and radiotherapy, have demonstrated their effectiveness issues from biochemical reactions inside the cell. These chemical reactions, such as all chemical reactions, are influenced by heat.

In physiological or pathological condition if the temperature of a cell is increased from 37C to 42C the action of these substances or these physical agents, such as radiation, is facilitated. Thus there is the first effect of hyperthermia which is an indirect effect of destruction of tumor cells; the second effect facilitates the action of drugs and radiation and the third effect is the simulation of immunity of the subject. So hyperthermia can have a significant role in cancer therapy, given also the fact that collateral effects are limited and low intensity.

The effect of hyperthermia can be locally obtained with magnetic fluids. These fluids, used in biomedical applications, are colloids containing magnetic nanoparticles to single domain dispersed in an organic matrix. Magnetic nanoparticles, with a size less than 50 nm (critical diameter), adopt a configuration with a single domain and superparamagnetic behavior. In addition, since they do not aggregate, it is possible to consider them as a system that do not interact.

In medicine, the magnetic hyperthermia uses the magnetic fluids to heat the tumor tissue in an uniform, targeted and effective manner applying an external magnetic field with a frequency between 100 and 500 kHz and amplitude of the order of  $kA/m$ .

The heating of the particles is primarily by the effect of relaxation processes: Brown and Neel. The relaxation of Brown is linked to the rotation of the particle in the fluid in which it is immersed and, in this case, the heat is produced by friction. While, in the relaxation of Neel there is a rotation of the magnetic moment and then the production of eddy currents that heat the tissue. The effectiveness of treatment is evaluated in terms of heat transmitted to the tumor tissue.

*In vitro*, the transmitted energy is related to the size and concentration of nanopar-

ticles and to the characteristics of applied magnetic field (frequency and amplitude). *In vivo* should be taken into account the effect of heat dissipation due to blood perfusion which can reduce the effective heating. [3] [19]



## Chapter 2

# The Nanosmart Project

Taking into account the large amount of information about technology and nanotechnology described in the first chapter of this thesis, University of Trento in collaboration with many international research centers has developed the Nanosmart project. The goals of this project are the study, preparation and experimental verification of iron oxide nanoparticles carriers for tumor diagnosis and therapy. They have been designed for diagnosis as contrast agents for magnetic resonance imaging and for therapy as drug delivery and hyperthermia carriers.

The scheme illustrated in Figure 2.1 describes the iron oxide nanoparticle pathway from injection to drug release inside the tumoral cells.

This was and continues to be a huge and innovative project. It has been written five years ago by six research center all over the world: Biotech - University of Trento, CNR-IBF (Trento), GeorgiaTech (Atlanta, USA), CNRS-U.M. (Montpellier, France), FBK-IRST (Trento), CNR-IFN (Trento) and Ludwig Boltzamm Institute for Cancer (Wien, Austria).

The project started 4 years ago and to be able to design a innovative carrier and

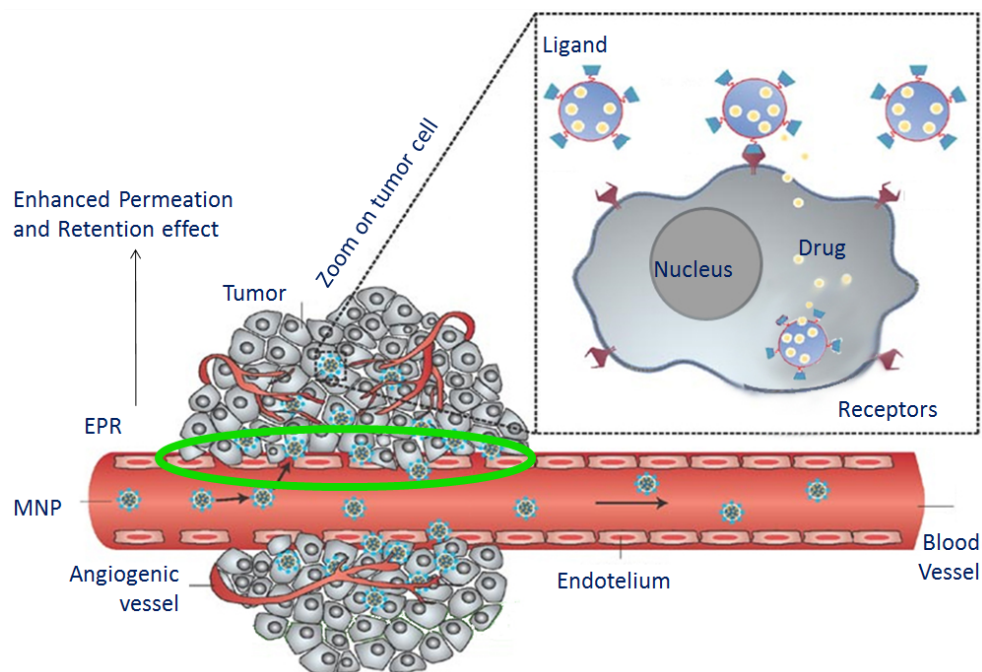


Figure 2.1: Scheme of pathway of MNPs after injection in blood stream [63]

eventually new commercial products it was very important to update our knowledge about nanotechnology, considering the information available in literature and the news for commercial nanoparticle products.

## 2.1 State-of-art of commercial nanoparticles

It is easy to get lost inside the literature about magnetic nanoparticles; there are many papers, books and works about this topic. The first works are more than 30 years old and at the same time a lot of new structure are discovered everyday. To obtain a good report about this research field it is useful to focus on nanoparticles ready to be investigated in clinical trials.

As time goes by some parts of this project are still underdeveloped and others were abandoned for many reason but this is not important because the idea was not to copy the structure but only to cross useful information about size, coating, drug entrapment and ligands to transfer to our iron oxide nanoparticles. [64]

The most interesting iron oxide nanoparticles are:

- **Feridex**, also called Ferumoxide and Endorem, is a sterile aqueous colloid of superparamagnetic iron oxide associated with dextran for intravenous administration as a MRI contrast medium for the detection of liver lesions that are associated with an alteration in the RES. Feridex is taken up by macrophages, found only in healthy liver cells but not in most tumors. Tissues such as metastases, primary liver cancer, cysts and various benign tumors, adenomas and hyperplasia retain their native signal intensity, so the contrast between normal and abnormal tissue is increased. Feridex is a black to reddish-brown aqueous colloid. In November 2008, AMAG Pharmaceuticals, Inc. decided to discontinue the manufacturing of Feridex.
- **Sinerem**, also Combidex is an ultrasmall superparamagnetic iron oxide (USPIO) to detect metastatic disease in lymph nodes. Metastatic nodes show less uptake of this MRI contrast agent, which results in less signal decrease and allows the differentiation of normal lymph nodes from normal-sized, metastatic nodes. Lymph node imaging with Sinerem is performed 24 to 36 hours after slow infusion. Normal lymph nodes turn black post contrast, namely on T2\* weighted images. Metastatic lymph nodes remain unchanged in signal intensity. Indication and Diseases: Cancer, Imaging for diagnosis, Lymphatic disorders. Guerbet decided in 2007 to withdraw its Marketing Authorisation Application (MAA) for Sinerem.

- **Lumirem** belongs to the negative oral contrast agents (same as GastroMARK). It used to distinguish the loops of the bowel from other abdominal structures and physiology. When Lumirem is ingested, it flows through and darkens the stomach and the small intestine in 30 to 45 minutes. By more clearly identifying the intestinal loops, Lumirem improves visualization of adjacent abdominal tissues such as the pancreas. Additionally, in Europe Lumirem is approved for rectal administration to delineate the lower intestinal system.
- **Resovist** is an organ-specific MRI contrast agent, used for the detection and characterization of especially small focal liver lesions. Resovist consists of superparamagnetic iron oxide (SPIO) nanoparticles coated with carboxydextran, which are accumulated by phagocytosis in cells of the reticuloendothelial system (RES) of the liver. The uptake of Resovist Injection in the reticuloendothelial cells results in a decrease of the signal intensity of normal liver parenchyma on both T2- and T1 weighted images. Most malignant liver tumors do not contain RES cells and therefore do not uptake the iron particles. The resulting imaging effect is an improved contrast between the tumor (bright) and the surrounding tissue (dark). Resovist can be injected as an intravenous bolus, which allows immediate imaging of the liver and reduces the overall examination time. A dynamic imaging strategy after bolus injection supports to characterize lesions. In comprehensive clinical trials, it demonstrated an excellent safety profile. In 2001, Resovist was approved for the European market. Resovist competed with Primovist, the other liver imaging agent of Bayer Schering Pharma AG. Due to this reason, the production of Resovist has been abandoned in 2009.
- **Clariscan** is an iron-based contrast agent with large molecular size, which prevents diffusion into body tissues and will be developed for MR imaging of

the liver (taken up by macrophages), tumor microvasculature and microvessel permeability. The blood half live of the particles with 11-20 nm diameter is 3-4 hours. At this time the development of Clariscan is discontinued.

- **Abdoscan** is a superparamagnetic oral contrast agent consists of large iron oxide particles, coated with insoluble material. Abdoscan particles have a mean diameter no less than 300 nm. Gastrointestinal superparamagnetic contrast agents are used for negative bowel enhancement. Abdoscan was approved in Europe but was taken off the market in 2000, and all sales stopped by the end of 2002.
- **VSOP-C184** means very small superparamagnetic iron oxide particles. This new class of contrast agents with smaller particle size than SPIO offers advantages for MR angiography. SPIO particles are usually coated with an organic polymer such as dextran, carboxydextran or polyethylene glycol, which limits the minimal overall particle size that can be obtained. VSOP-C184 consists of an aqueous solution of superparamagnetic iron oxide particles with a citrate coating and the overall particle size of 4-8 nm.

### 2.1.1 Interaction lived tissue and application

After the injection the first interaction of nanoparticles is with blood stream. In particular iron oxide nanoparticles are internalized into macrophages (Fig. 2.2) and other phagocytic cells. Every interaction of NP depends on a lot of variables: one of the most important is size. Size can strongly interfere with their capacity to be internalized into macrophages or other phagocytic cells following intravenous administration. Studies on different types of NP (sinerem) show different properties. NPs that have a hydrodynamic diameter very similar to iron oxide MNPs used in this work (15-30 nm)

show a long blood residence time, which allows them to easily access macrophages located in deep and pathologic tissues (such as lymph nodes, kidney, brain, osteoarticular tissues, etc.). This is very positive because it is difficult to access these organs respect to other organs.

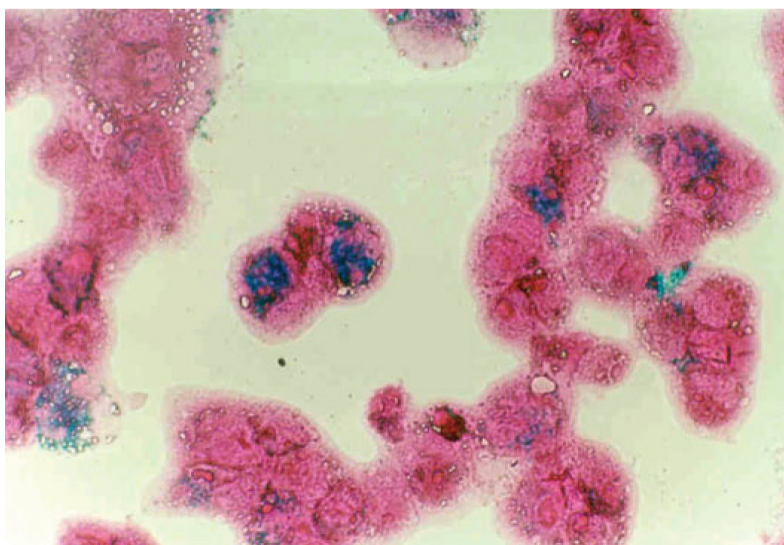


Figure 2.2: Intracellular localization of MNPs following a 24-h incubation with human monocytes. Iron staining with Prussian blue and counterstaining with eosin [65]

Iron oxide nanoparticles with a very small size such as resovist have a higher macrophage uptake; the effect of this is a faster blood clearance and, consequently, a more limited access time to the deep compartments. For example, the elimination half-life of VSOP-C184 in healthy volunteers is only 0.5-1.5 h after bolus injection. Conversely, pegylated Clariscan 1 because of the pegylation of the coating starch, can be regarded as "stealth nanoparticles" which are hardly recognized by the macrophage and probably not suitable for macrophage imaging, but they show a long blood residence time.

Not only the size is important for tissue interaction, but also the superficial

chemistry. It has recently been shown that superparamagnetic nanoparticles with an amino-functionalized PVA coating can interact with human melanoma cells without any cytotoxicity. This interaction of the nanoparticles with melanoma cells was found to be active, energy-dependent and saturable [66]. The increase of uptake in the presence of amino groups is consistent with the well-known uptake of cationic liposomes, mainly for transfection purposes.

A recent study compared anionic nanoparticles coated with hydrodynamic diameter 24 nm with ferumoxtran-10. In vitro ferumoxtran-10 enter easier the human prostatic adenocarcinoma cells than with ferumoxtran-10. According to their negative charged and hydrophilic coating, nanoparticles show different degrees of uptake by macrophage-like cells. The macrophage is a specialized host defense cell with endocytic properties. They are involved in a lot of diseases; for this reasons they are one of the most used pharmaceutical target. Apart from particle size, the phagocytic uptake is dependent on the surface properties of the nanoparticles; ionic carboxy-dextran coating NP enter easier the phagocyte easier than nonionic dextran coating NP .

Other studies show that the value of charge of coating gives to NP specific properties: the negative charged coating is more biocompatible, instead the positive one has a better interaction with cell membrane.[67]

### 2.1.2 Pharmacokinetics

To better design NP it is very important to understand the typical velocity of process that characterizes NP *in vivo*. Knowing this parameters is useful to prepare nanoparticles with specific amount of drug and particular drug release speed.

For example, Ferumoxtran-10 is completely degraded in the macrophage lysoso-

mal compartment within 7 days, and plasma elimination half-life is strongly species dependent: 2 hours in rats, 6 h in rabbits and 24-36 hours in human after intravenous injection. In both rats and rabbits, increasing the dose it is possible to have longer half-life because there is a saturation of uptake by liver and spleen.

Taking into account that the diffusion of NP in tissue strongly depends on blood residence time, animal imaging experiments are generally performed using high doses of nanoparticles of 200-1000  $\text{mmolkg}^{-1}$ , while for human experiments the used dose is about 45  $\text{mmolkg}^{-1}$ .

An unexpected parameter to characterize the uptake process is the patient age. In case of rats, after a injection of VSOP-C43, younger animals show a blood resistance value less than 50% respect to old animals. This fact suggests a higher macrophage uptake in younger animals.

The iron derived from the uptake of iron oxide nanoparticles is bioavailable and is incorporated into the normal body iron pools, such as hemoglobin. This is also showed by the increment of ferritin levels inside the body. Ferritin is a ubiquitous intracellular protein that stores iron and releases it in a controlled fashion. An example is dextran-coated iron oxide nanoparticles which are degraded by Kupffer cells (specialized macrophages located in the liver) to incorporate most of the iron they contain into ferritin and/or hemosiderin (when the intracellular concentration of ferritin becomes relatively high) before exocytosis. [68][69][70]

A use of Ferumoxtran-10 would be the detection of nodal metastases. After intravenous infusion, USPIO nanoparticles are distributed to the lymph nodes by two distinct pathways:

- direct transcapillary passage through venules into the medullary sinuses of the lymph node, followed by phagocytosis by macrophages

- non selective endothelial transcytosis into the interstitial space in the body, followed by uptake of the nanoparticles by draining lymphatic vessels and transport to the lymph nodes via afferent lymphatic channels

There are several methods to administrate iron oxide nanoparticles: slow intravenous infusion (Endorem 1 /Feridex 1), injected as a bolus (Resovist 1) and subcutaneous injections (ferumoxtran-10) Each of these possibilities has advantages and disadvantages depending on the NP type and on application. [71][72][73]

## 2.2 Nanosmart Project

Nanoparticles used for Nanosmart Project are designed, set up and produced according to the information described in the previous section of this chapter.

The ultimate structure includes:

- **NP core:** it is magnetite maghemite mixture produced by a thermo-decomposition of iron complex in a mixture of oleic acid and oleylamine. Both of them are strongly bound with the core and will be always present in final composition of nanoparticle.
- **NP coating:** it is made using amphiphilic molecules; it is a phospholipid attached to a polymer chain (PEG). This molecules can interact with oleic acid and oleylamine and form a hydrophilic external shell with polyethylene glycol.
- **NP functionalization:**
  - Labeling: iron oxide nanoparticles are magnetic properties but do not have fluorescent characteristics. DiI fluorescent dye is used to become fluorescent the NP. This dye is hydrophobic and can be entrapped inside the

hydrophobic double layer formed by oleic acid and the fatty acid of phospholipids with PEG.

- Targeting: a epidermal growth factor receptor (EGFr) antibody is attached on the external shell of NP. This antibody can interact with the EGFr of tumoral cells to increase uptake of nanoparticles.

- **NP drug loading:** the main application of this NP is drug delivery. Doxorubicin is the choose drug to delivered togheter with nanoparticles. It is very famous cancer chemotherapy. This drug has a particular behavior in solution: indeed, it is pH sensitive. At low values of pH (4-6) it is hydrophilic, at high values (7-8) hydrophobic. It is possible to exploit this characteristic as release mechanism. The drug enters the hydrophobic layer of NPs when they are suspended in basic solution and it can exit in acid solution, for example inside the lysosome (pH is about 4)

In the following chapter ideas, methods and protocols to obtain this type of nanoparticles will be described.

## Part II

# Experimental Part: Production



f



## Chapter 3

# Introduction

Main protocols, tests and results to verify the ideas and to keep the promise described in the previous chapter will be shown in this part. As often happens, ideas are very simple and clear, but their application is not so easy. The better fulfillment is a long pathway between failures, renounces and modification, but all problems could represent a new starting point for better discoveries and applications.

For that reason, the experimental approach for this work followed the philosophy of “step by step” and “trial and errors”.

The entire work was dived in different four tasks; the most relevant are: production of MNP, their functionalization, *in vitro* and *in vivo* tests. Easy to understand that it is impossible to deal oddly with these parts: functionalization depends on used production methods, results of *in vitro* tests depend on nanoparticle functionalization and so on.

For each of the four mentioned steps purposes, materials, protocols and results will be illustrated in the next chapters.

At the beginning, the most difficult decision was the choice of the material for

nanoparticles production. During these years even four different types of MNP have been taken into account to carry out the project:

- iron oxide nanoparticles produced at the University of Trento (Italy), called UNITN-MNP;
- iron oxide nanoparticles produced at GeorgiaTech of Atlanta (US), called GATECH-MNP;
- iron oxide nanoparticles produced at the University of Montpellier (France), called FRANCE-MNP;
- gold nanoparticles produced by FBK-IRST of Trento (Italy), called AuNP.

This thesis focuses only on UNITN-MNP and GATECH-MNP, describing work and results pertaining to them. Indeed, it is interesting to understand the synthesis process of UNITN group, while GATECH-MNP resulted the best and more suitable for our purposes.

To do this chapter more readable, materials, reagents and instruments used in chapter are described in section 5.4

## Chapter 4

# UNITN MNPs

### 4.1 MNP Synthesis and chemical-physical characteristics

This type of magnetic nanoparticles has been developed at the BIOtech research center of University of Trento. The synthesis protocol was based on microemulsion: highly monodispersed iron oxide nanoparticles were synthesized by using the aqueous core of aerosol-OT (AOT)/n-Hexane reverse micelles in N atmosphere. Reverse micelles have an aqueous inner core, which can dissolve hydrophilic compounds, salts, etc. A deoxygenated aqueous solution of ferric and ferrous salts (molar ratio 2:1, 1 M) was dissolved in the aqueous core of the reverse micelles formed by 0.05M AOT in n-hexane. Chemical precipitation was achieved by using a 1 M deoxygenated solution of sodium hydroxide. The reaction was carried out in nitrogen atmosphere at low temperature (4°C) with vigorous stirring. Hexane was evaporated and the particles were recovered by precipitation in an excess of an acetone-methanol mixture (9:1

ratio), followed by dialysis using 12-kD cutoff dialysis membrane against double-distilled water to remove unreacted iron salts. This solution was dried in an oven at 80° C and nanoparticles were suspended in toluene. [74].

MNPs, formed inside reverse micelle, have a hydrophobic surface; therefore they can be suspended only in a non-polar solvent like toluene. Moreover, these MNPs have high stability (several months). The shape of this NP is ellipsoidal with some little defects.

#### 4.1.1 Nanoparticle size measurement using DLS and TEM

In this experimental part, characterization and analysis were performed using transmission electron microscope (TEM) and dynamic light scattering (DLS). [51][52][53][54]

As regards TEM analysis, images were produced using the protocol based on the deposition of a drop of suspension of MNP on a carbon-film coated copper grid.

Figure 4.1 represents a series of TEM images: a direct, a doubly magnified and a detail of the latter.

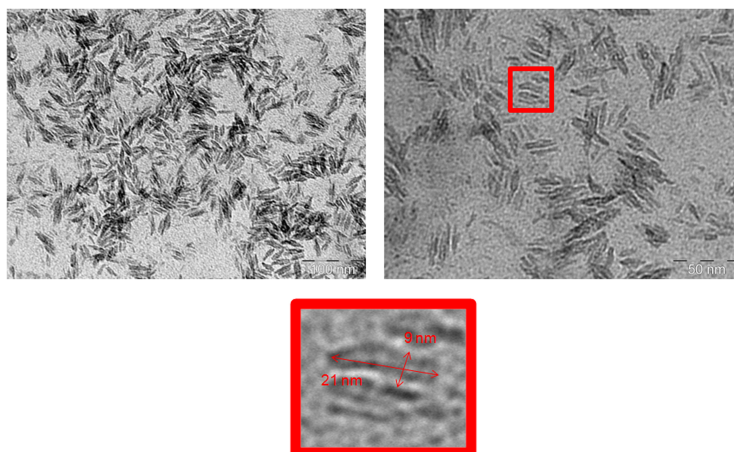


Figure 4.1: TEM images of iron oxide cores produces by UNITN group. Top left: direct image; right: magnified image twice. Below: detail of an isolated nanoparticle

Produced nanoparticles have an ellipsoid shape with diameter ranging between 9 and 21 nm, approximately.

Via TEM instrumentation was also carried out the microanalysis, in order to determine which elements compose the sample. Figure 4.2-left represents the frequency spectrum of the elements analyzed in microanalysis.

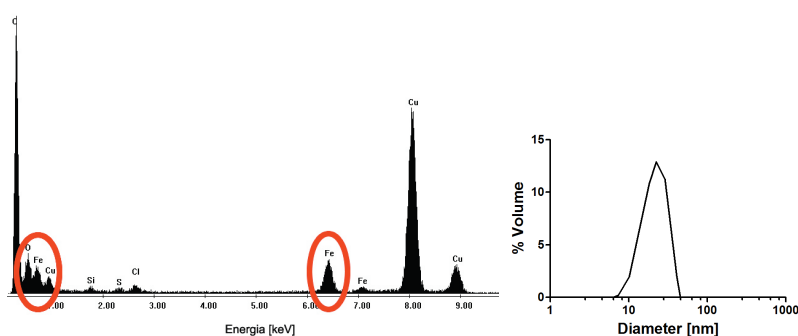


Figure 4.2: Left: Energy spectrum by microanalysis of a sample of synthesized MNP. Right: DLS analysis of iron oxide cores

The graph shows two very high peaks which represent carbon and copper. These two elements are present because they are the basic constituents of the grid: the support and coating. The other peaks represent the iron and oxygen which are the constituents of the iron oxide, components of nanoparticles.

As regards DSL analysis, figure 4.2-right represents size distribution and the average diameter of nanoparticles.

Produced nanoparticles have an average diameter of about 15 nm, with a very wide distribution.

The TEM and DLS comparison reveals a large discrepancy of measured dimensions and shape. This difference follows from the capability of TEM to analyze only one particle at a time and the ellipsoidal shape of nanoparticles is easily observable, while

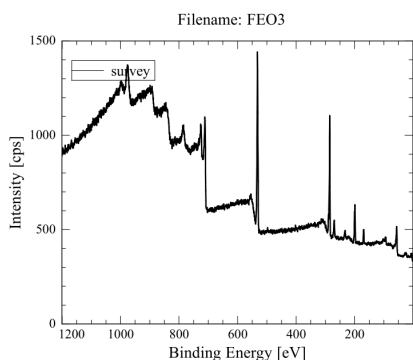
DLS results take into account the whole sample analyzed.

To fill this discrepancy there is the fact that the diameter measured by DLS results to be 15 nm, which is a value similar to the average between the greater diameter (21 nm) and the smaller diameter (9 nm) measured by TEM.

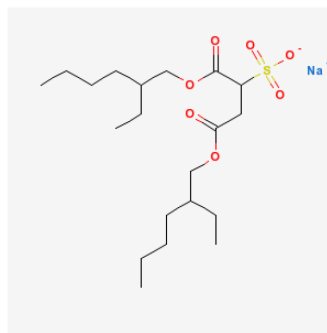
### 4.1.2 X-ray photoelectron spectroscopy XPS

All XPS analysis has been performed by Ph.D. Luca Minati at the FBK-IRST (Trento).

The XPS analysis of the MNP synthesized by UniTN show the presence of different kinds of contaminants. In addition to carbon (285 eV) oxygen (530 eV) and iron (710 eV), XPS also chlorine (200 eV) and sulphur signals are detected. The former is probably due to a non total reduction of the precursor while the latter derives from surfactant residuals (sodium bis(2-ethyl-1-hexyl)sulphosuccinate).



A



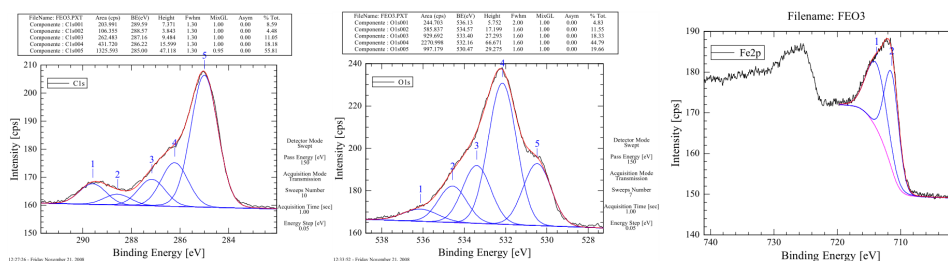
B

The fit of the C1s core line in the following figure shows a principal component at 285.0 eV associated to hydrocarbon chains. Higher spectra power is found in the regions 286 - 287 eV and 289-290eV associated to C-O, C=O and carboxylic bonds, respectively.

As for C1s, also the O1s core line is rather different from that of the previous

#### 4.1. MNP SYNTHESIS AND CHEMICAL-PHYSICAL CHARACTERISTICS 77

sample. Now the main component (at 532eV) is associated to C-O bonds whole that, corresponding to the iron oxide (530eV), has a pretty lower intensity. The remaining components are: carboxylic species at 533eV, at 534eV carboxylic bonds near SO<sub>3</sub>- and finally the component at 536 eV is associated to water residuals.



The Fe2p core line is quite different respect to the previous sample due to the presence of iron chloride. Each of the two peaks of the spin-orbit doublet can be resolved in two components deriving from Fe oxide and Fe chloride.



## Chapter 5

# GATECH MNPs

According to ideas described in chapter 2, also GATECH MNPs have a great potential as MRI contrast agent for molecular imaging thanks to their excellent T2 relaxivity and as drug delivery carrier considering their small size and high reactivity. However, it is necessary to modulate SPIOs to obtain optimal size, T2 relaxivity and surface functionality for specific applications.

The major part of the work has been done on these MNPs. They have followed a precise pathway from the first step of synthesis until the last *in vivo* results.

All experiments and results, good and bad ones, led to reach ultimate development described in section 2.2.

### 5.1 Synthesis and coating

Iron oxide cores were synthesized by thermo-decomposition of iron complex in a mixture of oleic acid and oleylamine. These nanoparticles have an external shell of oleic acid, which makes them to be suspended in toluene, limiting any possible biological

study. [16][17][75][76][77]

In figure 5.1 there are a graph of size distribution and a TEM image of bare NP as prepared by Atlanta lab.

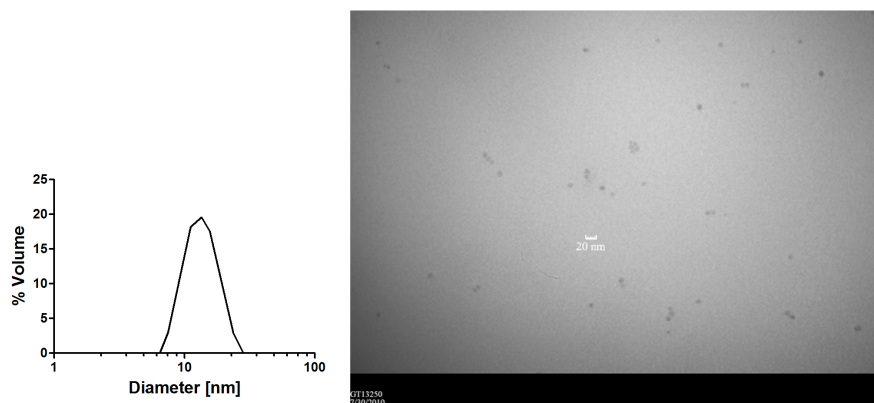


Figure 5.1: Left: Size distribution of bare MNP in toluene; Right: TEM image of same MNP

To make water soluble SPIO, iron oxide cores were coated with 1,2-distearoyl-sn-glycero-3-phosphoethanolamine-N-[methoxy (polyethylene glycol)-X] (DSPE-mPEG X) using a solvent exchange method. X is the molecular weight of methoxy (polyethylene glycol) ranging from 550 to 5000 (figure 5.2).

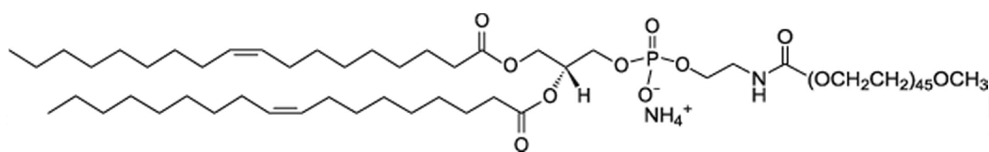


Figure 5.2: Chemical structure of 1,2-distearoyl-sn-glycero-3-phosphoethanolamine-N-[methoxy (polyethylene glycol)-2000

These molecules have polar head (hydrophilic) and non-polar tail (hydrophobic). This polymer is not toxic and is water soluble and biocompatible. There are different types of polyethylene glycol, classified by molecular weight and number of monomers.

Structures with different length have different physical properties (viscosity) and different applications, meanwhile the chemical characteristic is constant.

In this work, for the majority of cases core size and polymer coating used are:

- 6.5 nm core produced by GeorgiaTech group
- DSPE-mPEG2000 and composed by 43 monomers prepared by Avanti Polar Lipids Inc.

The coating protocol is the following: the GATECH iron oxide cores were dispersed in toluene and were insoluble in water prior to modification. A solution of DSPE-mPEG (4.8 ml at 5 mg/ml) is prepared in chloroform. MNPs in toluene (3 ml at 1 mg/ml) were added in this solution (fig. 5.3). The Iron-PEG ratio in weight is about 1:8.



Figure 5.3: Pictures of argon-flow (left) and rotovapor (right) apparatus to coated iron oxide core with dried film.

This mixture was then dried under argon gas and left in a vacuum desiccator for 48 h to remove all traces of organic solvents. The dried film was easily resuspended in deionized water with agitation. In this way, the PEG-MNPs were dispersed in water.

This protocol has been developed because another dried film technique using a rotovapor showed worse result. The main difference is the use of vacuum pump to eliminate toluene and chloroform instead our argon flow.

With both techniques, the obtained film is dried more in a desiccator connected with a vacuum pump for 16 hours and then MNPs are suspended in water using ultrasonification.

After this procedure, the solution is composed by:

- Coated nanoparticles (figure 5.4-right)
- Multicore nanoparticles
- Empty PEG micelle (figure 5.4-left)
- Free PEG molecules
- Aggregates.

Coated MNPs are the right structure to obtain. During the coating process and water re-suspension, it is possible to have unwanted products. In multicore NP different cores are coated by the same polymer shell. The size of this structure is larger than the required NP size. It is possible to obtain empty micelles too, where PEG chains in solution can react between them with hydrophilic heads outside and hydrophobic part inside. This free chain is the most dangerous structure for stability of correct MNP.

Moreover, it easy to find PEG free chains and other bigger aggregates so a purification processes has been developed of this multi-component suspension . The tree main steps are:

- centrifugation with specific filter tube (100 kDa) to eliminate free chain

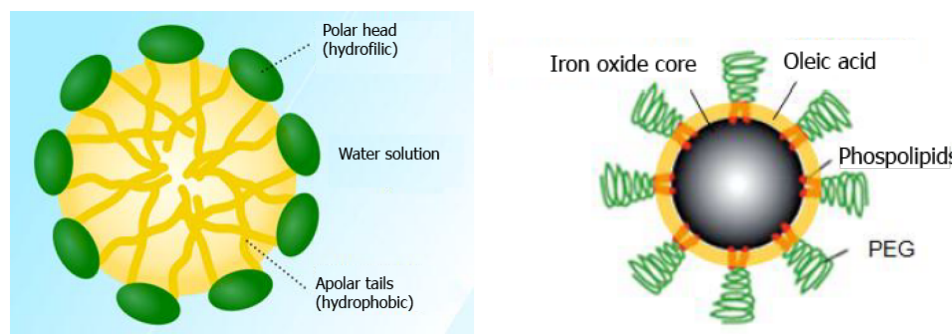


Figure 5.4: Left: structure of an empty micelle; Right: structure of PEG coated MNP

- ultracentrifugation (upper than 40000 rpm) to concentrate correct MNP and eliminate empty micelle
- 0,22 um filtration to eliminate aggregates.

It is possible to characterize bare MNP (non coated and in toluene) and coated MNP using dynamic light scattering (DLS) to evaluate size distribution. Figure 5.5-left shows the size distribution using both dried film methods: argon flow and rotovapor. The argon-flow MNPs have a sharp peak at 24 nm and a small peak around 90 nm. The 80% of MNPs has an average size of 24 nm. Rotovapor MNP have 2 high peaks at 59 and 130 nm. Comparing these distributions it possible to notice that the argon-flow protocol is much better than the rotovapor method. Taking into account that the objective of our project is the synthesis of 50 nm iron compound, argon-flow MNPs follow completely the specific requests. Using specific polymer-contrast resin for TEM, in figure (5.5-right), it is possible to assess PEG-MNPs size is around 30 nm.

For this type of nanoparticles there are advantages and disadvantages.

One of these disadvantages is the difficulty to bind polyelectrolytes with the chains

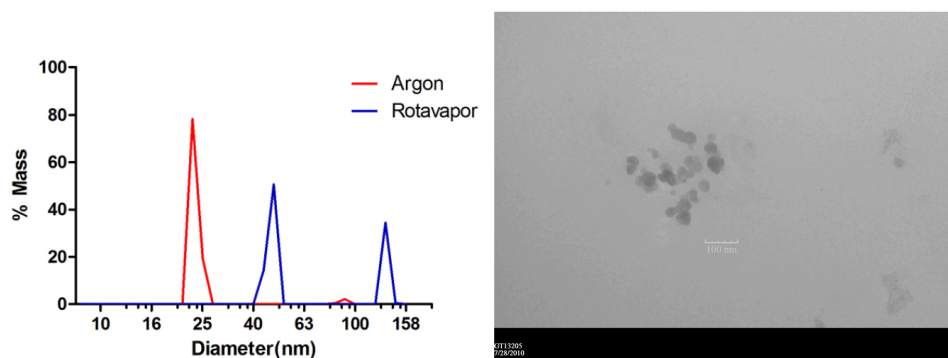


Figure 5.5: Left: comparison of argon-flow and rotovapor size distribution using DLS. Right: TEM image of coated MNP using specific polymer contrast resin

of PEG. Indeed, the structure described in figure 5.4-left is complete. There is a core, a hydrophobic double layer and a hydrophobic external layer and it is very difficult to add some other layers. However, using specific commercial molecules, it is possible to select the chemical group for MNP functionalization, for example COOH and NH<sub>2</sub> group that are used in several reaction to bind many types of molecules on the surface of MNP: antibody, dye, proteins and so on. Hence this disadvantage turns out to be an advantage.

### 5.1.1 Nanoparticle size measurement using DLS

Dynamic light scattering (DLS) measurement of 6.5 nm iron oxide core indicates that nanocrystals are well dispersed in toluene with an average hydrodynamic diameter of 8.12 nm (figure 5.6-left). Coated MNPs with dried film method show different diameter reliant on type of solution which they are suspended in. [53][54]

In water their average diameter is about 27.8 nm, while for DMSO solution this value reaches 34.6 nm. These results indicate that iron oxide nanocrystals are stabilized by DSPE-mPEG in DMSO and water.

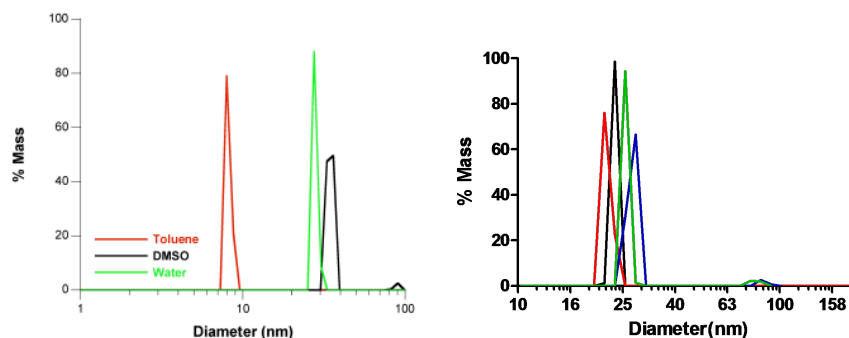


Figure 5.6: Left: DLS peaks of iron oxide core and coated MNP in DMSO and water. Right: DLS analysis of 4 different samples prepared in the same way

MIONs are slightly larger in DMSO than in water. This is presumably due to the increased solubility of DSPE-mPEG in DMSO so that the coating layer is more extended.

There is one more thing to take into account for coating process: it is very difficult to reproduce perfectly the entire process. In figure 5.6-right it is possible to notice 4 different peaks for 4 different batches of coated nanoparticles produced with same parameters. Measured diameter ranges from 18 to 28 nm.

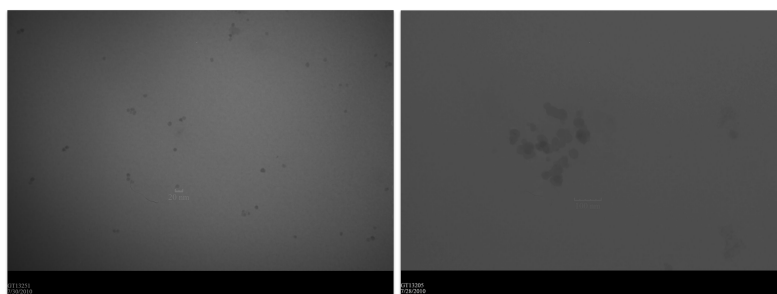
One of the most annoying parameter during this process is humidity because it can interact with the size of DPSE-mPEG layer around the core. And it is very difficult to control humidity during the process, so it is easy to find this little differences of diameter during measure.

For simplicity, these MNPs are also called PEG-MNPs.

### 5.1.2 Nanoparticle size measurement using TEM

Transmission electron microscopy (TEM) was used to determine the size of coated and uncoated MIONs with core diameters of 6.5nm and 17 nm. [51][52]

Empty micelles were separated from micellar nanoparticles by ultracentrifugation. 5  $\mu$ l nanoparticles solutions was dropped onto a carbon coated copper grid and negatively stained with 1% phosphotungstic acid. The following TEM images were recorded with a JEOL JEM-1210 transmission electron microscope connected to a CCD camera.

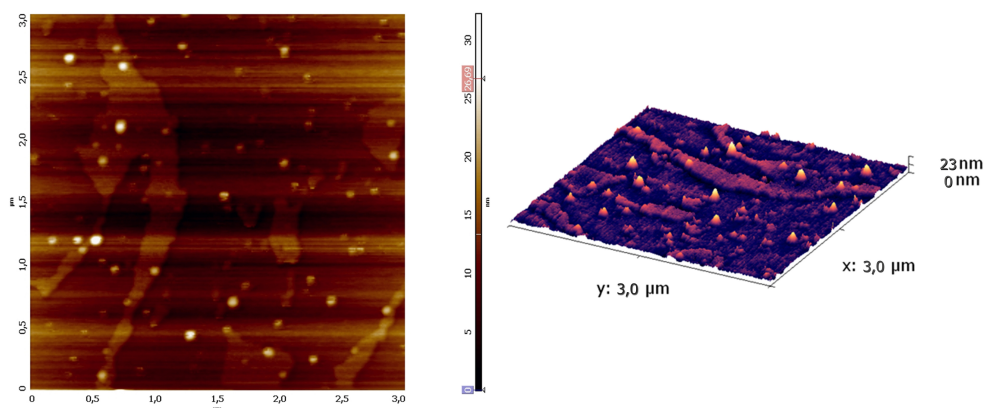


### 5.1.3 Nanoparticle size measurement using AFM

Also atomic force microscope AFM was used to determine nanoparticles size. [78][79][80]

A small amount of PEG-MNPs was dropped on a sheet of mica; after a long drying in N atmosphere the sample was ready for measurement.

The following two figures clearly show the presence of MNPs on the substrate surface. The analysis of the roughness leads to an average dimension of 20-30nm.



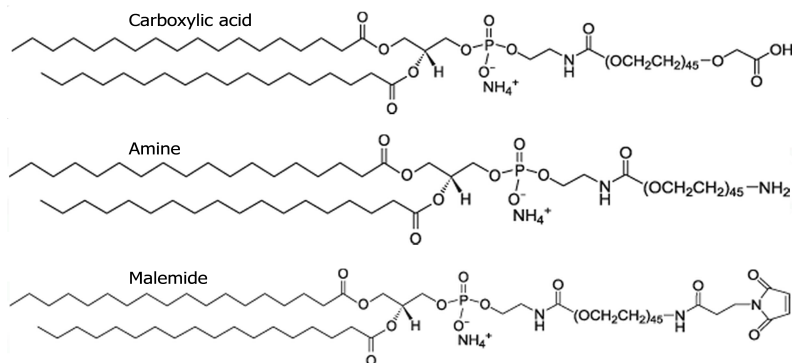
So it is possible to measure the size distribution of MNPs with AFM too, but this technique was abandoned because it is very complex respect to DLS or TEM.

#### 5.1.4 Change of coating recipe

Until now the coated MNP have been produced using only one type of phospholipids with PEG, but there are different structures of these. One of the most important difference concerns the functional group attached at the end of PEG polymer chain.

The first MNPs have been coated using DSPE-mPEG that ends with a methoxy group; it is a not reactive group.

For many purposes it is a good idea to use different chemical groups such as carboxyl COOH, amine NH<sub>2</sub>, maleimide and many more. These groups are illustrated in the following image.



These groups are very reactive and using specific crosslinker it is possible to exploit them to bind several molecules on the surface of nanoparticles. In the same way it is possible to change easily the total charge of the structure. For example, a MNP coated with DSPE-PEG-COOH is more negative respect to DSPE-mPEG MNP which it is more negative respect to DSPE-PEG-NH<sub>2</sub> nanoparticles.

The most part of described analysis is done using nanoparticles coated with 95% of DSPE-mPEG and 5% of DSPE-PEG-NH<sub>2</sub>, called NH<sub>2</sub>-PEG-MNPs or simply PEG-MNPs, the reason of this choice will be explained in next sections of this work.

Also the length of the polymer is a variable parameter. In this work DSPE-mPEG-2000 and DSPE-PEG-NH<sub>2</sub>-2000 are always used to coat iron oxide core. MNPs with different length of PEG have been tested, only for coating protocol verification.

As showed in figure 5.7, DLS points out different size distributions of MNP coated with 350, 2000 e 5000 kDA PEG using a Iron/PEG ratio of 1:8

It is possible to notice that PEG-5000 have same size distribution of PEG-2000 just shifted to the right of 5-8 nm. Instead, the size distribution of PEG-350 is very bad. Probably the ratio 1:8 is not the right one for this kind of molecules and it is possible to find multicore NP and aggregates.

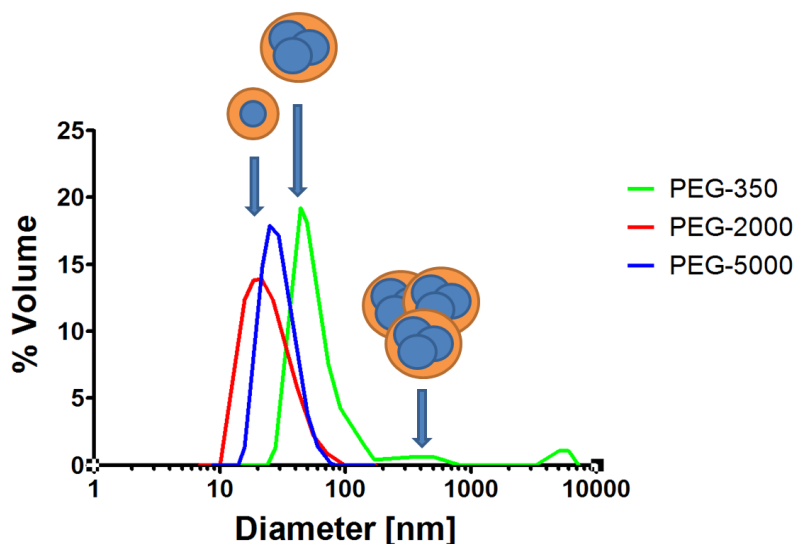


Figure 5.7: DLS analysis of coated MNP using PEG with different lengths

### 5.1.5 Change of coating protocol

During the work, a large amount of nanoparticles has been developed. The synthesis process is expensive because a lot of reagents, tools and instruments are used. The most expensive reagent is DSPE-mPEG because it is a very particular molecule and it is not so diffuse in industry. The process ratio used between iron of core and DSPE-mPEG was 1:8. At the beginning of our research this ratio has been the first one to show good results for coating of MNP. Indeed, the number of phospholipids with PEG has to be always larger than NP number because otherwise it is possible to have multicore NP or aggregates.

Since, unfortunately, this ratio makes MNP very expensive, another ratio has been tested: Iron:PEG=1:4. This permits to save half quantity of DSPE-mPEG.

In figure 5.8 it is possible to notice two synthesis batches (B1 and B2) produced at different times.

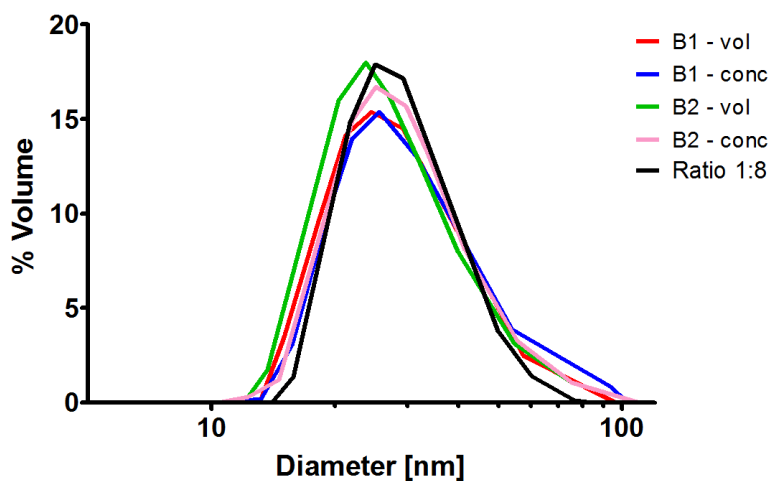


Figure 5.8: DLS analysis of 2 different samples: “B1 - vol” are MNP produced from the first batch maintaining constant volume, ‘B1 - conc” are MNP produced maintaining constant concentration, ‘B2 - vol” are MNP produced from the second batch maintaining constant volume, ‘B2 - conc” are MNP produced maintaining constant concentration and “Ratio 1:8” are MNP produced with with the previous ratio between iron and PEG

In the same batch, two conditions have been tested:

- **Same concentration:** thereby half volume. There is a half quantity of solution respect to 1:8 ratio.
- **Same volume:** thereby half concentration. There is a half value of concentration respect to 1:8 ratio.

DLS analysis illustrates that there are not big differences between different methods, in case of constant volume or concentration, and between different ratios.

So using the coating dried film method based on argon flow it is possible to obtain a very good size distribution using a ratio 1:4, instead of more expensive 1:8.

### 5.1.6 Protocol for the determination of Fe concentration

To know directly the right number of nanoparticles in solution or uptaken by cells is very difficult. One way to achieve this target is to measure the amount of iron ions of NP breaking the iron oxide molecules that compose them.

So the iron content of MIONS was determined using a ferrozine assay. In brief, 50  $\mu\text{l}$  sample solution was mixed with equal volume of HCl 12 M and incubated at room temperature for 30 minutes. Then, 240  $\mu\text{l}$  of 2 M NaOH, 55  $\mu\text{l}$  of 4 M ammonium acetate and 110  $\mu\text{l}$  of 5% hydroxylamine HCl were added to the solution. After 30 minutes incubation, the solution was mixed with 0.02% ferrozine solution. Light absorption was read at 562 nm with 810 nm as the reference with a microplate reader.

This method is very useful to know the right concentration of produced nanoparticles because it is impossible to estimate it taking into account the leaks during several filtrations, washing and centrifuge processes.

During several batches of PEG-MNPs, the amount of recovered nanoparticles ranges from 75 to 80% of total amount of iron used in the first steps of coating process. [81]

### 5.1.7 Stability of MNPs

After a long coating process nanoparticles stay suspended in water. In this situation they are pretty stable but after some days, weeks or months it is possible to notice precipitates on the bottom of the storage vial.

In most cases these aggregates are formed by free DSPE-mPEG molecules that interact with themselves and form precipitates.

MNPs have to be stable in different situations. To simulate them as good as possible three categories are defined:

- Storage: it is possible to store MNPs in water at different temperature and different concentration
- pH: during several process it is possible that the pH of solution is not always 7
- particular solution: MNPs could be dissolved in many solutions with different amounts of salts.

To verify stability, MNPs of a concentration of 100 ug/ml are suspended in different solutions. After defined experimental time, the samples are centrifuged (2000 rpm for 10 minutes) and a little amount (about 10 ul) is taken from the top of solution. These aliquots were analyzed with ferrozine protocol (5.1.6) to measure the concentration.

#### **Storage:**

To verify which is the best way to store MNPs, a big experiment was set up; nanoparticles have been stored in water at different temperature ( $-80^{\circ}\text{C}$ ,  $-20^{\circ}\text{C}$   $+4^{\circ}\text{C}$  and room temperature RT) with different concentrations (50, 100 and 500 ug/ml).

Figure 5.9 shows the percentage of MNPs remaining stable in solution. For instance, if the value related to a sample is 80% this means that the 80% of amount of iron is inside of suspended MNPs while the 20% of iron is inside the precipitated aggregates.

#### **pH**

The stability of MNP in different pH solutions has been tested in a experiment similar with the previous one. Small MNP amount (50  $\mu\text{g}$ ) was suspended in 500  $\mu\text{l}$  of pH solution so the final concentration was 100  $\mu\text{g}/\text{ml}$ . The vials that contained these solutions have been maintained at room temperature for 3 and 6 days.

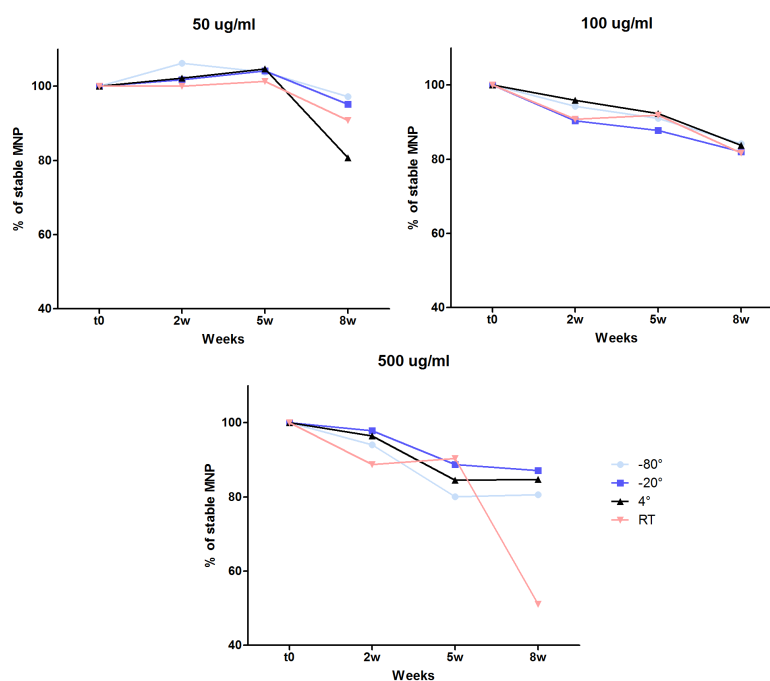


Figure 5.9: Stability graph of MNPs sample at different storage conditions: concentration and time

The pH value of used solution are: 1.92, 2.53, 3.30, 5.10, 6.00, 6.50, 7.40, 8.70, 10.90 and 12.00.

The data illustrated in figure 5.10 are normalized to 100% at starting value of concentration.

From this graph it is possible to notice that the MNP are pretty much stable at most pH value. The biggest problems has been found at boundaries pH value: 1.92 and 12 pH mainly.

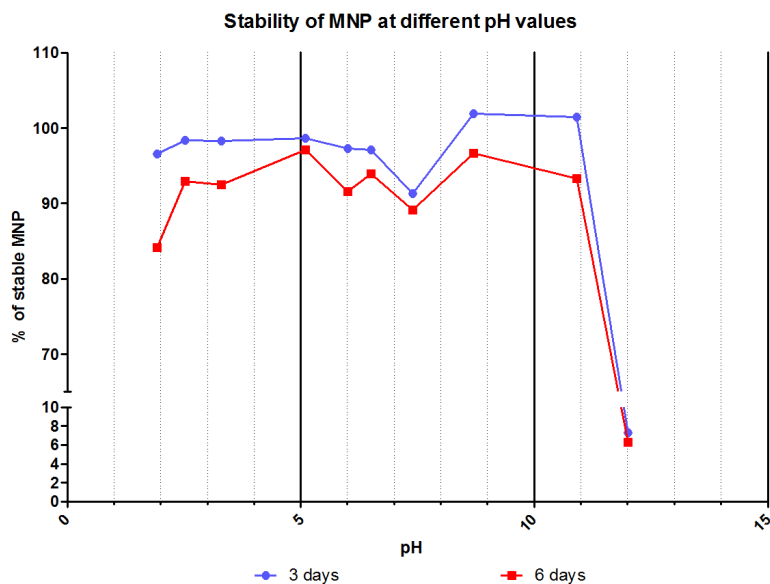


Figure 5.10: Stability graph of MNPs suspended in solution with different pH values at  $100 \mu\text{g}/\text{ml}$  concentration and maintained at room temperature for 3 and 6 days.

#### Particular solution:

The stability of MNP in different solution has been tested in a experiment similar with the previous ones but using different buffer. These buffer are widely used in many biological laboratory. Small MNP amount ( $50 \mu\text{g}$ ) was suspended in  $500 \mu\text{l}$  of these buffer, so the final concentration was  $100 \mu\text{g}/\text{ml}$ . The vials that contained these solutions have been maintained on a shaker at  $37^\circ$  for 1, 3 and 5 days.

The buffer used for this stability experiment was:

- Fosfate buffer 10 mM ph7
- 2M KCl
- KCl 200 mM

- $CaCl_2$
- Tris-Cl pH9 1M
- Destain solution
- PBS 1X
- PBS 10X
- KOH 4N
- KOH 0.4N
- NaOH 2N
- Cell medium
- Water (as a control)

The data illustrated in figure 5.11 are normalized to 100% at starting value of concentration.

From this graph it is possible to notice that the MNP are stable in most buffer. There are problems with high concentration of ions buffer and with solution that contain OH ions as KOH and NaOH, also at low concentration (0.4N KOH)

### 5.1.8 Chemical surface analysis of MNPs using $\zeta$ -potential

$\zeta$ -potential is the potential difference between the dispersion medium and the stationary layer of fluid attached to the dispersed particle.

In figure 5.12-left there is a scheme of  $\zeta$ -potential of a general colloid.

This techniques measures the surface charge of structures. This is a important parameter to know the stability of nanoparticles.

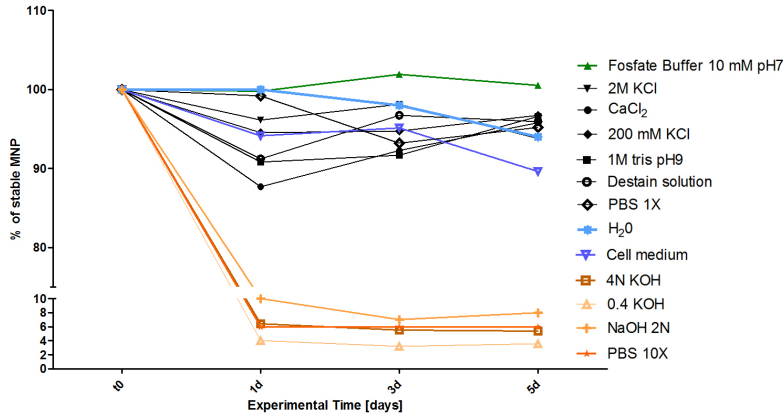


Figure 5.11: Stability graph of MNPs suspended in different buffer at 100  $\mu\text{g}/\text{ml}$  concentration and maintained on a shaker at 37 ° for 1, 3 and 5 days.

The following table described the stability of colloid that have different values of  $\zeta$  potential.

$\zeta$ -potential [mV]	Colloid stability
$\pm[0, 5]$	Aggregation
$\pm[10, 30]$	High instability
$\pm[30, 40]$	Moderate stability
$\pm[40, 60]$	Good stability
$\geq 60$	Excellent stability

Another reason to measure this potential is to understand the interaction with lived tissue.

In previous section of this work the charge of MNPs was described as very fundamental parameter because a negative charged surface makes MNPs more biocompatible, while a positive charge increases the interaction between MNPs and cells but is more toxic too.

Figure 5.12-right shows  $\zeta$ -potential analysis of PEG-MNP sample. It is to notice

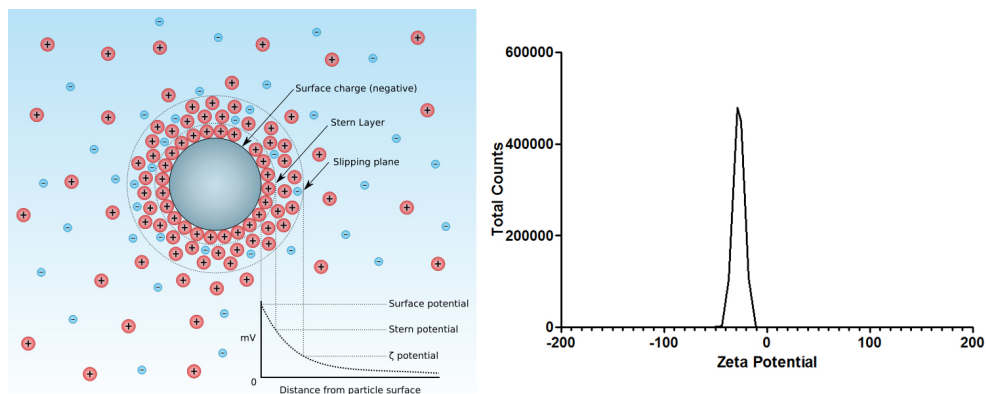


Figure 5.12: Left: scheme of surface potential of general colloid. Right:  $\zeta$ -potential measurement of PEG-MNPs

that the value is about -27.3 mV. And according with the table and the stability tests of previously section it is possible to affirm the the MNPs are pretty stable

### 5.1.9 Magnetic $T_2$ relaxivity of PEG-MNPs

All magnetic measures are executed using a 9.7T NMR Bruker Avance 400 spectrophotometer installed at the Bio-organic Chemistry of University of Trento.

The MNP sample are prepared by dilution from mother solutions 0.13 mg/mL (=0.56 mM) in  $Fe_3O_4$ . Taking into account that a mole of  $Fe_3O_4$  contains 3 mole of  $Fe$  and the relaxivity  $r_2$  is described by following equation:

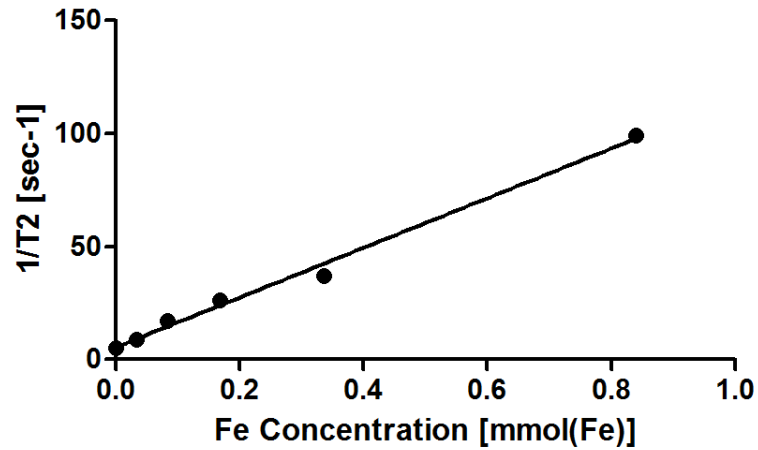
$$\frac{1}{T_2} = \frac{1}{T_2^0} + r_2 \cdot C \quad (5.1)$$

where  $T_2$  is the relaxation time  $T_2$  of  $^1H$  of water and  $C$  is the concentration of iron expressed in  $mmol(Fe)$ . The relaxivity unit is  $[sec^{-1} \cdot mmol(Fe)^{-1}]$ .

Table of relaxation time  $T_2$  is:

MNP concentration [mg/ml]	Fe Concentration [mmol(Fe)]	T2 [msec]
0	0	0.199
0.048	0.034	0.114
0.121	0.084	0.059
0.241	0.168	0.038
0.482	0.336	0.027
1.206	0.840	0.010

And the following graph describe linear proportional relationship between concentration  $n$   $C$  and the inverse of relaxation time  $T_2$ .



Fitting linear this graph, it is easy to find  $\frac{1}{T_2^0} = 5.456 \pm 1.735 \text{ msec}^{-1}$  and  $r_2 = 109.9 \pm 4.597 [\text{sec}^{-1} \cdot \text{mmol}(\text{Fe})^{-1}]$ .

The relaxivity of other commercial product is: Feridex 160, Sinerem 160, Resovist 151 and Clariscan 35  $[\text{sec}^{-1} \cdot \text{mmol}(\text{Fe})^{-1}]$

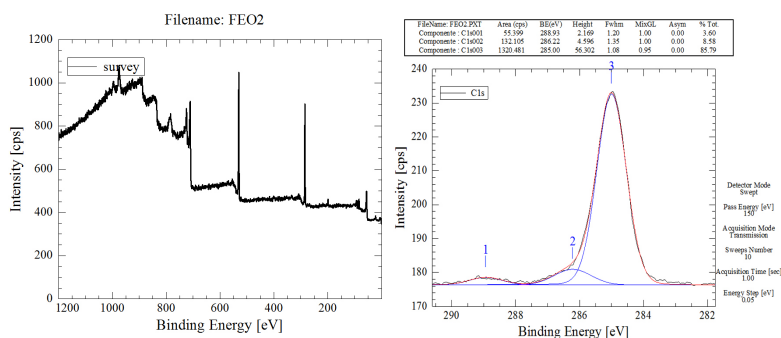
Comparing them with our MNPs it is possible to affirm that the our value of relaxivity  $r_2$  it is good enough for clinical practice.

### 5.1.10 X-ray photoelectron spectroscopy

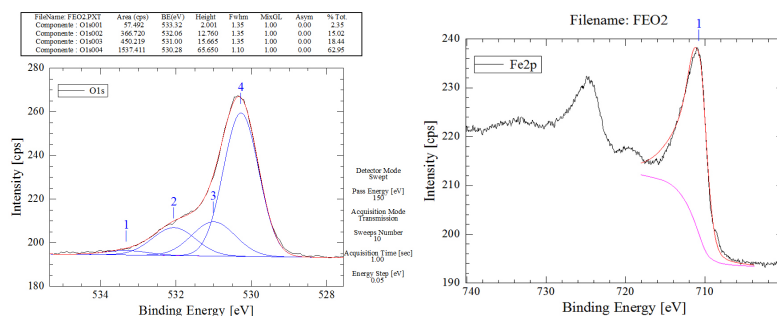
All XPS analysis has been performed by Ph.D. Luca Minati at the FBK-IRST (Trento).

#### Iron oxide core

The survey allows the identification of the atomic species present in the sample. In particular detect carbon (C1s peak at 285 eV) oxygen (O1s peak at 530 eV), iron (Fe 2p doublet at 710 and 720 eV) and traces of chlorine (component around 200 eV). Other peaks derive from Fe3s and Fe3p components and from the Auger structures of the detected elements.



Example of C1s peak fitting. The Core line shows a principal component a 285.0 eV associated to hydrocarbon chains, the component at 286eV is associated to -C-O-C- and C-OH bonds while at 289eV falls the carboxylic bond. The C1s core line is compatible with the presence of a high amount of oleic acid and oleamine chains (used as surfactants) present on the nanoparticle surface. This is revealed also by the extremely sharp peak at 285 eV (0.95 eV) that is an indications of the presence of well ordered carbon chains as in the case of oleic acid and oleamine.



The O1s core line presents one main component at 530 eV associated to metal oxide. The additional three components at around 531, 532 e 533.5 eV are associated to carbon- oxygen bonds.

The Fe2p core line shows two peaks coming from the spin-orbital splitting at energies of 710 eV e 726 eV which are associated to iron oxide.

#### Quantification results

Line	di core	Area	BE (eV)	Height	Fwhm	RSF	CONC. %at
Cl_Survey		126.60				0.770	1.61 %FeCl3
Cl1s001		55.39	288.93	2.17	1.20	0.296	1.83 % (C=O) -O-
Cl1s002		126.07	286.22	4.08	1.45	0.296	4.17 %C-O
Cl1s003		1320.48	285.00	56.30	1.08	0.296	43.63 %CH2-CH2
O1s001		57.49	533.32	2.00	1.35	0.730	0.77 % (C=O) -O*-
O1s002		366.72	532.06	12.76	1.35	0.730	4.91 %-O-C-O-
O1s003		450.22	531.00	15.66	1.35	0.730	6.03 % (C=O*) -O-
O1s004		1537.41	530.28	65.65	1.10	0.730	20.60 %Fe3O4
Fe2p001		3010.44	710.73	36.94	2.20	1.790	16.45 %Fe3O4

#### Application of spectral modeling to discriminate magnetite and hematite in MNPs

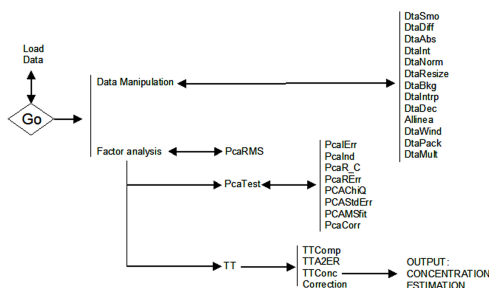
Fe has different oxidation states giving origin to four different forms of iron oxides. Wustite is formed by FeO in a cubic crystalline form. In magnetite Fe and O are

arranged in an octahedral crystalline structure where iron assumes oxidation state 2 and 3. Hematite is formed by  $\text{Fe}_2\text{O}_3$  and assumes a trigonal crystalline structure. Finally maghemite can be considered as an oxidized form of magnetite where the previous forms coexists in a rather complex crystalline arrangement. In nature the more diffuse form of iron oxide are magnetite and hematite. Also during the nanoparticle (NP) synthesis of iron oxide nanoparticles leads to aggregates formed by different stoichiometries between Fe and O composed prevalently by a mixture of  $\text{Fe}_2\text{O}_3$  hematite and  $\text{Fe}_3\text{O}_4$  magnetite. Following the literature the maximal intensification of NMR images is obtained using magnetite-based NPs. It is then important to estimate the composition of the two different iron oxides inside the NP in order to possibly maximize the  $\text{Fe}_3\text{O}_4$  content. Unfortunately there are very small differences between the Fe 2p spectral core lines of hematite and magnetite which render the discrimination between the two oxides and their quantification impossible. There is a second problem which adds to this first difficulty. The inverse micelle process used to synthesize the NPs leads to a considerable amount of polymeric residuals on the NP surface as discussed previously. Unfortunately this kind of contamination contains a certain amount of oxygen. It is not possible to use directly the O1s core line to quantify the hematite and the magnetite considering the different Fe : O stoichiometries in these two compounds. Although the problem is rather complex, a way to produce meaningful estimation of the hematite and magnetite content in the NPs exists. It is a method based on a statistical estimation. This work is referring to the Factor Analysis (FA) which is quite used as an analytical approach in chemistry. Specifically FA is able to determine the concentrations of some chemical components in a given solution. The FA is a multivariate technique used to reduce matrices of experimental data at their lower dimensionality. This is performed through specific transformations of the original data (the XPS spectra) in new vectors in an abstract space. These

transformations allow a reduction of the numbers of vectors needed to describe the experimental observations. In our case the experimental data are XPS spectra and in particular the valence band (VB) spectra. Using the FA it is possible to try to generate the XPS VB of the nanoparticles through a composition of the VB from hematite and magnetite. The coefficients of this composition represent the concentrations of hematite and magnetite in the MNPs.

A considerable part of the work was dedicated the development of a software to perform data manipulation and the FA spectral analysis. The software was developed in the Matlab since it is very efficient in handling matrices. As indicated in the following flow chart, the program is roughly composed by two parts:

- Data manipulation to prepare data for the statistical analysis;
- Factor Analysis;



As stated above, the first step is to acquire the hematite and the magnetite standards to be able to generate the spectra from the NPs synthesized by the GT research group. At this aim hematite 99.8% and magnetite 99.99% purity were bought from Sigma Aldrich. High resolution XPS valence band spectra were acquired for each of the two standards. Same experimental conditions were used to analyze the NPs from GT. The valence bands of the standards are showed in figure 5.13

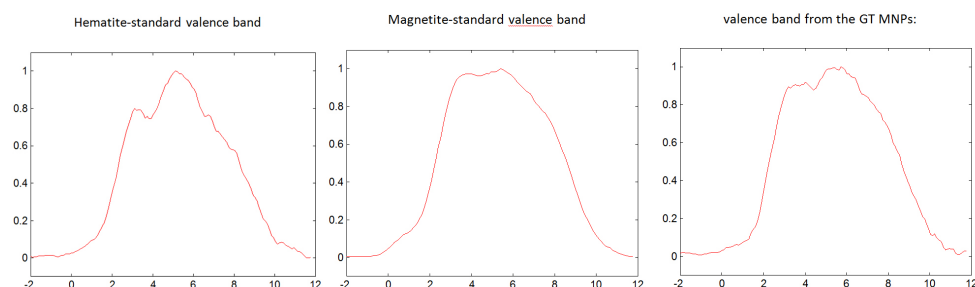


Figure 5.13: XPS standard Valence band of Hematite (left), Magnetite (center) and iron oxide core from GeorgiaTech (right)

The FA transforms these spectra in abstract vectors. It is important to verify that these abstract vectors are able to reproduce the original experimental data. Results are showed in figure 5.14-left and 5.14-center.

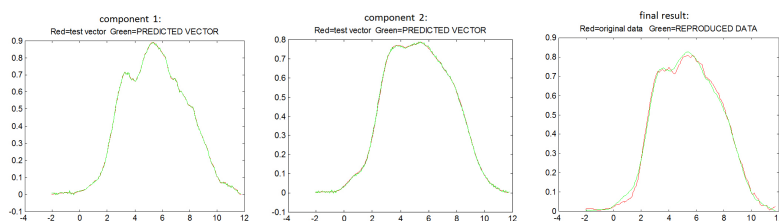


Figure 5.14: Comparison between real and model data of Hematite (left) and Magnetite (center). Right: Result of predictive model and real valence band

The abstract vectors are able to perfectly reproduce the original valence band spectra of hematite and magnetite. If the hypothesis that the MNPs are composed by hematite and magnetite holds for true, components 1 and 2 should be able to correctly reproduce the valence band spectrum of the GT- MNPs. The result obtained from the Factor analysis is shown in 5.14-right

As it can be appreciated a good reproduction of the MNP valence band which is obtained using 38% hematite and the 62% magnetite. [82]

### PEG coated MNPs

After XPS core analysis, measurements of PEG-MNPs has been done.

In fig. 5.15-left the C1s core lines of the SPIO NPs before and after the reaction with the PEG chains are reported. The as-produced SPIO NPs show an intense carbon signal placed at 285 eV associated to the presence of hydrocarburic chains. These are ascribed to the presence of the oleic acid and oleamine stabilizing agents on the surface of the NPs. The presence of hydrocarburic chains clearly explains the hydrophobicity of the SPIO NPs. After the reaction with the polyethylene glycol, the C1s core line show the presence of a high intensity peak at around 286 eV assigned to the CH<sub>2</sub>-O- bonds that are the fingertips of the PEG chains.

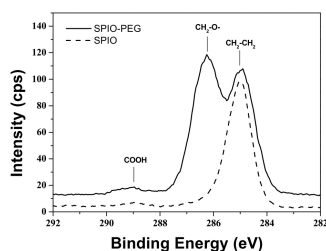


Figure 5.15: X ray photoelectron spectroscopy analysis of the C1s core line of pristine SPIO NPs (dashed)

Finally, the C1s core line of the SPIO-PEG nanoparticles shows the presence of a small feature at around 289 eV associated to the carboxylic groups of the oleic acid chains [12]. The same feature visible on the C1s core line of the pristine SPIO NPs proves the bond formation between the hydrophobic portion of the phospholipid-PEG polymer and the oleic acid chains. As a result of this hydrophobic interaction, the SPIO-PEG nanoparticles show high solubility in water. [83]

## 5.2 Functionalization

Iron oxide nanoparticles have two main properties with consequent advantages: nanometric size and paramagnetic behavior.

So these MNPs could be exploited just as MRI contrast agents.

To make these MNPs usable as carrier for drug delivery, it is necessary to functionalize them to entrap drug, to label with fluorescent dye and to improve uptake by cells.

### 5.2.1 Labeling with fluorescent dye

Obtain fluorescent skill for our MNPs it is very useful since it allows us to give another property to nanoparticles other than magnetic behavior. It is used a specific dye, which is called DiI. In following figure there are the structure and the absorption-emission spectrum of this molecules. The values of absorption and emission are so strong that this molecule can be used as colorimetric and fluorescent probe.

This molecule is hydrophobic and can be entrapped inside the hydrophobic shell of MNPs, formed by oleic acid and phospholipid chains. When the dyes enter this shell, the entire MNP becomes a fluorescent probe.

The protocol to obtain an effective entrapment included:

- PEG-MNPs suspension in water
- DiI molecules suspension in DMSO
- Mix of PEG-MNPs and DiI solutions at  $\frac{[MNP]}{[DiI]} = \frac{80\mu g/ml}{5\mu g/ml} = 16$

Figure 5.16-bottom shows the difference between spectra and max intensity for a fixed wavelength value of MNPs with and without dye. This graph confirms that DiI

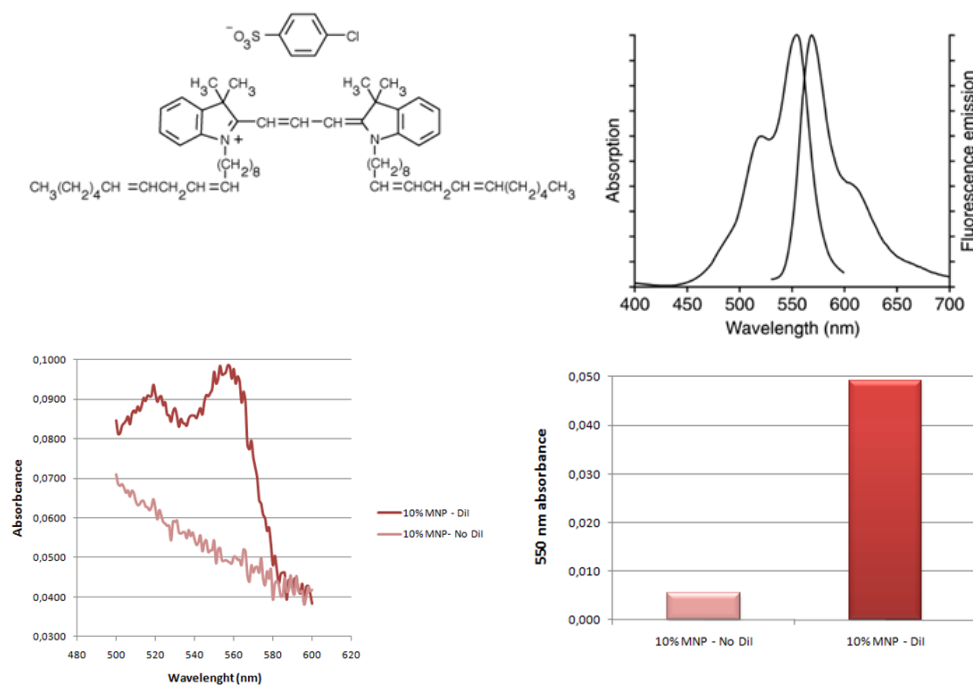


Figure 5.16: Top: Structure (left) and absorption and emission spectrum (right) of DiI dye. Bottom: Absorption spectrum (left) and absorbance at 550 nm (right) of MNPs with and without DiI

molecules can be used for example, as fluorescent probes for confocal microscopy and cytofluorimetry

In figure 5.17 two different confocal microscope images are showed This pictures are taken with different methods: different cells, different instruments and different staining preparation; but in both cases it is clear that MNPs are locate inside the cells but not inside the nucleus.

One possible improvement to complete the project purpose is to label MNP with different dyes, so it would be possible to exploit these properties to verify different behaviors. For example, if two types of MNPs with different properties (different

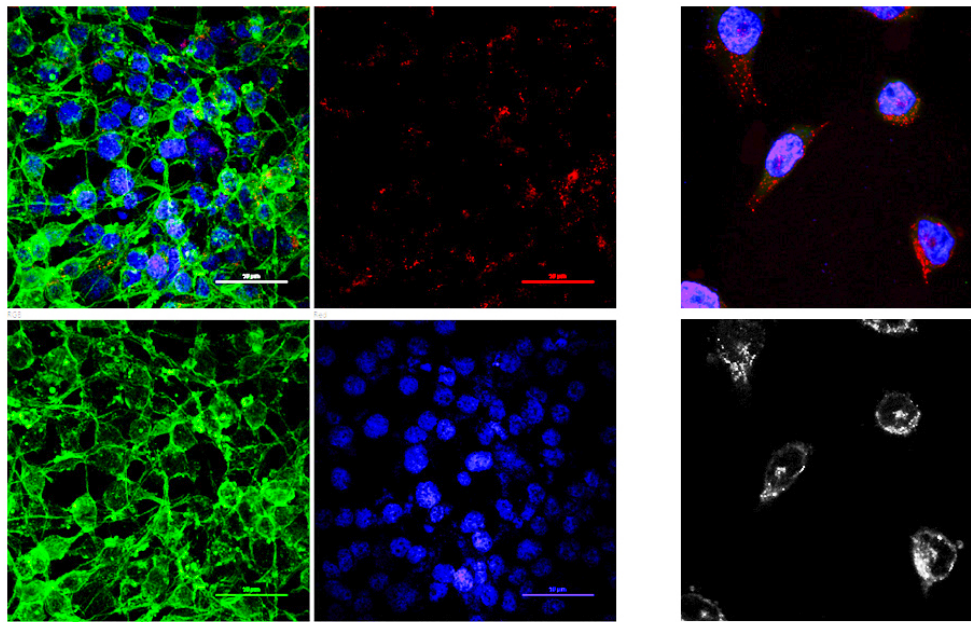


Figure 5.17: 2 examples of confocal microscope images taken using DiI-MNPs. Left: ES2 cell staining to map cell nucleus (DAPI, blue), cytoskeleton (Oregon Green Phalloidin, green) and MNPs (red). Right: 3T3 cell staining to map cell nucleus (DAPI, blue) and MNPs (red)

antibodies, drugs, charge, size,...) ore labeled with two different color it would be easy to understand the behavior of the 2 MNPs in the same experiment reducing the costs and saving time.

### 5.2.2 Antibody conjugation to MNP

A good idea to improve the uptake of MNPs by cells is to increase their reciprocal interaction. To do this it is possible to use a lot of specific molecules designed to promote diffusion of MNPs into cells. But this molecules could probably interact with all types of cells (healthy or diseased) and this is not good because for drug delivery it is important to enter only the tumor cell. For this reason, the ligand

selected to specifically enter tumor cells is the antibody for epidermal growth factor receptor EGFr.

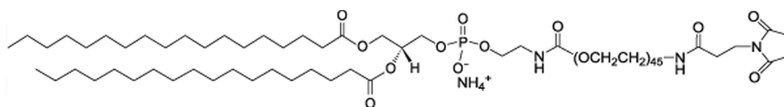
The epidermal growth factor receptor (EGFr; ErbB-1; HER1 in humans) is a receptor located on cell membrane. It is a member of the epidermal growth factor family (EGF-family) and belongs to extracellular protein ligands. Epidermal Growth Factor was discovered by Rita Levi-Montalcini for which received the Nobel prize in Physiology or Medicine in 1986.

Mutations affecting EGFr expression or activity could result in cancer. This is very important for the purpose of the project because the majority of cancer cells has high gene expression of this specific protein.

This protein is important for cancer cell because regulates the viability and proliferation of cells. A high concentration of this on the membrane surface can increase the cellular proliferation rate.

The EGFr antibody has been produced by specific hybridoma cells by dr. Valeria Antonini (CNR-IBF, Trento). The entire process is described in section 6.3.

The first method used to attach EGFr to MNP is based on thiol-maleimide reaction. The iron oxide cores were coated with a mixture of DSPE-mPEG and DSPE-PEG-maleimide. The weight ratio between total DSPE-PEG and iron was 8:1 and the molar ratio of DSPE-PEG-maleimide in the mixture was 2% (following structure).



The disulfide bond in the antibody was reduced with 2-Mercaptoethylamine-HCl. After 2-Mercaptoethylamine-HCl was removed by a centrifugal filter tube (MW = 10,000, Millipore), the reduced antibody was mixed with the MNPs in PBS solution at 1:1 ratio and incubated at 4°C overnight. Free antibody fragments were removed

by ultracentrifugation.

In the preliminary test this method worked very good, but the presence of maleimide compromised the stability of nanoparticles because this functional group is very reactive.

To fix this problem another way to bind the antibody has been developed. The nanoparticles were coated with mixtures at DSPE-mPEG-2000 and DSPE-PEG-NH<sub>2</sub>-2000 (1,2 and 5%) different ratio. At this point a crosslinker to bind the AB to MNP was used: this crosslinker is Sulfosuccinimidyl-4-(N-maleimidomethyl)cyclohexane-1-carboxylate (Sulfo-SMCC) provided by Thermo Fisher Scientific Inc.

This molecule is used as bridge molecule between amine groups of MNP and sulfhydryl groups of antibody, treated with 2-Mercaptoethylamine-HCl in the same way described before. A scheme protocol is described in figure 5.18. In this way, there is a step more respect to the previous method, but the MNPs coated with DSPE-PEG-NH<sub>2</sub> are more stable (months at 4°C) respect to the same MNPs coated with DSPE-PEG-maleimide (2-3 days at 4°C).

The nanoparticles functionalized with EGFr antibody are called AB-MNP.

#### **Determination of MNP targeting using mouse IgG on ELISA plate**

To verify the presence of antibodies on MNP surface, a ELISA-ferrozine hybrid protocol has been developed.

First, a 96-well ELISA plate was coated with mouse IgG specific for EGFr antibody suspended in bovine serum albumin (BSA). In brief, mouse IgG was dissolved at 2  $\mu\text{g}/\text{ml}$  in PBS. Serial dilutions of the IgG solution were performed directly in the plate. The plate was incubated at 4°C for 24 hours and washed with PBS containing 0.05% Tween-20. Then, the plates were incubated with 1% BSA solution in PBS at 4°C for 24 hours. In the coated plate, the amounts of mouse IgG were different but

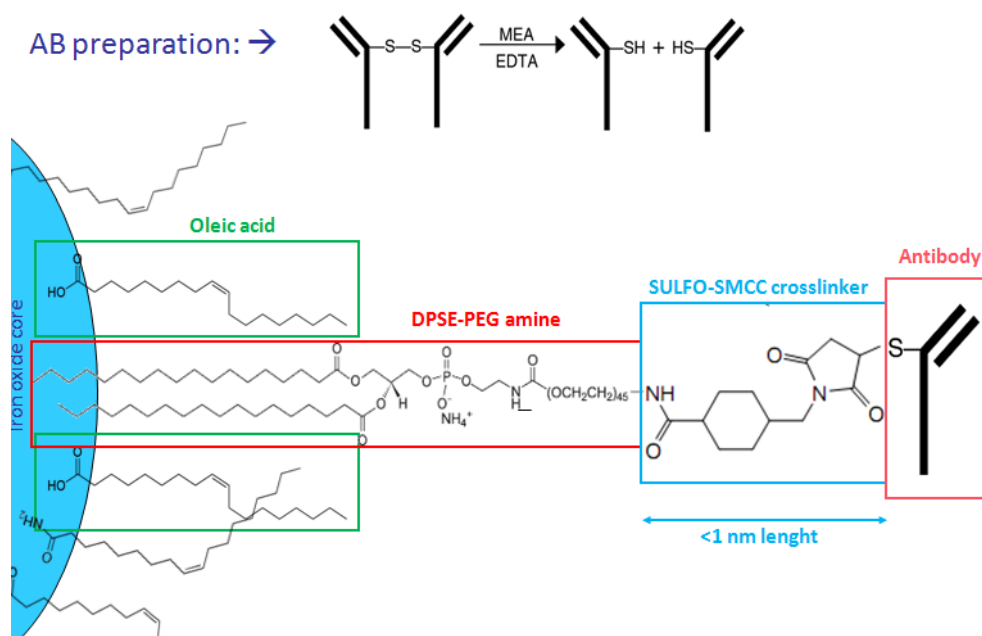


Figure 5.18: Scheme of antibody binding using DSPE-PEG-NH<sub>2</sub> and Sulfo-SMCC crosslinker

the BSA was approximately the same on the surface of each well.

Each well was loaded with 100  $\mu$ l of AB-MNPs. The concentrations of the MIONs were fixed at 2  $\mu$ g/ml. The plate was incubated at 37°C for one hour and washed with PBS containing 0.05% Tween-20. To measure the amount of bound MIONs, the wells were incubated with 50  $\mu$ l of 6N HCl for 30 minutes at room temperature. Then 120  $\mu$ l of 2 N NaOH, 25  $\mu$ l of ammonium acetate buffer, 25  $\mu$ l of 5% hydroxylamine HCl and 30  $\mu$ l of 2% ferrozine were added sequentially. The iron content was determined by light absorption at 562 nm with 810 nm as reference.

The following table illustrated the amount combination between MNP, crosslinker and antibody.

MNP 1%, 2% and 5%	EGFr antibody	Crosslinker Sulfo-SMCC
400 $\mu g$	100 (low) and 200 (high) $\mu g$	60 $\mu g$
	2:1 and 1:1 MNP/AB molar ratio	1500:1 MNP/SMCC molar ratio

Figure 5.19 shows the results about effectiveness of binding using MNPs with different amount of amine group and different concentration of antibody.

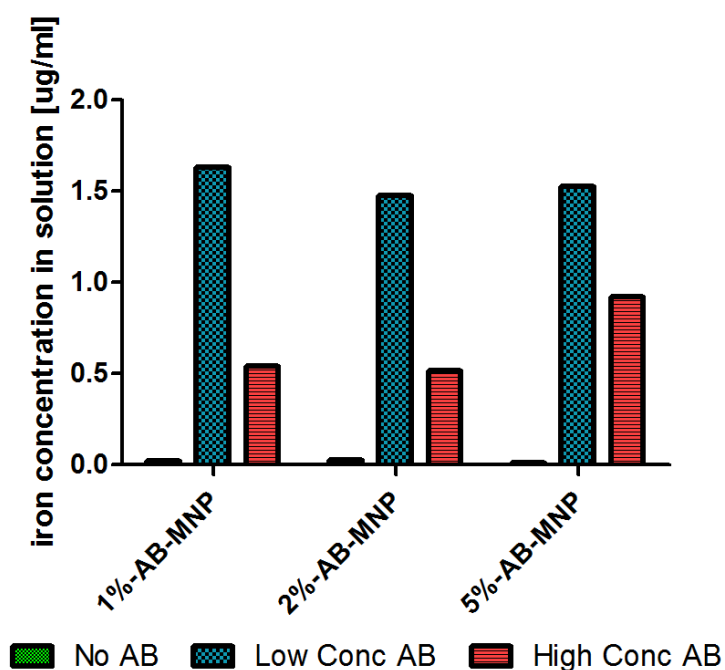


Figure 5.19: ELISA analysis of MNPs with and without antibody.

The type of nanoparticles that returned better results was 5%-AB-MNPs showing higher values for both low and high AB concentration. From this point this protocol with these parameter has been used for following tests and results. For simplicity the 5%-AB-MNPs are called AB-MNP.

These AB-MNPs were tested to verify if the presence of AB facilitates MNP uptake

by cells and these results will be showed *in vitro* test part (section 6.4.3)

### 5.3 Drug loading

One of the most important thing during the design of a carrier for drug delivery is the loading and release of drug. For this purpose doxorubicin (DOX) has been selected as a standard drug. Doxorubicin is a very used drug for cancer therapy. Furthermore DOX has been chosen for its chemical properties:

- Hydro -phobic or -philic behavior is pH sensitive.
- it possible to use it as fluorescent probe: it has excitation and emission at 480 and 580 nm.

Taking into account the behavior at different pH, the drug could be entrapped inside the hydrophobic layer of MNPs in the same way of DiI fluorescent dye.

To get acquainted with the behavior of this molecules and with the protocol, the first DOX entrapping procedure was carried on using water solution (pH 6.5) starting from the parameters used with DiI dye.

One of main problem of drug entrapment is the elimination of free drug from solution of nanoparticles. The method use in these preliminary tests is ultracentrifugation exploiting the big difference between drug (500 Da) and MNPs (380 kDa) molecular weight.

This work is still in progress; the first thing has been done is the evaluation of the correct ratio between drug and MNP to obtain the better loading. Different DOX:MNP ratios have been analyzed to verify which one is the best producing a higher drug loading: 2, 5, 10 and 50 ug of DOX for 80 ug of MNPs (1 ml solution with a concentration of 80 ug/ml).

Just for a complete information, there is a experimental protocol, developed in collaboration with Georgiatech, to measure  $\chi$  value.  $\chi$  is an indicator of entrap efficiency of drug carrier. It is calculated after a centrifugation of solution with MNPs and free drug as described in figure 5.20.

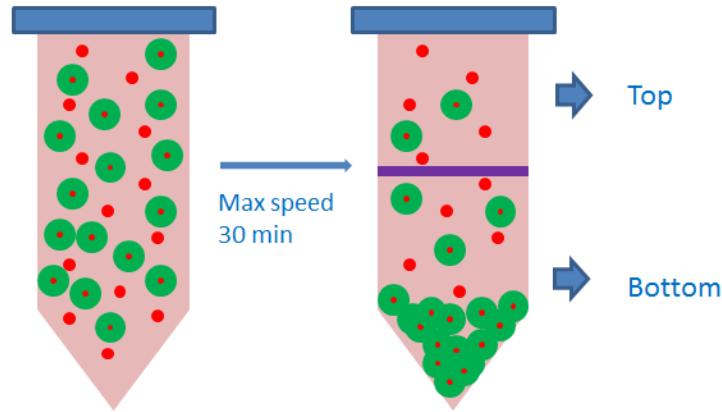


Figure 5.20: Process to prepare the solution for  $\chi$  analysis

The physical principle of this technique is:

$$C_{D-Total} = C_{D-free} + C_{D-entrapped} = C_{D-free} + \chi \cdot C_{SPIO} \quad (5.2)$$

where  $C_{D-Total}$  is the total amount of drug,  $C_{D-free}$  is free drug,  $C_{D-entrapped}$  is drug entrapped in MNPs and  $C_{SPIO}$  is MNPs concentration of solution.

Taking into account that  $C_{D-free}^T \cdot OP = C_{D-free}^{BOTTOM}$ , it is obtained:

$$\chi = \frac{(C_{D-T}^T - C_{D-T}^B)}{(C_{SPIO}^T - C_{SPIO}^B)} \quad (5.3)$$

and it was observed that  $\frac{\chi}{C_{free}}$  is constant for different samples.

To try this method samples (2, 5, 10, 50 ug of dox for 80 ug of MNPs) have been used.

The following table reports the results for each sample:

ug	2	5	10	50
$\chi(10^{-3})$	6,26	6,96	7,40	2,80
$\frac{\chi}{C_{free}}$	0,0017	0,014	0,011	0,001

From this data it is possible to affirm that the 10 ug has a better entrapping because its value is the highest respect to others. Also the value of  $\chi/C_{free}$  is pretty similar for all samples but the 50 ug, that has a concentration too high for this amount of MNPs as showed before.

All this preliminary data have been produced handling DOX in water solution. For a complete analysis it is important to verify drug behavior as regards stability, light absorbance and fluorescence at different pH.

The used pH values are: 1.92, 2.63, 3.3, 5.1, 6, 6.5 (dH2O), 7.4, 8.7, 10.9 and 12.



Figure 5.21: Picture of DOX molecules suspended in different pH solutions: solutions between 1.92 and 7.40 are stable, the 8.70 pH solution have drug aggregates inside and upper pH values show particular stability and absorbance properties.

The stability of DOX solution is illustrated in figure 5.21: it is possible to notice that at pH 8.7 DOX molecules become hydrophobic and aggregate. Both at lower

and higher pH, DOX seems stable. At pH 10.9 and 12 the chemical structure of DOX molecules is probably modified because the solutions change color and no precipitation was observe.

In figure 5.22-left it is possible to analyze what happens at the fluorescence signal and light absorbance of DOX molecules at different pH.

Both parameters are stable for low pH from 1.92 to 7.4 and start to be not so effective at higher value of pH. This is a good thing because high value of pH is just used to entrap DOX into MNPs, but the release happens at low pH (inside the lysosome: 3-4 pH) and the drug has to be active and useful in this condition.

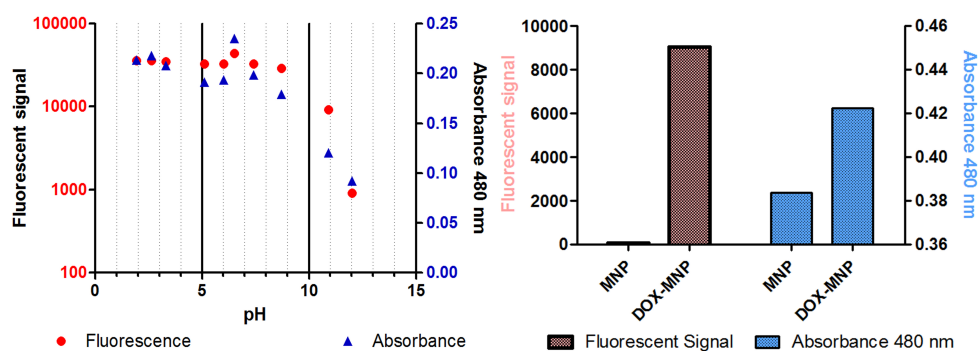


Figure 5.22: Left: Graph of fluorescence and absorbance signal of nanoparticles with and without doxorubicin DOX. Right: Graph of fluorescent signal and absorbance at 480 nm of DOX at different pH values

It is interesting to notice that MNPs with and without entrapped DOX molecules show different fluorescence and absorbance behavior (figure 5.22-right). Both fluorescence and absorbance spectroscopies will thus allow to measure the amount of DOX entrapped in the MNPs preparing a standard curve with fixed amount of MNPs ( $7 \mu\text{g}$ ) and different concentration of DOX ranging from 0 to  $100 \mu\text{g}$ . The measured value is  $1.1 \mu\text{g}/\text{ml}$  of DOX for  $35 \mu\text{g}/\text{ml}$  of MNPs.

Taking into account our experience with doxorubicin and nanoparticles, it is easy to affirm that one of the most complicated step is the removal of free DOX molecules from DOX-MNPs solution.

several methods have been tested and many others are still underdeveloped to obtain a solution as free as possible from DOX molecules.

The method used and to try is: ultracentrifugation, magnetic separation, filtration by filter tube, desalting by spin column, dialysis and many others.

Each of this methods has some disadvantages: they are time consuming, very expensive, MNP leaking and other problems.

At the same time, new DOX entrapment protocol based on different pH solution will be tested. Once obtained best drug loading, MNP will be tested to measure release.

## 5.4 Material, Reagent and Instruments

### 5.4.1 Experiment materials of chapter 4

The used reagents are described in the following table:

Nome	Company	Code	Purity
Iron(III) chloride hexahydrate	Sigma-Aldrich	31232	> 99.0%
Iron(II) chloride tetrahydrate	Sigma-Aldrich	220299	> 99.0%
Aerosol AOT	Fisher	B01930	100.0%
Sodium Hydroxide	Sigma-Aldrich	480878	99.98%
n-Hexane	Sigma-Aldrich	139386	> 99.0%
Acetone	Sigma-Aldrich	179124	> 99.5%
Methanol	Fluka	65550	> 99.5%
Toluene	Sigma-Aldrich	24529	> 99.5%

**The used instruments were:**

- The used transmission electron microscope is a TEM Philips CM12 spectrometer equipped with EDAX 9100. The Olympus is a CCD MegaView II. The acceleration voltage is between 20 and 120 KV, the resolution is 0.3 nm and the magnification is of between 46x to 280.000 x.
- The size distributions were analyzed by Malvern's Zetasizer 1000. The laser mounted on the instrument had a wavelength of 690 nm. The diffusion of light was measured at an angle of 90 degrees.
- The XPS measurements on MNP were carried out using an ESCA200 instrument (Scienta-Gamdata ESCA 200 Uppsala Sweden)

## 5.4.2 Experiment materials of chapter 5

### Section 5.1

MNP core were provided by Laboratory of Biomolecular engineering and Nanomedicine at GeorgiaTech in Atlanta (US)

The DSPE-PEG molecules were supplied by Avanti Polar Lipids, Inc. Used products were:

Name	Code
DSPE-PEG-methoxy 2000	880120P
DSPE-PEG- amine 2000	880128P

Toluene (24529) and Chloroform (650498) was supplied by Sigma-Aldrich. While the filtration tube was a commercial product for Sartorius: Vivaspin 20 (VS2002) with a cutoff of 10 kDa.

#### The used instruments were:

- The ultracentrifugation was a BeckMan Coulter Optima L-100K. The used rotor was: 70.1 Ti Rotor, Fixed Angle, 12 x 13.5 mL, 70,000 rpm, 450,000 x g
- The used trasmission electron microscope is a TEM Philips CM12 spectrometer equipped with EDAX 9100. The Olympus is a CCD MegaView II. The acceleration voltage is between 20 and 120 KV, the resolution is 0.3 nm and the magnification is of between 46x to 280.000 x.
- The size distributions were analyzed by Malvern's Zetasizer 1000. The laser mounted on the instrument had a wavelength of 690 nm. The diffusion of light was measured at an angle of 90 degrees.

- The XPS measurements on MNP were carried out using an ESCA200 instrument (Scienta-Gamdata ESCA 200 Uppsala Sweden)
- The used atomic force microscope is a AFM NT-MDT Solver Pro software and NOVA. The height and phase are acquired in the mode of intermittent contact with non-contact tips with curvature typical of 10nm and spring constant of 5.5 N / m, the typical frequency resonance: 150 kHz.
- The used transmission electron microscope is a TEM Philips CM12 spectrometer equipped with EDAX 9100. The Olympus is a CCD MegaView II. The acceleration voltage is between 20 and 120 KV, the resolution is 0.3 nm and the magnification is of between 46x to 280.000 x.

#### Section 5.1.4

In this part materials and instruments are similar to the previous one, the only difference is the use of other DSPE-PEG molecules.

Used products were:

Name	Code
DSPE-PEG-methoxy 350	880420P
DSPE-PEG-amine 5000	880220P

#### Section 5.1.6

All reagents are provided by Sigma Aldrich and are listed in the following table:

Name	Code
Hydrochloric acid	H7020
Ammonium acetate	431311
Thiosemicarbazide	T33405
Ferrozine	160601
Hydroxylamine hydrochloride	159417

To measure the absorbance of samples produced by ferrozine prococol, a microplate reader TECAN Infinite 200 PRO series has been used.

#### **Section 5.1.8**

To measure the  $\zeta$ -potential of MNP solution a Malvern Zetasizer Nano Z has been used.

#### **Section 5.2.1**

For the labeling of MNP a fluorescent dye has been used. This dye was provided by Invitrogen, Life Technologie Corp.

The chemical name of this product is 1,1'-Dilinoleyl-3,3,3',3'-Tetramethylindocarbocyanine, 4-Chlorobenzenesulfonate, called DiI. The product code is D-7756

To produce fluorescent images a confocal microscope has been used: Nikon A1. The excitation wavelength of this instrument are: 457, 488 and 514 nm.

#### **Section 5.2.2**

In this part a lot of new reagents have been used.

<b>Nome</b>	<b>Company</b>	<b>Code</b>
DSPE-PEG(2000) Maleimide	Avanti Pola Lipids Inc.	880126P
2-MercaptoethylamineHCl	Thermo Scientific	20408
Sulfo-SMCC	Thermo Scientific	22322
Unconjugated Horse Anti-Mouse IgG Antibody	Vector Lab.	AI-2000

### **Section 5.3**

The used drug in this part was supplied by Sigma Aldrich. The commercial name is Doxorubicin hydrochloride and its product number is D1515.

To measure the absorbance and the fluorescent of samples loaded with DOC, a microplate reader TECAN Infinite 200 PRO series has been used.



## Part III

# Experimental Part: Biological Tests



# Chapter 6

## *In vitro* tests

### 6.1 Introduction

The general aim of this part is to investigate interactions and effects of nanoparticles on tumor cell lines. In particular the cytotoxicity has been investigated: internalization and localization of the nanoparticles in different condition. All the experiments are performed in vitro using both 2D and 3D cell cultures.

Preliminary studies has be done on the delivery and availability of the NP and/or drug into the cytosol or intracellular targets.

The cell lines used in this part of work belong to 3 different types of cancers. They are:

- **Lung cancer:** >30% estimated death; it is considered one of the most difficult solid tumours to be targeted. Lung cancer incidence in females is raising, due to the fact that while the number of men who smoke is decreasing, the number of females who start smoking is still increasing. App. 20% of all lung cancers

are independent of smoking.

- **Colon cancer:** >10% estimated death; invasive and if recognized too late, metastasis to the liver, bone, etc.
- **Ovarian cancer:** ~4% of estimated new cases in females = attention to gender issues.

Five cell lines has been chosen to start our analysis. They are list in the table below.

Type	Cell lines	EGFR expression level
Colon Cancer	HCT116	Intermediate
	HT29	High
Ovary Cancer	ES2	High
Lung Cancer	A549	Intermediate
	KNS62	Not determined

The use of all these cell lines would determined a huge work, hence only some of these were used, in particular HT29, ES2 and HTC116.

Other cell lines has been used for test: 3T3 fibroblast and SW480 colon tumor cells. These cells show a negative gene expression for EGFR.

## 6.2 Cell characterization

### Flow cytometric

By flow cytometry the EGFR protein expression has been tested of five cell lines (HTC116, HT29, ES2, A549, KNS62) plus 2 negative ones (SW480 and 3T3 cell lines).

Analysis has been performed two weeks after the cell thawing. In order to confirm the EGFr expression was not lost by cells during the culturing time the analysis was repeated also 1 month and 50 days after. Selection pressure for high EGFr expression was kept adding recombinant EGF (5 ng/ml for 3 days) on the 21st and 47th days, just few days before the 2nd and 3rd cytofluorimeter analyses. Analysis was repeated 3 times:

- 1st experiment: 16 days after cell thawing
- 2nd experiment: 15 days, and 50 days after cell thawing
- 3rd experiment: 14 days, 28 days, and 50 days after cell thawing.

In all the analyses each cell line was tested for: cell without antibody (CTRL), a-human EGFr-1 Abs + FITC (fluorescein) secondary Abs (aEGFr), FITC (fluorescein) secondary Abs (FITC) and PSMA (Prostate Specific Membrane Antigen) Abs + FITC secondary Abs (D2B)

The data obtained show that EGFr expression early time points (14th-15th-16th days after thawing) are similar in the 3 different analyses. In the 3rd analysis SW1990 lost EGFr expression after 28 days. At 50th day the most of the cell lines still express EGFr. Another important result is that SW480 and 3T3 are EGFr negative, as it was expected from the Affymetrix data.

These data were obtained with the collaboration of dr. Valeria Antonini (CNR-IBF, Trento)

### 6.3 Production of EGFr antibodies

A big amount of antibody was needed in order to make targeting nanoparticles. This is why it was decided to produce them by ourselves. The entire process and showed

FACS ANALYSIS DATA

Type	Name	EGFR	14th day		15th day		16th day		17th day		18th day		19th day		
			FLTC Mean	% positive											
Colorectal Cancer	HCT116	Int.	Ctrl	34	0.1			45	0.3	130	0.2			87	0.4
			αEGFr	364	85.4			308	75.7	419	21.3			280	36.8
			FITC	42	0.1			66	2.8	141	0.2				
HT29	High	Ctrl	Ctrl	22	0.1	40	0.1	50	1.6			28	0.1	67	0.9
			αEGFr	260	81.7	248	76.7	225	80.3			335	92.2	418	79.4
			FITC	23	0.2	42	0.7	56	2.2			29	0.1	81	1
SW620	Low	Ctrl	Ctrl							136	0.4				
			αEGFr								178	0.7			
			FITC								181	0.6			
Pancreas Cancer	AsPc1	High	Ctrl	42	0.4			36	0.6			104	0.6	106	0.3
			αEGFr	1563	99.6			528	88			1788	97.1	213	14.6
			FITC	46	0.4			49	1.8			114	1.1		
SW1990	High	Ctrl	Ctrl	62	0.1			46	0.4						
			αEGFr	575	78.5			440	93						
			FITC	71	0.3			45	0.4						
Ovarian Cancer	ES2	High	Ctrl	59	0	77	0.4	46	0.6			74	0.1	47	0
			αEGFr	712	97.6	1078	99	705	98.6			620	90	452	77.2
			FITC	69	0.2	82	0.4	45	0.7			75	0.3		
Lung Cancer	A549	intermediate	Ctrl	41	0	82	0.1	51	0.3	105	1.2	87	0.1	82	0.2
			αEGFr	897	98.3	787	94.4	660	96.2	1482	99.1	676	88.9	515	77.7
			FITC	50	0.6	86	1.2	55	0.8			89	0.2	84	0.5
KNS62	not determined	Ctrl	Ctrl	22	0.3	52	0.9	35	0.2			52	0.2	47	0.1
			αEGFr	293	93.7	282	94.7	226	84.4			323	86	274	73.1
			FITC	48	1.8	54	1	40	0.8			54	0.2	56	2.9
MOUSE fibroblast	3T3ras negative	Ctrl	Ctrl			81	0.7	38	0.1					91	0.5
			αEGFr			86	1	78	1					122	1.6
			FITC			85	1.4	42	0.4					117	1.2
SW480	Low	Ctrl	Ctrl	28	0	52	0					57	0.4	0.36	0
			αEGFr	35	0	54	0.1					60	0.4	52	3.1
			FITC	32	0	53	0.1					59	0.4	52	1.2

Figure 6.1: Flow Cytometric analysis at different culturing cell times using anti human EGFr1, FITC, and PSMA. This data is obtained with the collaboration of dr. Valeria Antonini (CNR-IBF, Trento)

results were carried out by dr. Valeria Antonini (CNR-IBF, Trento). HB-8508 hybridoma was purchased from ATCC. It's B lymphocyte type hybridoma produced in animals that were immunized with partially purified EGF receptors from A-431 cells. Spleen cells were fused with NS-1-503 myeloma cells. The produced antibody is a mouse IgG1 Abs clone 225 that blocks EGF/TGF -induced activation of EGFr and efficiently arrests tumor growth in vivo. It has no effect on tyrosine kinase activity of the receptor. The antibody binds to a single class of receptor sites on A-431, HeLa

and human fibroblasts, and it blocks EGF stimulated phosphorylation of membrane proteins.

### 6.3.1 Hybridoma Adaptation to Medium without Horse Serum

In order to make all the purification protocol easier it was tried to culture the hybridoma in medium without the presence of serum. Different kinds of medium has been used and Hybridomed Medium (Biochrom AG) turned out to be the one giving the best performance.

Figure 6.2-left shows western blotting analysis of hybridoma IgG production after 4 day culturing. The arrows indicate the IgGs present in the supernatant of the hybridoma cultured with Hybridomed Medium without serum. Also reduced and not reduced conditions are shown.

### 6.3.2 IgG production

For production of IgG antibody, CELLLine Two-Compartment bioreactor technology (IBS integra Biosciences) was used. This system is designed to overcome the problems of oxygen and nutrient supplying and inhibiting metabolic waste products removal. At the same time it enables cell proliferation to very high cell density within the cell compartment. In order to establish a working protocol, supernatants at different time points were harvested, and both cell density viability and expression of Abs were checked. Nine days culturing resulted to be the best supernatant harvesting time.

Figure 6.2-right shows western blotting of IgG production at different times. Also reduced and not reduced conditions are shown.

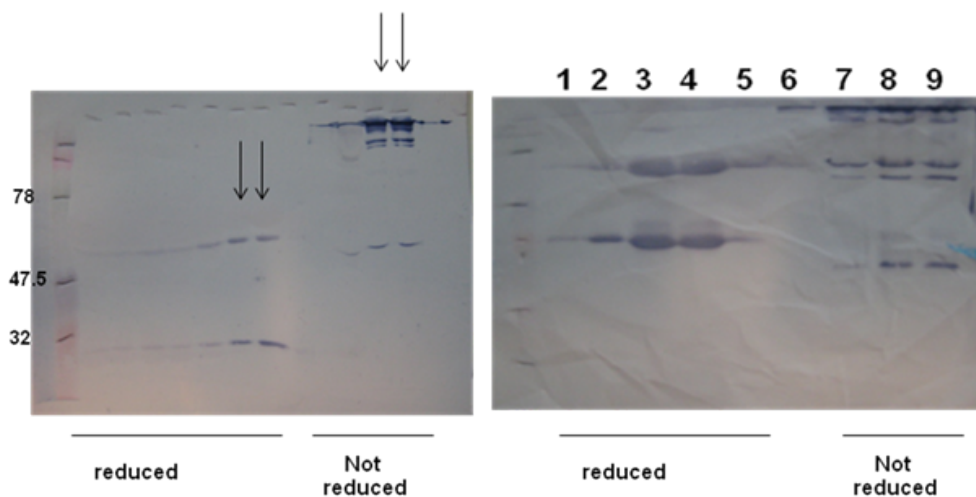


Figure 6.2: Left: Western blotting of hybridoma IgG production after 4 day culturing. The arrows indicate the IgGs present in the supernatant of the hybridoma cultured with Hybridomed Medium without serum (reduced and not reduced conditions are shown). Right: IgG production time points: western blotting of different harvesting time points. Reduced and not reduced conditions are shown. Legend: (1) 2 days reduced, (2) 4 days reduced, (3) 7 days reduced, (4) 9 days reduced, (5) medium, (6) 2 days not reduced, (7) 4 days not reduced, (8) 7 days not reduced, (9) 9 days not reduced,

### 6.3.3 IgG purification

Supernatant was first filtered ( $0.22 \mu m$ ) and then loaded onto a protein G sepharose column. IgGs were eluted using 0.1 mM glycine pH 3 (1M tris-HCl to neutralize the eluate). The sample was collected and it was dialyzed against PBS in order to remove all the amino groups of the buffer that could create problems during the IgG linking to the nanoparticles.

Comassie staining gel of IgG purification steps (reducing and not reducing conditions) are showed in following figure.

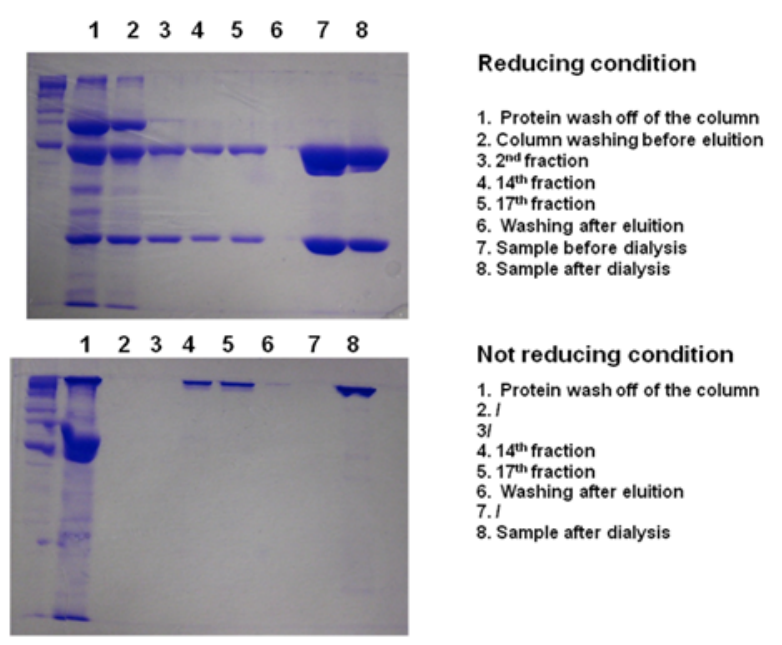


Figure 6.3: Comassie staining gel of IgG purification steps. Reducing and not reducing conditions are shown.

### 6.3.4 EGFr IgG quality testing

The quality of the produced antibodies was tested both by flow cytometry and cell proliferation inhibition analyses. FACS analysis of AsPc1 pancreas cell line using the EGFr antibody purchased by AbCam (left panel) and the EGFr produced by us (right panel) are compared in the figure below. As shown, the antibody worked fine in flow cytometric test.

Moreover antibody effects on 8 cell lines (ES2, HCT116, HT29, KNS62, A549) thawed 1 week before the experiment was tested by viability analysis. 10.000 cells of each cell lines were plated in 96 wells Costar. After 6 hours they were treated with EGFr 200nM. After 18 hours and 42 hours the number of viable cells was determined,

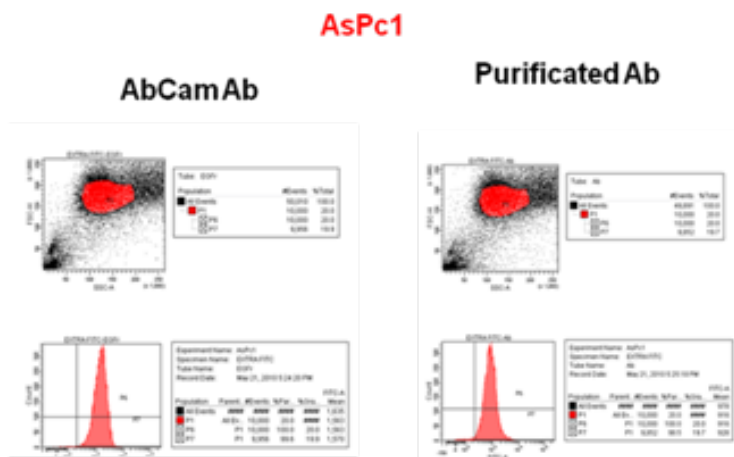


Figure 6.4: Cytometric analysis of AsPc1 cell line using the EGFr antibody purchased (AbCam ab30) left panel and the EGFr produced by us (right panel)

as reported in the next two tables.

Viability relative to untreated cells after 18hrs:

	HT29	HTC116	ES2	A549	KNS62
CTRL	100	100	100	100	100
aEGFr 200 nM	38	92	96	93	77

Viability relative to untreated cells after 42hrs:

	HT29	HTC116	ES2	A549	KNS62
CTRL	100	100	100	100	100
aEGFr 200 nM	8	66	72	73	94

After 42 hrs of treatment almost all the cell lines show a decreased cell numbers except SW1990 and SW620 both the 1week and 2months old cells cultures. This indicates that the antibody can arrest cell proliferation or can induce cell death.

## 6.4 GATECH MNPs

All experiments of this section are carried out using 5%-NH<sub>2</sub>-PEG-MNP (or PEG-MNP simply). These MNPs, dependent on type of experiment are functionalized with fluorescent dye (DiI-MNP), EGFr antibody (AB-MNP and DiI-AB-MNP) and DOX drug (DOX-MNP).

### 6.4.1 Interaction NP-cell

A first step is to investigate the direct interaction of the NPs (in the absence of any drug) with the selected cell lines, using particles with different sizes and coating/functionalization. Preliminary analysis on the viability of ES2 cell lines after 2 and 4 day incubation with PEG-MNP at 35 ug/ml concentration has been performed.

The results (fig. 6.5-left) shows that cell treated with MNPs feel the presence of these structure and the proliferation is slowed down. But it is possible to affirm that the MNPs are biocompatible.

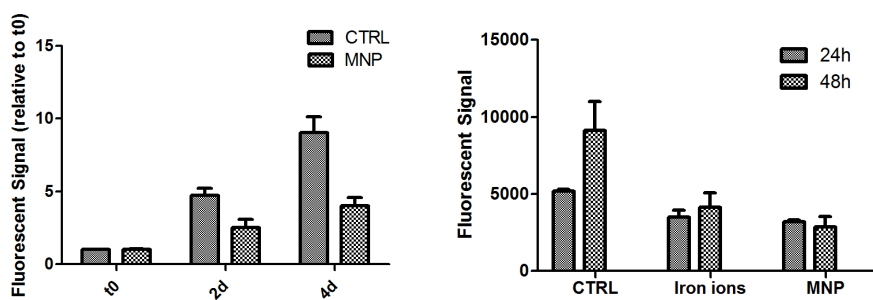


Figure 6.5: Left: Alamar test to verify viability of ES2 cell treated with PEG-MNP. Right: Comparison between viability of ES2 cells treated with MNPs and iron ions

### 6.4.2 Toxicity of MNPs

In previous section, experiment described that MNPs are biocompatible. But to investigate in depth the interaction between MNPs and cells, it is interesting to evaluate if the possible iron ions released by nanoparticles can modify viability and proliferation of cells.

The parameters of this experiment are:

- ES2 cell lines
- cell medium with MNPs (iron concentration of 35  $\mu\text{g}/\text{ml}$ )
- cell medium with iron ions (iron concentration of 35  $\mu\text{g}/\text{ml}$ )
- alamar blue test to measure cell viability after 24 and 48 hours

In figure 6.5-right it is possible to notice a behavior similar to previous case. Cell without treatment proliferated faster than cell with iron or MNPs in medium. Other cells have pretty much the same behavior: presence of iron and MNPs modifies proliferation and viability, but this change can not be correlated just to concentration of ions or to structure of MNPs.

### 6.4.3 Measurement of uptake of AB-MNP by cells

One of most important analysis to reach objective of the project is the measurement of uptake of MNPs by the cell. This parameter gives useful information to design a perfect carrier for diagnosis and above all drug delivery. Knowing the amount of MNPs enter the cell, it is possible to understand the right dose of MNPs to inject.

As described in section 5.2.2, the antibody is attached on the MNP surface exploiting maleimide groups of Sulfo-SMCC crosslinker. One of interesting things to do

it very if presence of antibody or maleimide increases uptake by cells respect to not functionalized PEG-MNP.

To check this possibility, a experiment with 5 different kinds of MNPs has been set up.

- MNP: nanoparticles just with PEG-MNP;
- Cross: nanoparticles with Sulfo-SMCC crosslinker;
- Cross+Block: nanoparticles with Sulfo-SMCC crosslinker and cysteine;
- AB-MNP: nanoparticles with attached AB and free crosslinker;
- AB-MNP+Block: nanoparticles with attached AB and free crosslinker and cysteine;

Cysteine transform the maleimide group in a COOH group that does not modify the MNP uptake by cells.

To be more precise as possible, also two cell lines has been used:

- ES2 ovary cell: EGFr high gene expression
- SW480 colon cell: negative control

with 4 days of MNP incubation.

To analyze the amount of iron inside the cell has been used the ferrozine protocol (fig 6.7-left): this is a quantitative technique to measured the concentration of MNPs inside the cell using colorimetric method described in section 5.1.6

The figure 6.4.3 shows the MNP uptake measured with ferrozine method. For the ES2, it is possible to notice that the AB-MNP enter easier the cell respect to other samples. The different of obtained values with or without blocking is not essential.

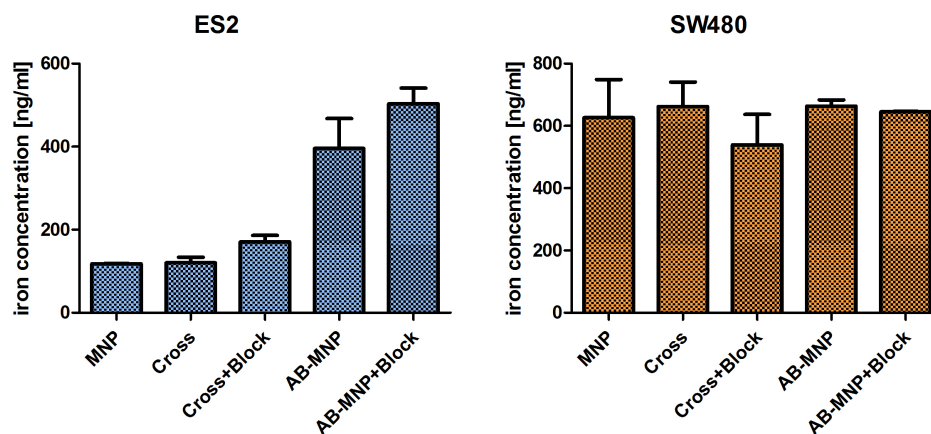


Figure 6.6: Left: Measurement of MNP uptake in ES2 cell line - Right: Measurement of MNP uptake in SW480 cell line

For SW480 cell line, there are not different between MNPs with or with antibody or blocking.

According to this data, it is possible to affirm that the presence of maleimide group does not increase or decrease the MNP uptake by cell.

Taking to account this results and to prepare the future *in vivo* test, another cell line has been selected; it is a EGFR high gene expression cell line: it is HT29 colon cancer cell.

In addition to ferrozine protocol, cytofluorimetry technique has been used to measure MNP uptake by cell (described in fig. 6.7-right). In this technique MNPs become fluorescent when functionalized with DiI dye. This is an advantage because the MNPs that enter cells that become a fluorescent structure. So it is possible to verify the relative amount of uptaken DiI-MNP using a FACS cytofluorimeter.

With both techniques, the uptake has been analyzed using cells with a high gene

expression for EGFR (HT29) and with negative control (3T3) to verify if the presence of the antibody is important for the internalization of MNPs.

The experimental times for FACS are 1 and 3 hours and for Ferrozine is 4 days.

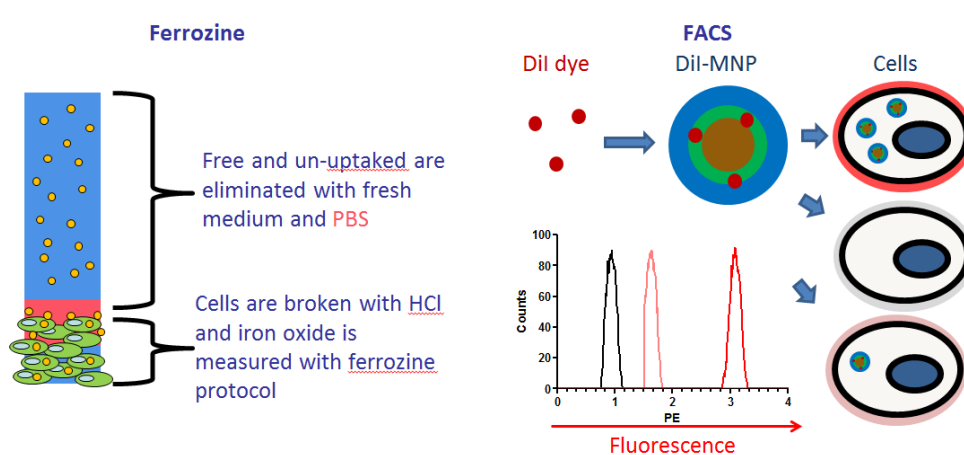


Figure 6.7: Ferrozine and FACS methods to measure the uptake of MNPs by cells

Figure 6.8 shows the iron ion amount for both cell lines and for MNPs with and without AB. It is possible to affirm that AB-MNP enter easier the cells with a high gene expression respect to MNP without antibody. While the behavior of MNPs with and without AB is very similar.

#### 6.4.4 Effectiveness of DOX entrapped in MNPs

At this point it is interesting to verify if chosen drug is effective to kill cell and to test if DOX-MNP if effective as free DOX.

The first thing to do is to verify if the DOX concentration inside the MNPs are good to kill cell. In section 5.3 the concentration of DOX inside MNPs has been calculated and this value is  $1.1 \mu\text{g}/\text{ml}$  of DOX for  $35 \mu\text{g}/\text{ml}$  of MNPs.

Taking into account this value, experiment has been set up with the following

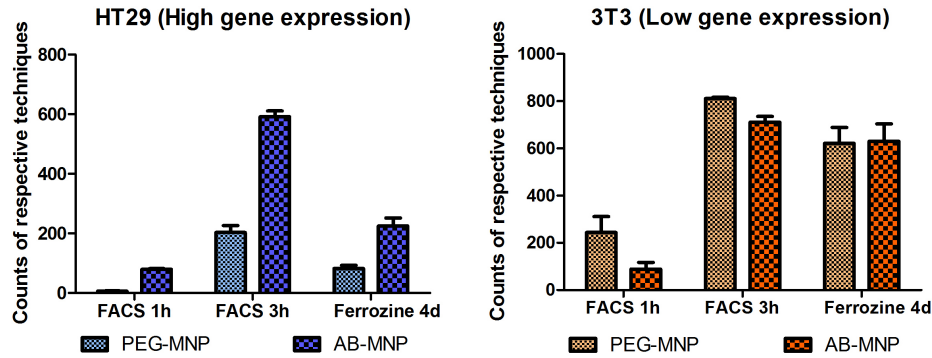


Figure 6.8: Uptake results for HT29 and 3T3 cells using MNPs with and without antibody

parameters:

- ES2 and HT29 cell lines
- 3 different DOX concentration in medium: 11  $\mu\text{g}/\text{ml}$  (DOX10), 1,1  $\mu\text{g}/\text{ml}$  (DOX1) and 0,11  $\mu\text{g}/\text{ml}$  (DOX01).
- alamar blue test to measure cell viability at t0 (starting point before MNP diffusion), 1, 2, 3, 5 and 8 days for ES2 and t0, 2, 3, 5 and 7 days for HT29

Results for both cell lines (fig 6.9 shows that higher concentration of DOX (11 and 1  $\mu\text{g}/\text{ml}$ ) have a good efficacy in the first 3 days. For low concentrations cell viability has strange behavior.

For ES2, DOX starts to kill cells after 5 days, probably this drug needs an accumulation to be effective. For HT29, in the first days low concentrations have the same behavior of DOX10 and DOX1, but afterwardt cell proliferation start to increase again. One possible reason is that in first days t cell proliferation and cell dying are balanced; in the following days there is a imbalance in favor to proliferation

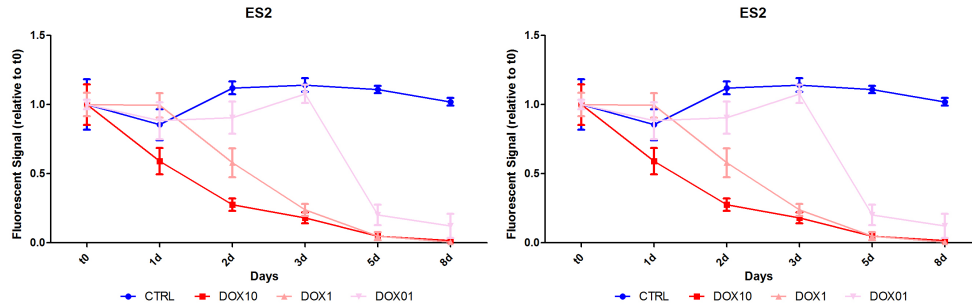


Figure 6.9: Alamar blue test to verify viability of cell treated with different concentration of DOX drug: 11  $\mu\text{g}/\text{ml}$  (DOX10), 1,1  $\mu\text{g}/\text{ml}$  (DOX1) and 0,11  $\mu\text{g}/\text{ml}$  (DOX01). Left: ES2 cell line. Right: HT29 cell line

and number of cell increases.

Taking into account these results, it is easy to prepare an experiment to verify the efficacy of MNP loaded with DOX drug. Parameters are similar to previous experiment, but in this case there are 3 different samples:

- free DOX with a concentration of 1,1  $\mu\text{g}/\text{ml}$  (DOX1);
- MNP loaded with drug following the protocol described in the first part of section 5.3, iron concentration of 35  $\mu\text{g}/\text{ml}$  (DOX-MNP);
- common PEG-MNP: they are the same used to prepare DOX-MNP (MNP).

Other parameters are:

- ES2 and HT29 cell lines
- alamar blue test to measure cell viability at t0 (starting point before MNP diffusion), 2 and 4 days

Figure 6.10 shows the behavior of viability of cells treated with different samples.

For both cell lines, control cell (CTRL) and cell with DOX (DOX1) follow the same trend of previous experiment. CTRL cells continues to proliferate day by day. Conversely, the DOX1 cell population tends to zero after 4 days.

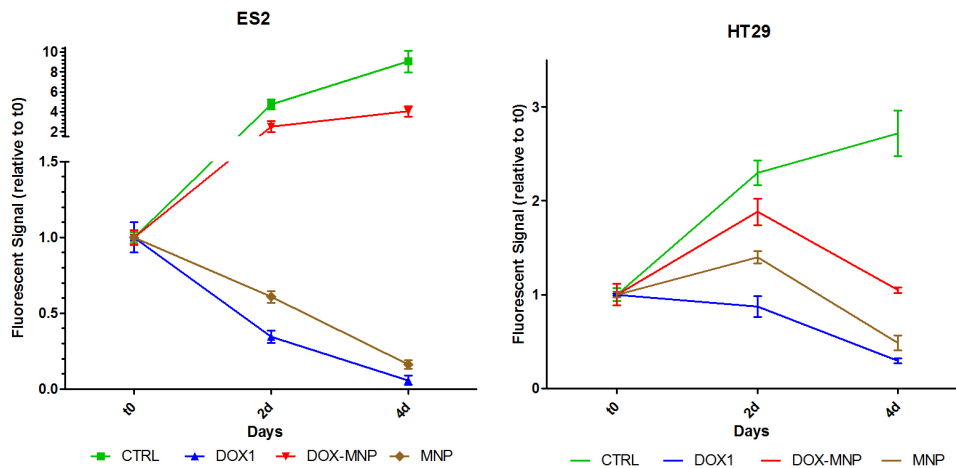


Figure 6.10: Alamar blue test to verify viability of cell treated with different sample: free DOX drug (DOX1), nanoparticles loaded with DOX (DOX-MNP) and just nanoparticles without drug (MNP). Left: ES2 cell line. Right: HT29 cell line

For DOX-MNP sample two different things happen dependent on types of cell line. For ES2, the only one effect of DOX-MNP is to limit the proliferation of cell that become retarded. On the contrary, DOX-MNP effect on HT29 is better: after growing for 2 days, the number of cell starts to decrease. But after 4 day, their effect is not so efficacious as free DOX.

For MNP sample something strange happens for both cell lines. This sample of nanoparticle without drug kills cells in a similar way to free DOX, in particular in case of ES2 cell line. There are possible reasons to explain the particular behavior of MNP sample respect to DOX-MNP tes and they are illustrated in following paragraphs.

As described in section 5.1, after coating, PEG-MNPs are purified with filtration

tube, vacuum pump and ultracentrifugation. After this batch, MNPs are stored in 4C fridge, ready to use.

The protocol to produce DOX-MNP starts taking an aliquot of this MNPs and continues as described in section 5.3. Cell medium solutions with MNPs and DOX-MNP are prepared adding small quantity of MNPs (with few number of washing steps) and DOX-MNP (more purified). Probably this difference of purification can show strange behaviors of previous tests. It is possible that MNPs contain traces of chloroform or toluene from coating process. Also small amounts of this molecules (parts per million ppm) can be very toxic for all types of cells.

Correlated with this explanation, there is another possible reason: the difference in purification steps can modify the  $\zeta$ -potential of MNPs. Different superficial charge could modify the interaction of MNPs with the cells and MNPs may result toxic or not totally biocompatible.

Figure 6.11 shows the  $\zeta$ -potential curves of MNPs and DOX-MNP samples.

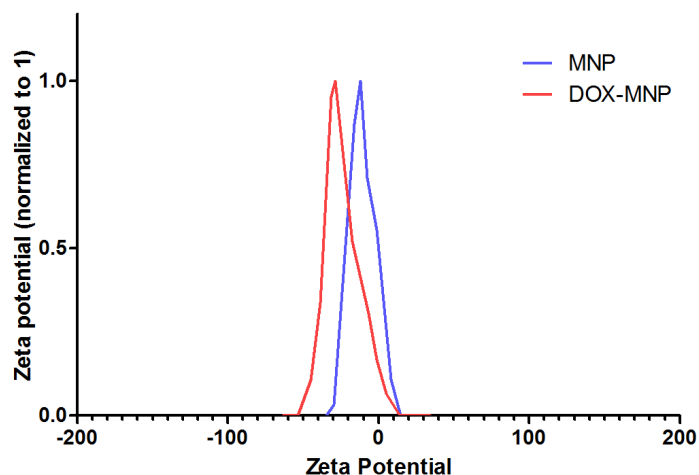


Figure 6.11: Zeta potential curve of MNPs and DOX-MNP samples

It is possible to notice that MNP sample has a peak more shifted to right respect to DOX-MNP. This modification of superficial charge can change the interaction of nanoparticles with cells. moreover MNP sample has a bigger positive component, that can increase the interaction with the cells but it is toxic too.

In the next experiment, nanoparticles to use as MNPs and DOX-MNP sample have to stand the same better purification and washing protocol to eliminate traces of solvent and to have similar  $\zeta$ -potential

#### 6.4.5 Bioreactor experiment: Introduction part

Until now all *in vitro* tests have been done in regular culture method. Cells have been seeded on the bottom of wells of commercial plate. The cell medium, with or without nanoparticles, was added on top of them. All measures has been carried out with a regular 2D layer of cell attached on well bottom.

Referring to future *in vivo* tests there are two things to take into account:

- cancer cells that form a neoplasm are not in a bidimensional layer but in a more complex 3D structure.
- MNPs are injected in blood stream, so when they interact with cell are moved by Brownian motion and blood flow mainly.

Trying to mimic this condition, bioreactor experiment has been set up. The idea is to use 3D insert to simulate a tridimensional structure of cells and to build a perfusion bioreactor to mimic blood circulation condition.

The complete protocol permits to compare result of 3 different types of culture:

- static 2D culture (called S2): it is the regular method used in previous tests

- static 3D culture (called S3): it very similar to S2 method but in this case cells are not seeded on the bottom of well but are attached on the 3D insert and this is leaved in a not treated for adhesion plate or in a petri dish
- dynamic 3D culture (called D3): the 3D insert described in S3 case is hold inside a chamber connected to a perfusion pump that can simulate blood flow.

The first things to do are the selection of better 3D insert dependent on our purpose and on methods used to reach it and the setting up of functional and practical bioreactor.

The selected insert has to be a good 3D model that can show similar behavior than tumor tissue and has to support adhesion, migration and proliferation of cells. It has to be able to resist in static and dynamic condition and has to further proliferation, morphology, distribution and viability of cells

In all steps of this experiment ES2 cell line has been used. The first choice of 3D insert was fibroin sponge produced at Biotech/UNITN lab. These sponges are built using salt-leaching method with NaCl particles (425-1180 nm). Sponge diameter is 6 mm and height is 4 mm. In figure 6.12-left there is a picture of them and of their structure obtained by SEM. It is easy to notice the nanoporous structure of scaffold with pore size between 10 and 30  $\mu\text{m}$ .

But this choice has shown problems and difficulties during the analysis. Sponges are sensitive to dye and other reagents used in biological analysis but the main problem is that each sponge is different to another one. So, these sponges have been abandoned and a commercial 3d insert has been selected (3D Biotek 3D Insert PS scaffold, Sigma Aldrich). These microfabricated inserts are in polystyrene (same material of regular culture plate) plasma treated to promote cell adhesion (figure 6.12-right

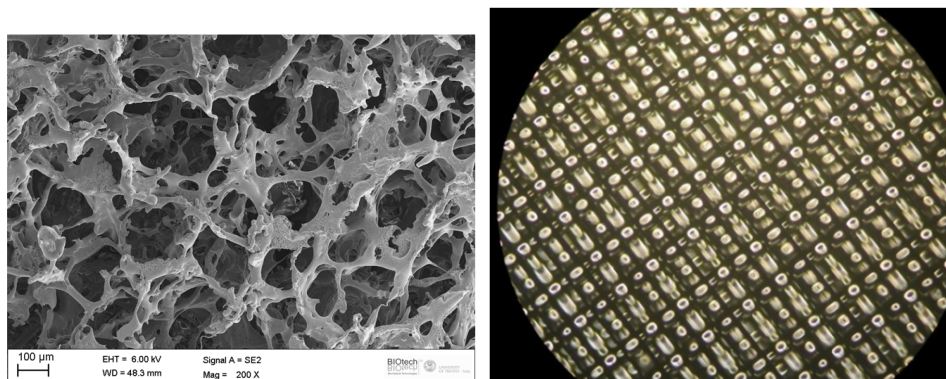


Figure 6.12: Left: SEM images of fibroin sponge, Right: optical images of 3d insert

The main characteristics are:

- Diameter: 5 mm
- Height: 0,5 mm
- Fiber size: 150  $\mu\text{m}$
- Pore size: 200  $\mu\text{m}$ .

The most important skill of this insert is the type of material: it is transparent, not sensitive for dye and reagents and each scaffold is similar to another one. This fact is very important for reproducibility and uniformity of samples.

A perfusion bioreactor has to provide an appropriate environment for biological organism. In most cases, a bioreactor is a container that allows chemical reactions of micro-organisms or molecules derived from them. In a more specific way, a bioreactor is an apparatus that can reproduce physiological condition, to maintain and promote tissue regeneration (for example for growing of tissue of bone, cartilage, hearts and blood vessel).

In an advanced bioreactor, every culture condition can be modified to study their influence on tissue growing. The main physiological conditions are:

- diffusion of nutrients: cell medium
- pH
- temperature
- concentration of  $CO_2$  and  $O_2$ .

In particular bioreactors it is possible to apply mechanical and biochemical stimuli to improve tissue properties. It is important for a bioreactor to guarantee sterility to cell culture and to correct oxygenation; for this purpose all components of a bioreactor must be sterilizable. To avoid contamination and growth of bacteria, filters for air and solution (cell medium,...) are attached to entrances of apparatus. But these filters and the polymer tubes have to further oxygen and  $CO_2$  transit.

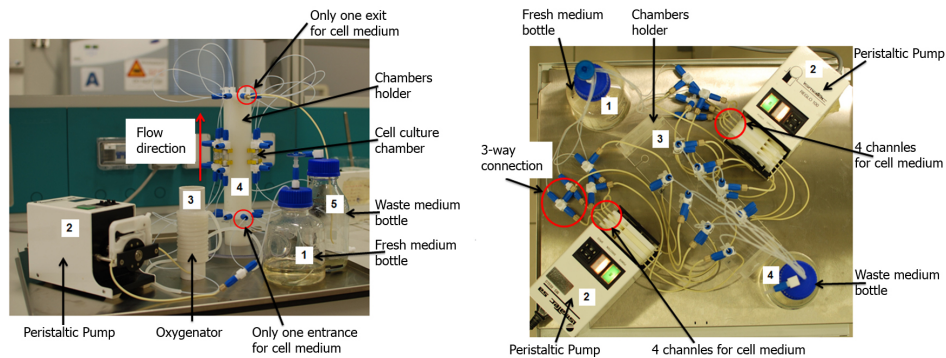


Figure 6.13: First (left) and last (right) configuration of bioreactor used for dynamic condition experiment

The developed bioreactor is a perfusion one; it has 8 polycarbonate chamber, 3-way connections, PTFE (Polytetrafluoroethylene) tubes and flexible Tygon tube used

with peristaltic pumps. Scaffolds are located inside the chamber where the medium is flowed perpendicular to samples (perfusion). The medium flow is maintained constant using a peristaltic pump and its direction is from bottom to top to avoid air bubbles.

Many bioreactor configurations have been tested to obtain good quality of perfusion and reproducibility of experiments.

The first bioreactor is described in figure 6.13-left and the last one is showed in the right part of the same image. There are big differences between them. The first version has only one pump to perfuse fresh cell medium taken from a plastic bottle into 8 chamber. For the main part of the experiment, injection of MNPs, the fresh medium bottle was replaced with a bottle of MNP enriched cell medium. The different flow pression in chambers and the large quantity of MNPs needed for the experiment marked the failure of this bioreactor. After many test versions, the ultimate bioreactor has been built (6.13-right). It has 2 peristaltic pumps, each with 4 channels. The total number of chambers is 8 and each chamber has a pump with the same flow condition.

The working scheme of this bioreactor is described in figure 6.14-top and it has to 2 configurations:

- Seeding - No MNPs: the medium is taken from the bottle, passed by pump and through the chamber and is trashed in another bottle (fig. 6.14-left).
- Testing - MNPs: the medium with MNPs is injected inside the chamber and the apparatus is modified to create a recycle that brings MNPs inside the chamber more times. This has two advantages: to reproduce the recycle of blood stream and to save a large amount of MNPs (fig. 6.14-right).

For a better quality of analysis, the recycle is not close on the same chamber but MNPs are mixed and pass in every chamber.

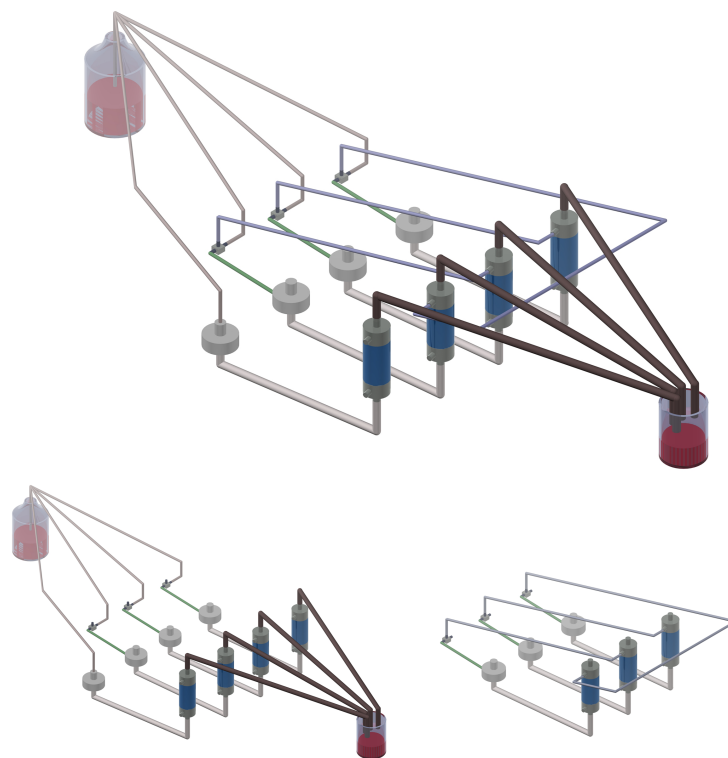


Figure 6.14: Scheme of bioreactor: green tube is for recycle and brown tube is for open configuration

About biological test, a large number of plates and inserts has been performed to permit statistical analysis of each valuation:

- Cell proliferation with AlamarBlue kit
- Morphological behavior and viability with confocal microscope
- Internalization with confocal microscope and colorimetric molecules (ferrozine)
- Trypsinization and cell count
- Quantification of DNA.

Each of these techniques is useful to characterize and understand the efficiency and ability of our bioreactor and our experiments.

## 6.4.6 Bioreactor experiment: Results and Comments

### 2D Static

**Proliferation:** in figure 6.15 it is possible to notice that the proliferation of cells increased in 4 days and after MNP injection the value is pretty much the same; the small difference can be related to confluence of cells inside the well.

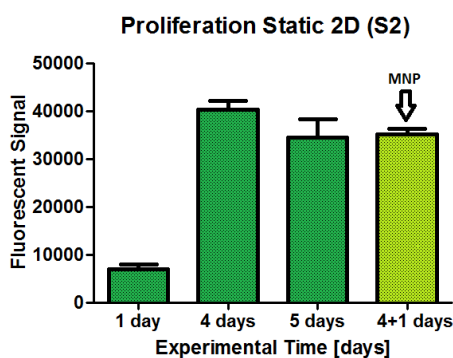


Figure 6.15: Proliferation of ES2 cells in static 2D culture, at different experimental time. “1 day”: after 1 day of static culture; “4 days”: after 4 days; “5 days”: after 5 days (no MNPs); “4+1 days”: after 4 days of static culture and 1 day with MNPs

**Morphology and MNP uptake with confocal microscope:** in fig.6.16 it possible to verify morphology and adhesion of cells. They are good and show good health. Red spots are MNP labeled with a fluorescent dye (DiI). According with figure it is possible to affirm that MNPs are inside the cells and not on the membrane because there are not red spots in nucleus.

### Trypsinization and cell count

Samples have been trypsinized to remove cells from insert and to count them

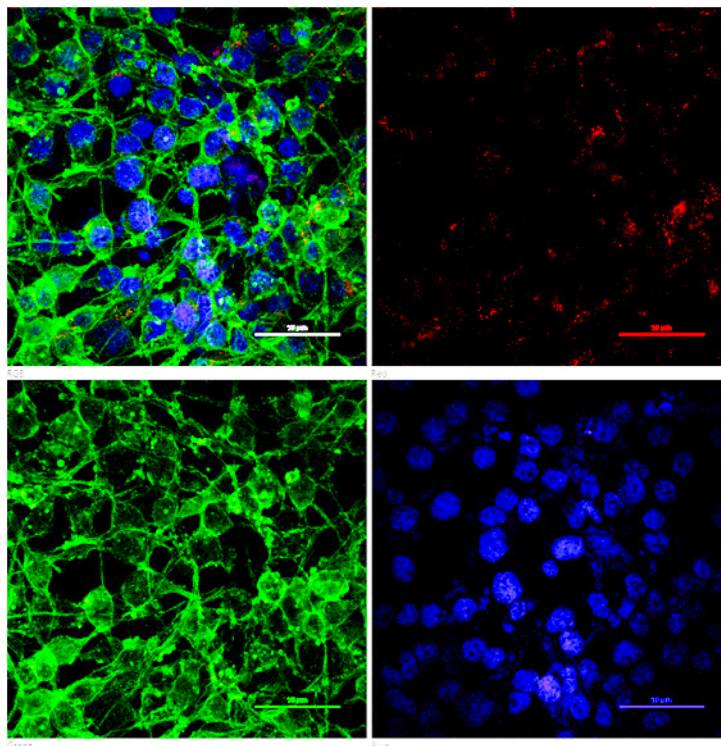


Figure 6.16: ES2 cells in 2d static condition and functionalized MNPs with DiI after 1 day. Magnification 60X. The 4 images is the 3 spectral component and merged picture

with Cellmeter Auto-T4, Nexcelon Bioscience. This method is not so accurate, but it is a quick way to discriminate alive and dead cells.

The obtained value is:  $(1,0 \pm 0,2) * 10^6$  cells for well.

#### **Quantification of DNA**

To obtain this value a specific assay has been used. This method is very accurate but counts both cells, alive and dead.

The obtained value is:  $(9,4 \pm 0,4) * 10^5$  cells for well.

So from these results and the precedent one, it is possible to have complete infor-

mation about viability and proliferation.

#### **Internalization of MNPs**

To obtain the value of MNP uptake for one cell, the amount of iron ions of sample (calculated with spectrophotometric analysis with ferrozine) is correlated to number of cells in sample. The number of cells is calculated using the one obtained with DNA quantification calculated considering the viability measured with cell counter.

The obtained value is:  $(0,8 \pm 0,1)pg/cell$ .

#### **3D static and dynamic**

To perform this part of work 2 cell cultures have been carried out at the same time: 3D in static and dynamic condition. The goal is the same of 2D static. For a further control 2D cell culture has been performed.

Cells ( $1.5 * 10^5$ ) are seeded on 3D inserts of polystyrene in 96-well plate not-treated for cell adhesion, moved after 6 hours in a 48-well plate and maintained in 37°C and 5% of  $CO_2$  incubator.

For dynamic condition, the previously described bioreactor has been used. The first part of protocol is the same of static condition, but after 6 hours inserts are moved in chambers of bioreactor instead of 48-well plate.

**Proliferation:** From 6.17 it is possible to notice that proliferation of S3 increased at day 4, hence it is a normal proliferation of cell. Then this value is constant until day 5. Between day 1 and 4, D3 samples for D3, maintain a comparable value of proliferation, but there is a reduction after 1 day. It is possible to explain the difference between static and dynamic condition at day 4 taking into account the different seeding environment. Probably static condition improves better proliferation respect to dynamic one. Then the injection of MNPs does not change the cell behavior and viability for S3 and D group either.

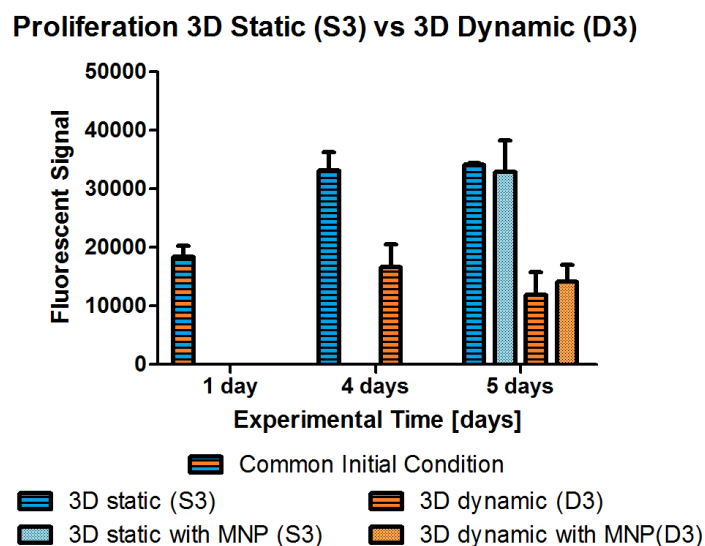


Figure 6.17: Comparison between ES2 cell proliferation on a insert in static and dynamic conditions. MNPs injection happens at day 4

**Morphology and MNP uptake with confocal microscope:** From both S3 (figure 6.18) and D3 (figure 6.19) images (left and right) it is possible to notice that cells have a good adhesion on scaffold. Cells have a correct distribution and are attached on fibers at different depth. Day by day each passing day there is increasing of cell rug, that means health, good proliferation and migration. At day 5, red spots show the position of dye-MNPs inside the cell around the nucleus. Injection of MNPs does not change adhesion, morphology and distribution of cells.

#### **Viability with confocal microscope**

In figure 6.20, the red spots (PI) indicate dead cells and green dyes (FDA) indicate alive cells. According to this, it is easy to affirm that, in the same way for S3 and D3 samples, the number of dead cell increased day after day. Also the injection of MNPs does not raise the number of dead cells.

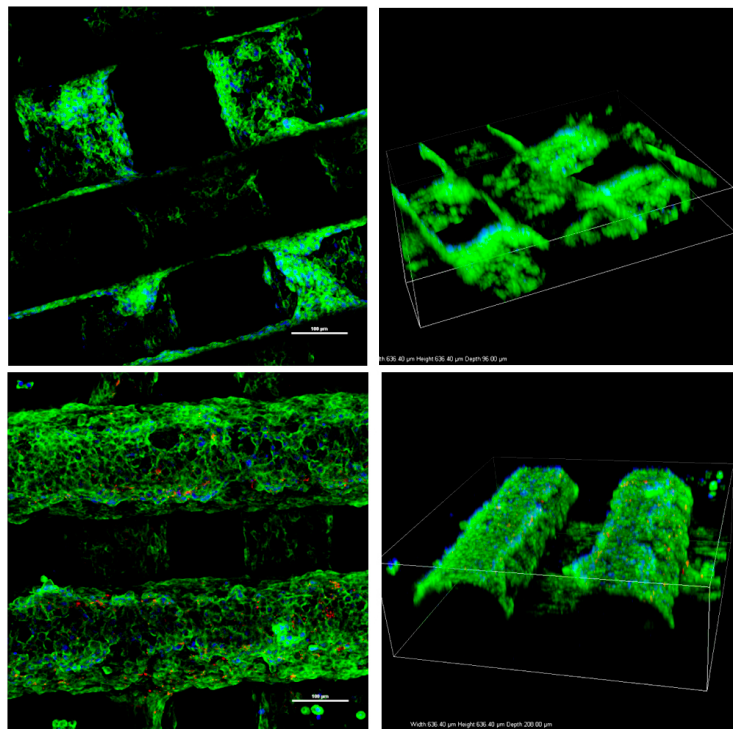


Figure 6.18: Upper: Polystyrene insert, ES2 cell line, static condition, day 4. Magnification 20x and 3d reconstruction. Down: Polystyrene insert, ES2 cell line, static condition, day 5 after MNP injection. Magnification 20x and 3d reconstruction

According to the proliferation results, cell death is a physiological condition of cell seeding process.

**Trypsinization and cell count:** Polystyrene inserts are trypsinized to remove cells and to count them with Cellometer Auto-T4, Nexcelon Bioscience. This method is not so accurate, but it is a quick way to discriminate alive and dead cells. For a complete analysis S2 values are reported too.

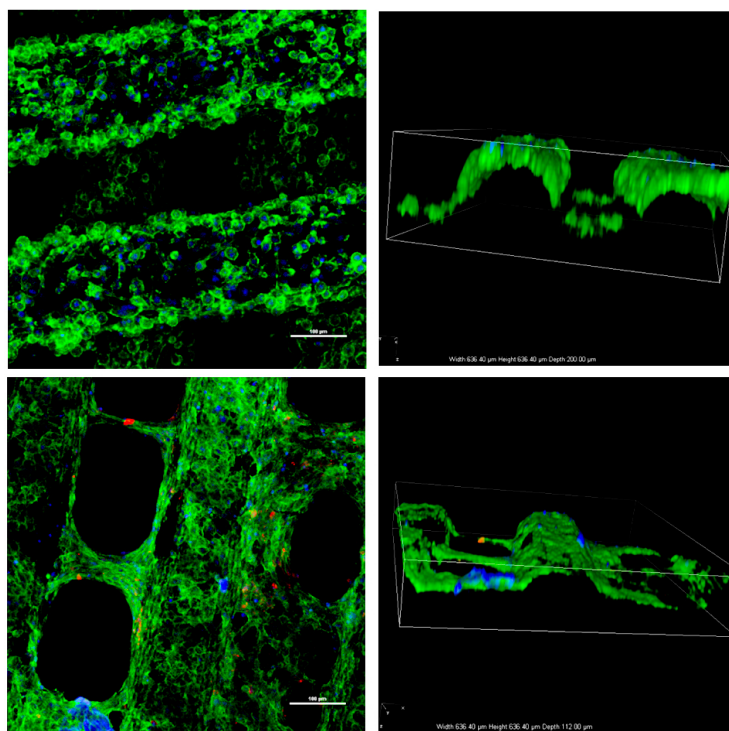


Figure 6.19: Upper: Polystyrene insert, ES2 cell line, dynamic condition, day 4. Magnification 20x and 3d reconstruction. Down: Polystyrene insert, ES2 cell line, dynamic condition, day 5 after MNP injection. Magnification 20x and 3d reconstruction

The obtained values are:

Samples	Cell number
D3-MNP	$(8 \pm 2) \cdot 10^4$
S3-MNP	$(2.2 \pm 0.7) \cdot 10^5$
S2-MNP	$(1.0 \pm 0.2) \cdot 10^6$

#### DNA qualification:

To obtain this value a specific assay has been used. This method is very accurate but it counts both cells, alive and dead. For a complete analysis S2 values are reported

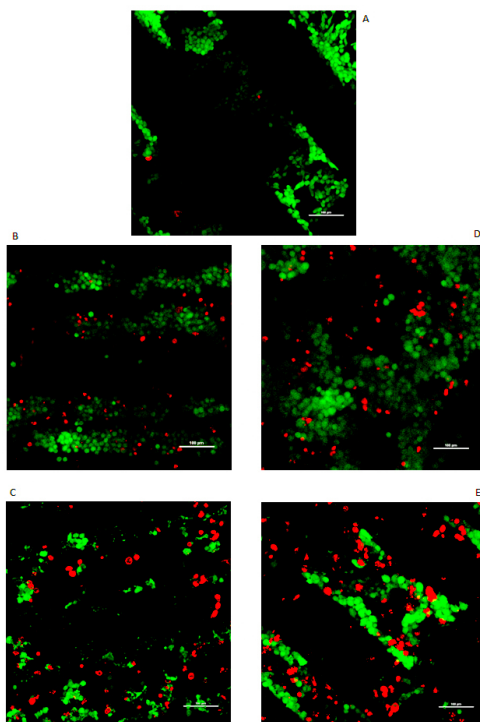


Figure 6.20: A. Insert for live(green)-dead (red) analysis at day 1; B. Same as A at day 4; C. Same as A at day 5 after MNP injection; D. Insert moved in bioreactor at day 4; E. Same as D. at day 5 after MNP injection;

too.

The obtained values are:

Samples	Cell number
D3-MNP	$(1.97 \pm 0.04) \cdot 10^5$
S3-MNP	$(2.9 \pm 0.4) \cdot 10^5$
S2-MNP	$(9.4 \pm 0.7) \cdot 10^5$

### Internalization of MNP

To obtain the value of MNP uptake for one cell, the amount of iron ions of sample

(calculated with spectrophotometric analysis with ferrozine) is correlated to number of cells in sample. The number of cells is calculated using that obtained with DNA quantification calculated taking into account the viability measured with cell counter.

The obtained values are:

Samples	Uptake [pg/cell]
D3-MNP	$1.0 \pm 0.3$
S3-MNP	$(0.9 \pm 0.3)$
S2-MNP	$(0.8 \pm 0.1)$

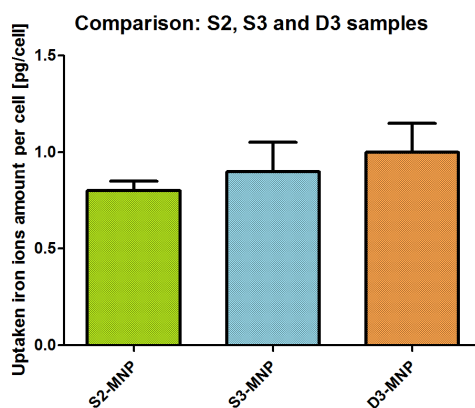


Figure 6.21: Recap of all experiments: amount of iron ions in picogram for 1 cell

Figure 6.21 shows a comparison of uptake results for 3 samples: S2, S3 and 3D. It is possible to notice that ES2 cells internalize in a tridimensional model the same quantity of MNPs for both culture conditions: static and dynamic. The amount of 2D samples is lightly less but in the same order of magnitude. But the value of S2 sample (cell on the bottom of well) is probably overestimated because the bottom and wall of the well can absorb MNPs, which increase the total signal.

Inserts do not suffer for the same problems, because it is possible to move them from the place where the experiment has been carried on. To obtain better result for

each group (S2, S3 e D3) a lot of blank samples have been prepared: wells with cells and without MNPs, inserts with cells and without MNPs, inserts with MNPs and without cells.

It possible to affirm that cells in a 3D model slightly aim to internalize MNPs easier respect to cells in a 2D model. The substitution of a 3D culture instead of a 2D model does not show disadvantage, leak of information or efficiency. There is the same behavior also changing the culture condition (static and dynamic); hence performing experiments in dynamics condition does not compromise this measurement.

Rather, the bioreactor has physically flexible components and adjustable characteristics: flow speed, the possibility of having different circuit (close, to lose and with inter-connections). That makes possible the design of different bioreactors for several types of experiments: gradient of MNPs concentration tunable at different time. Moreover it is possible to use the bioreactor for other samples instead of nanoparticles as enzyme, protein or growth factors.

## Chapter 7

### *In vivo* tests

#### 7.0.7 Results

##### Ferrozine protocol applied to *ex vivo* analysis

According with recent literature, most used techniques to verify the presence of iron oxide nanoparticles in the tissue are histology, electron microscopy or nuclear magnetic spectroscopy. About these methods there is a large amount of papers or books.

On the contrary, it is very difficult to find work about a precise quantitative characterization of MNPs inside the tissue.

In *In vivo* situation the analysis is very complicated, but also *ex vivo* it is not easy to find standard procedures.

The idea developed in this section is to exploit the ferrozine protocol (described in section 5.1.6) to measure the amount of iron ions inside the tissue. In literature there are not papers describing a ferrozine-based procedure to quantitative measure the uptaken MNPs by tissue.

To do this, frozen pieces of liver, kidney and tumor from LBI-CR research group

have been used. These pieces have been cut in smaller pieces to have the possibility to carry about many trials.

The possible ways to effect this process have been reduce to two and called:

- “brute force”: the tissue sample is destroyed and burned with high concentrated HCl for a long time. In this way tissue, cell, protein and MNPs are disrupt and iron ions from MNPs are measured with ferrozine protocol.
- “clever trick”: different molecules (as Proteinase K) are used to disrupt just protein and dissemble the tissue or trypsin are used to recover cell to analyze in the same way described in section 6.4.3.

For “brute force” the HCl solution with the tissue has been heated up with a silicon oil bath or in oven for 16 hours at 120°C. For “clever trick” proteinase K and trypsin (used in cell culture) have been used. To help this molecules the samples have been homogenized with an electrical homogenizator.

Besides the tissue, an iron ion solution has been tested to verify the possible false-negative or false-positive results.

Figure 7.1 shows the result of use both of these techniques on a pieces of liver taken from mice treated with AB-MNPs and engrafted with HCT116 and HT29 cell lines

It is possible to notice that there are signals from oil and oven techniques for MNPs and control liver and from iron ion solution. There are not signals from “proteinase K” and Trypsin spending more time and homogenizing the samples.

For these techniques a problem with the pH occurs. The ferrozine molecule works fine in a narrow pH range, probable buffer of these molecules move the pH of final solution and it is not possible to have a signal.

So taking into account the result of HCl oil bath and oven, another explorative experiment has been carried out.

In this case, there is a comparison of these two techniques using liver, kidney and iron ion solution as samples to analyze.

In figure 7.2 it is possible to notice that the results of “oil bath” and “oven” are pretty similar in behavior and value.

So taking into account the facility of experiment preparation and reproducibility, the “oven” method has been selected to better analysis to try to quantify the amount of MNPs in tissue.

Until now, just one experiment has been carried out: uptakes of MNPs by liver after 4h and 24h have been compared. The procedure is schematized below:

- Total used liver samples were 7: 1 as a control, 3 for 4h analysis and 3 for 24h
- Each sample two little pieces (about 20 mg) were taken
- Each pieces was disrupt with HCl at 120°C. Each piece was separated respect to similar one
- After 16 hours, two small aliquots (50 ul) from the same solution were used to measurement of iron ion amount with ferrozine method
- At the end of ferrozine protocol, two duplicates were measured at 562 nm in absorbance

According with this protocol for each mouse 8 measures have been performed. So according with the first point of previous list, there are 8 measures for the control and 24 measures for both 4h and 24h analysis.

Figure 7.3 shows the graph of amount of iron ion ( $\mu g$ ) uptaken by 1 mg of tissue.

It is not easy to see big difference between 4h and 24h samples. There is a little distinction between control and MNP treated sample.

On possible reason for this difference is that the analysis is not on the entire organ (liver in this case) but just on a small section of it. Probably the large distribution of value depends on this fact, indeed larger distributions is for treated MNPs not for the control. Probably the MNPs can not diffuse homogeneously into tissue and the final value of uptake depends on the section that has been taken.

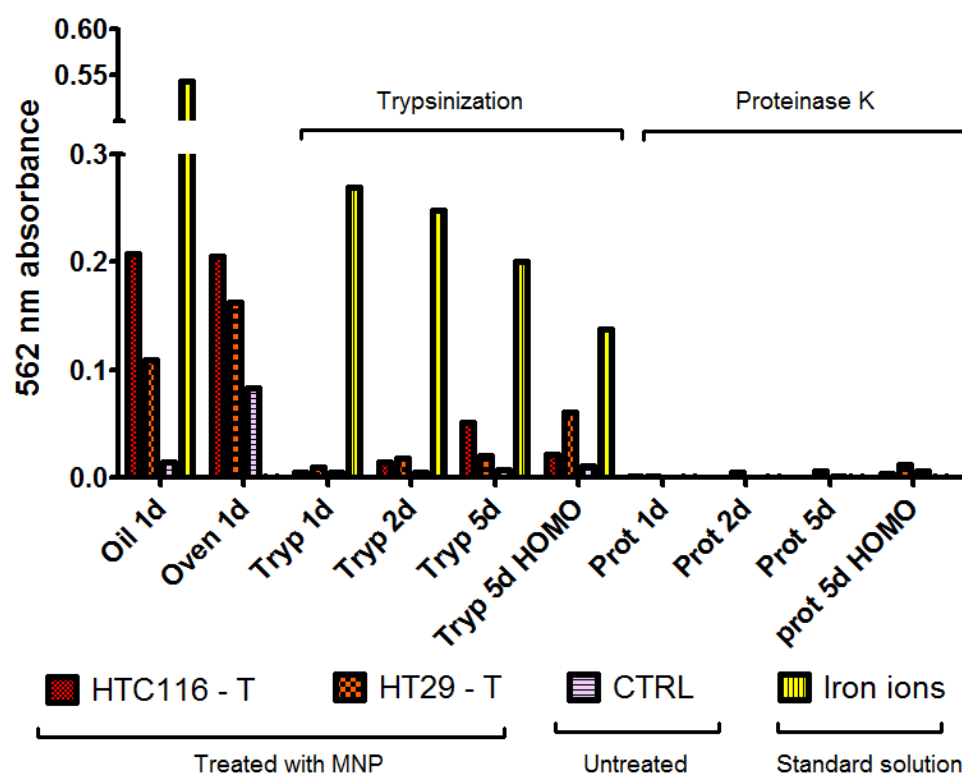


Figure 7.1: Uptake measurement of MNPs by liver tissue calculated using different methods (“oil bath”, “oven”, with proteinase K and trypsin) based on ferrozine protocol. Sample are: MNPs treated liver tissue, control liver tissue and standard iron ion solution

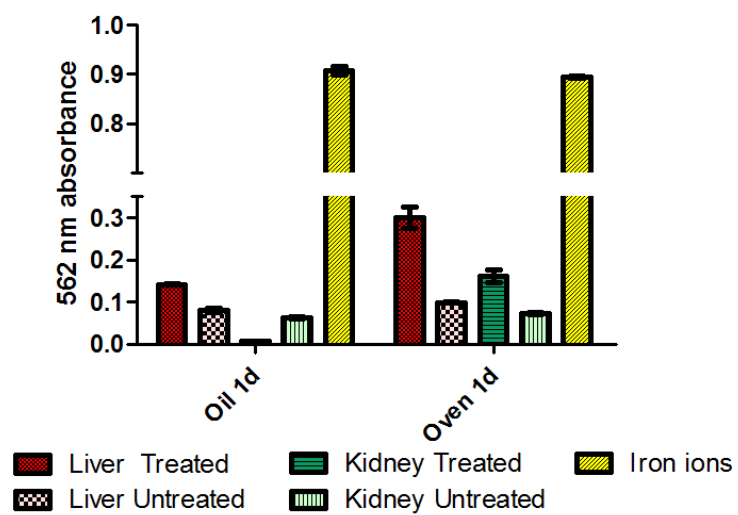


Figure 7.2: Uptake measurement of MNPs by liver and kidney tissues calculated using different methods (“oil bath” and “oven”) based on ferrozine protocol. Sample are: MNPs treated liver and kidney tissue, control liver and kidney tissue

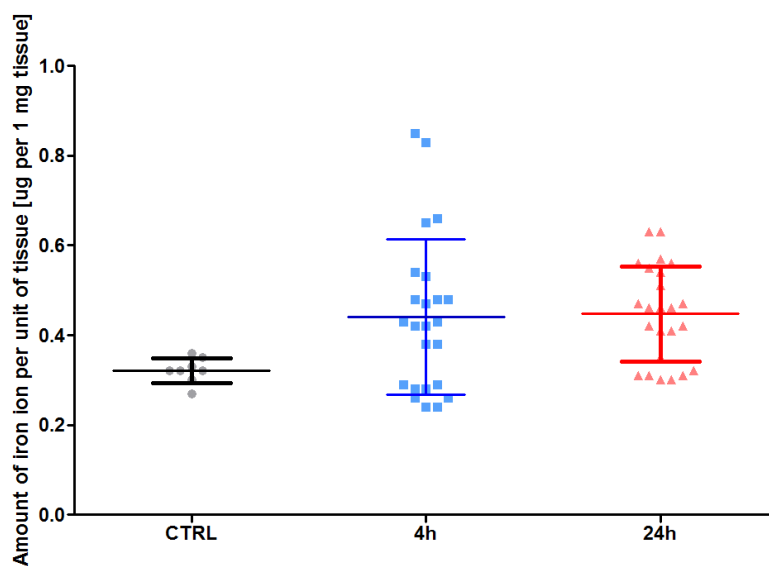


Figure 7.3: Uptake measurement of MNPs by liver tissues calculated using “oven” method based on ferrozine protocol. Sample are: 4h and 24h MNP treated liver and control liver tissue. The spots are the single value, the long central bar is the sample mean and other bars are the standard deviation of the sample



# Conclusions

The production of iron oxide nanoparticles with the ability to be used as contrast agent and as drug delivery carrier was the first purpose of the Nanosmart project. This implied several secondary objectives: indeed, we needed to verify if our MNPs satisfied specific characteristics. To be an effective contrast agent, they have to show high magnetic properties and they have to be biocompatible, but not to be recognized as foreign bodies by the immunity system they must be biomimetic. Moreover, to be a good carrier for drug delivery, MNPs must have good drug entrapment capability and controlled cell interaction.

Just after verifying and reaching these abilities, it would be possible to affirm the realized MNPs are an excellent tool for tumor diagnostics and therapy.

The purpose of this thesis work was an in-depth characterization of every single potentiality offered by iron oxide nanoparticle. According to the characteristics described in section 2.2, several analysis were performed, permitting the design and the production of the best possible structure.

The first challenge was the investigation and the improving of the synthesis and functionalization of MNPs; we demonstrated the accuracy and the reliability of such techniques towards MNPs production. According to our results MNPs came out to be

a complex structure, stable in different buffers at various temperatures and different concentrations. However, these nanoparticles showed also a very modular structure, in which it was not difficult to change the size of iron oxide inner core or to select different thickness or particular electrical charge of external layers.

Further, these nanoparticles also exhibited a high value of magnetic relaxivity  $r_2$ , comparable with that of commercial products; so it is possible to affirm that MNPs can be effectively used as MRI contrast agents.

A critical milestone for the project was the verification of the biocompatibility of the nanoparticles. Several studies demonstrated that MNP are not toxic, however, there was just a collateral effect: the cell proliferation was retarded in presence of MNP.

Another result to underline is the measure of MNP uptake by cells. The most interesting point is that nanoparticles with EGFr antibody entered easier within the cells that had high gene expression for EGFr respect to nanoparticles without the antibody. On the contrary, nanoparticles without antibody entered easier into cells with a negative gene expression for EGFr respect those with antibody.

The drug loading is still an open aspect of this work. Only in the last months, research attention has been focused on this topic. Preliminary results seem promising; nonetheless, it is important to improve DOX loading into MNP and to verify its release and *in vitro* effectiveness.

One of the most stimulating and riveting aspects of this work has been the design and fabrication of a perfusion bioreactor. According to the results in this thesis work, it is possible to affirm that this apparatus, combined with the use of the 3D cell culture insert, enables for an environment capable to simulate a native tumor tissue and blood stream conditions as would be expected for MNPs uptake.

The last and the most important milestone has been the preliminary *in vivo* verification of MNP ability. Here we confirmed that MNP can spread over the tumor region

within as little as 4 hours from injection. Histology also demonstrated that MNPs do not have adverse interaction with kidney tissue. According to these results the liver accumulated MNPs, thereby indicating it is the first mechanism to remove MNP from the blood stream.

Regarding the tumoral uptake, there is not a significant difference between 4h and 24h uptake, also for MNP and AB-MNP samples. The dominant variable in this case seems to be the EGFr gene expression, AB-MNPs entered with slightly higher difficulty the HCT116 cells (intermediate EGFr gene expression) with respect to raw MNP, while AB-MNP entered the HT29 (high EGFr gene expression) easier than raw MNP.

According to these promising, but still preliminary results, it is possible to hypothesize that our nanoparticles have a chance to become in a future a commercial product, usable both for diagnostic and therapeutic applications. Just this double ability is the main strong point of our nanoparticles, beyond the modularity and facility of production.

In the next months, an experiment to verify the tumor shrinking will be performed using the complete MNP structure: iron oxide nanoparticles loaded with DOX drug and functionalized with EGFr antibody.

This experiment will indeed shed further light onto the efficacy of MNPs for tumor therapies, giving us a key proof that could, eventually, open the door to the years-long clinical trials.

In conclusion, these data offer substantial promise and encouragement to continue the work on this research field using this structure and methodology. With improvement and better analysis the MNPs here designed, fabricated and validated may offer considerable interest to the scientific community, in particular with regard to tumor therapies.

# Acknowledgment

This work was supported by Nanosmart Project granted by Provincia Autonoma di Trento (Grandi progetti 2006).

I am grateful to all the people that I met over the years and that helped me to realize this work.

My first thanks goes to Professor Claudio Migliaresi, Professor Antonella Motta and dr. Devid Maniglio, who believed in my abilities and left me the responsibility to participate this big and prestigious project. It was not such an easy task but I had the possibility to visit many research centers all over the world and to learn a massive quantity of information about nanoparticles.

Regarding new experiences, I wish to thank to Professor Gang Bao who gave me the possibility to visit and attend his laboratory at GeorgiaTech in Atlanta. I want to thanks also Sheng Tong, Nazanin Hoshyar and Annie Zheng for their help, patience and precious suggestions.

I want to thank Professor Michel Vert and his group at University of Montpellier (France) for long and challenging discussions about nanoparticles and polymers.

In the same way, I am grateful to Professor Richard Morrigl and his group (Dr.Marc

Wiedner and Dr. Harini Nivarthi) who instructed me about the *in vivo* tests and for the beautiful histology of chapter 6.

A special thanks to Dr. Valeria Antonini (and her boss Mauro Dalla Serra at CNR-IBF) and Dr. Luca Minati (and his boss Giorgio Speranza at FBK-IRST) because I bothered them a lot of times for many reasons.

A personal thanks to all people of BIOtech group for the support and the assistance inside and outside the lab. In particular to Dr Marta Rigoni for assistance during the bioreactor experiment and a special one to Ph.D. Cristina Foss for the constant help and suggestions about *in vitro* tests and for everything we shared in and outside the laboratory.

I am grateful to all friends that play along these years with me: Vale, Marcolla, Laretta, Larcher, Moretti, Ema, Benetti and all others that I forgot.

A huge acknowledgment to all of my old friends: Anna, Mikel, il Puma, Gerry, Dassa (the architect that has drawn figure 6.14), Zanna, Giuly, Fabien, Kaya, Tambu and all others that I forgot.

In the end, I want to thank my parents and my sister for all the rest.

# References

- [1] Nanotechnologies for the Life Sciences Vol. 10, Nanomaterials for Medical Diagnosis and Therapy. Edited by Challa S. S. R. Kumar **2007** WILEY-VCH Copyright 8
- [2] L.G. Gutwein, T.J. Webster TJ; American Ceramic Society 26 th Annual Meeting Conference Proceedings, **2003**
- [3] Nanosmart, Grandi Progetti PAT, anno 2008
- [4] The Royal Society, Nanoscience and nanotechnologies:opportunities and uncertainties, **2004** 1-49
- [5] M.Bruchez, M. Moronne, P. Gin P,S. Weiss; Science 281, **1998** 2013-2016
- [6] H. Mainul, W. Chaoming, S. Ming; Appl. Phys. Lett. 97, **2010** 263704
- [7] C. Mah, I. Zolotukhin, T.J. Fraitos, J. Dobson; Mol Therapy 1, **2000** S239
- [8] J.R. Garrett, X. Wu, J. Sha, K. Ye; Biotechnol. Prog. 24, **2008** 1085-1089
- [9] D. Panatarotto, C.D. Prtidos, J. Hoebeke, F. Brown, E. Kramer, J.P. Briand; Chemistry&Biology 10, **2003** 961-966

- [10] R.L. Edelstein, C.R. Tamanaha, P.E. Sheehan; *Biosensors Bioelectron* 14, **2000** 805-813
- [11] R. Mahtab, J.P. Rogers, C.J. Murphy; *J Am Chem Soc* 117, **1995** 9099-9100
- [12] J. Ma, H. Wong, L.B. Kong, K.W. Peng; *Nanotechnology* 14, **2003** 619-623
- [13] J. Yoshida, T. Kobayashi T; *J Magn Magn Mater* 194, **1999** 176-184
- [14] R.S. Molday, D. MacKenzie; *J Immunol Methods* 52, **1982** 353-367
- [15] R. Weissleder, G. Elizondo, J. Wittenburg, C.A. Rabito CA; *Radiology* 175, **1993** 489-493
- [16] S. Tong, S. Hou, Z. Zheng, J. Zhou, G. Bao; *Nano Lett.* 10 **2010** 4607-4613
- [17] S. Tong, S. Hou, B. Ren, Z. Zheng, G. Bao; *Nano Lett.* 11, **2011** 3720-3726
- [18] W.J. Parak, R. Boudreau, M.L. Gros, D. Gerion; *Adv Mater* 14, **1994** 882-885
- [19] F. Dughiero, A. Candeo, E. Sieni; Dipartimento di Ingegneria Elettrica, Universit di Padova;  
  
[www-1.unipv.it/et2008/memorie/Dughiero.pdf](http://www-1.unipv.it/et2008/memorie/Dughiero.pdf)
- [20] OV Salata, *Journal of Nanobiotechnology* 2:3, **2004** 1-6
- [21] J.M. Wilkinson; *Med. Device Technol.* 14, **2003** 2931
- [22] M. Sprintz, C. Benedetti, M. Ferrari, *Minerva Anesthesiol.* 71, **2005** 419-423
- [23] T. Kubik, K. Bogunia-Kubik, M. Sugisaka; *Curr. Pharm. Biotechnol.* 6 **2005** 1733
- [24] D. F. Emerich, C. G. Thanos; *Expert Opin. Biol. Ther.* 3 **2003** 655-663

- [25] D. F. Emerich; *Expert Opin. Biol. Ther.* 5 **2005** 1-5
- [26] K.K. Jain; *Curr. Opin. Drug Discov. Dev.* 7 **2004** 285289
- [27] D. Proske; *Appl. Microbiol. Biotechnol.* 69 **2006** 367374
- [28] M. Thompson, A. K. Deisingh; *Can. J. Microbiol.* 50 **2004** 6977
- [29] B.A. Holm; *Mol. Crystals Liquid Crystals* 374 **2002** 589598
- [30] P. Prasad; *Mol. Crystals Liquid Crystals* 415 **2004** 17
- [31] P. Gould; *Materials Today* 7 **2004** 3643
- [32] K.K. Jain; *Med. Device Technol.* 13 **2002** 1418
- [33] P. Gould; *Mater. Today* 7 **2004** 36
- [34] X.Zhao; *Anal. Chem.* 75 **2003** 34763483
- [35] X. Zhao; *Analytical Chemistry* 75 **2003** 34763483
- [36] S.A. Wickline, G. M. Lanza; *Circulation* 107 **2003** 10921095
- [37] L. Dalbosco; *Realizzazione e valutazione, fisica e biologica di nanoparticelle magnetiche da utilizzare per l'imaging e la terapia tumorale* University of Trento, Faculty of Science, **2006**
- [38] J.A. Coplan; *Mol. Imaging Biol.* 6 **2004** 341349
- [39] R.A. Farrer; *Nano Lett.* 5 **2005** 11391142
- [40] G.A. Silva; *Surg. Neurol.* 61 **2004** 216220
- [41] A.G. Tkachenko; *J. Am. Chem. Soc.* 125 **2003** 47004701

- [42] J.Klaveness; Runge VM (Ed.). Mosby, St Louis, MO, **1989**, *117128*
- [43] V.J. Mohanraj, Y. Chen; Tropical Journal of Pharmaceutical Research 5 **2006**  
*561-573*
- [44] M. Senna, Dekker Encyclopedia of Nanoscience and Nanotechnology; **2004** *1525*
- [45] <http://www.nanoamor.com>
- [46] {<http://webmineral.com/data/Maghemite.shtml>}
- [47] {<http://webmineral.com/data/Magnetite.shtml>}
- [48] {<http://www.galleries.com/Magnetite>}
- [49] {<http://www.mindat.org/min-1856.html>}
- [50] K. Raj, B. Moskowitz, R. Casciari; Journal of Magnetism and Magnetic Materials  
149 **1995** *174180*
- [51] Yvan Bettarel, Teleshore Sime-Ngando, Christina Amblard, Henri Laveran; Applied and Environmental microbiology **2000** *2283-2289*
- [52] G. Palasantzas, S.A. Koch, T. Vystavel, J.Th.M. De Hosson; Journal of Alloys and Compounds 449; **2008** *237-241*
- [53] Marta Sartor; Dynamic Light Scattering; University of California, San Diego
- [54] R. Xu; Particle Characterization:Light Scattering Methods; Kluwer **2002** *323-341*
- [55] S. Benderbous, C. Corot, P. Jacobs, B. Bonnemain; Acad Radiol. 3 **1996**  
*292S294*
- [56] A. K. Gupta, S. Wells; IEEE Transactions on nanobioscience 3; **2004** *66-84*

- [57] [http://www.ultrasonic-systems.com/ultrasonics/precipitation\\_01.html](http://www.ultrasonic-systems.com/ultrasonics/precipitation_01.html)
- [58] J. Vidal-Vidal, J. Rivasb, M.A. Lopez-Quintela; Colloids and Surfaces A: Physicochem. Eng. Aspects 288; **2006** 44-51
- [59] X. Zeng, Z. Wang, Y. Liu, M. Ji; Appl. Phys. A 80; **2005** 581-584
- [60] M.D. Barankin, Y. Creighton, A. Schmidt-Ott; Journal of Nanoparticle Research 8; **2006** 511-517
- [61] A.K. Gupta, M. Gupta; Biomaterials 26; **2005** 3995-4021
- [62] A.Petri-Fink, M.Chastellain, L.Juillerat-Jeanneret; Biomaterials 26; **2005** 2685-2694
- [63] D. Peer, J. M. Karp, S. Hong, O.C. Farokhzad, R. Margalit, R. Longer; Nature Nanotechnology 2 **2007** 751-760
- [64] {<http://www.mr-tip.com/serv1.php>}
- [65] M. Song, W. Kyung Moon, Y. Kim, D. Lim, I. Song, B. Yoon; Korean J. Radiol. 8 **2007** 365-371
- [66] A. Petri-Fink, M. Chastellain, L Juillerat-Jeanneret, A. Ferrari, H. Hofmann; Biomaterials 26 **2005** 26852694
- [67] S. Metz, G. Bonaterra, M. Rudelius, M. Settles, E.J. Rummeny, H Daldruplink; Eur. Radiol. 14 **2004** 18511858
- [68] E Schulze, J.T. Ferrucci, K. Poss, L. Lapointe, A. Bogdanova, R. Weissleder; Invest. Radiol. 30 **1995** 604610.
- [69] W. Leenders; Ferumoxtran-10. Drugs 6 **2003** 987993

- [70] J. Schnorr, M. Taupitz, S. Wagner, H. Pilgrim, J. Hansel, B. Hamm; *J. Magn. Reson. Imaging*. 12 **2000** 740744
- [71] R. Weissleder, G. Elizondo, J. Wittenberg, C.A. Rabito, H.H. Bengele, L. Josephson; *Radiology* 175 **1990** 489493.
- [72] M.F. Bellin, C. Beigelman, S. Precetti-Morel, *Eur.J. Radiol.* 34 **2000** 257264
- [73] H.H. Bengele, S. Palmacci, J. Rogers, C.W. Jung, J. Crenshaw, L. Josephson, *Magn. Reson. Imaging* 12 **1994** 433442
- [74] A. K. Gupta, S. Wells; *IEEE Transactions on nanobioscience* 3 **2004** 66-84
- [75] N. Nitin, L.E.W. LaConte, O. Zurkiya, X. Hu, G. Bao; *J Biol Inorg Chem*; **2004** 706-712
- [76] N. Nitin, P.J. Santangelo, G. Kim, S. Nie, G. Bao; *Nucleic Acids Research*; **2004** 1-8
- [77] L. LaConte, N. Nitin, G. Bao; *NanoToday*; **2005** 32-39
- [78] E. Balnois, K.J. Wilkinson; *Colloids and Surfaces* 207; **2002** 229-242
- [79] K.J. Wilkinson, E. Balnois, G.G. Leppard, J. Buffle; *Colloids and Surfaces* 155; **1999** 287-310
- [80] L.P. Silva, Z.G.M. Lacava, N. Buske, P.C. Morais and R.B. Azevedo<sup>1</sup>; *Journal of Nanoparticle Research* 6; **2004** 209-213
- [81] E. Viollier, P.W. Inglett, K. Hunter, A.N. Roychoudhury, P. Van Cappellen; *Applied Geochemistry* 15 **2000** 785-790
- [82] L. Minati, V. Micheli, B. Rossi, C. Migliaresi, L. Dalbosco, G. Bao, S. Hou, G. Speranza; *Applied Surface Science* 257 **2011** 10863-10868

- [83] G. Speranza, L. Minati, S. Torrenco, B. Rossi, C. Migliaresi, D. Maniglio, L. Dalbosco; *Advances in Science and Technology* **76** **2010** 165-170
- [84] T.K. Jain, M.A. Morales, S.K. Sahoo, D.L. Leslie-Pelecky, V. Labhasetwar, *Molecule pharmaceutics* 2:3; **2005** 194-205
- [85] G. Bao, S. Suresh; *Nature materials* **2003** 715-726
- [86] C. Corot, K.G. Petry, R. Trivedi, A. Saleh, C. Jonkmanns, J.F. Le Bas, E. Blezer, M. Rausch, B. Brochet, P. Foster-Gareau, D. Baleriaux, S. Gaillard, V. Dousset; *Invest. Radiol.* 39 **2004** 619-625
- [87] G. Schmidt, *Nanoparticles*, Wiley VCH, **2004** 199-230